Enhancing energy recovery from industrial wastewater using microbial fuel cells

Fapetu, S.

Enhancing energy recovery from industrial wastewater using microbial fuel cells

FAPETU SEGUN

A thesis submitted in partial fulfilment of the requirements of the University of Westminster for the degree of Doctor of Philosophy.

January 2018

University of Westminster
115 New Cavendish Street, London, W1W 6UW.

Abstract

Microbial fuel cells (MFCs) hold great promise for the simultaneous treatment of wastewater and electricity production. However, the electricity recovery needs improvement if MFCs are to compete with already established technologies e.g. anaerobic digestion. The aim of this study was to investigate ways of enhancing electricity recovery from (synthetic) industrial wastewater. Initial studies investigated the use of defined cocultures as a way of improving turnover of substrate and hence electricity produced by exploiting mutualistic relationships such as syntrophy or ability of facultative microoganisms (*Saccharomyces cerevisiae*) to consume residual oxygen from the anode. A coculture of *Shewanella oneidensis* and *Clostridium beijerinckii,* investigated here for the first time, gave a power production of 87 mW m^{-2} compared to 48 mW m^{-2} for *S. oneidensis* alone or 60 mW m^{-2} for *C. beijerinckii* alone. Substrate degradation was also improved significantly from 20% (*S. oneidensis* alone) to 67% using the coculture. Similar improvements were observed for novel cocultures of *G. sulfurreducens, S. cerevisiae* and *C. beijerinckii* as well as cocultures of *C. beijerinckii, S. oneidensis* and *S. cerevisiae.* To improve electricity recovery from MFCs, mechanisms of electron transfer need to be understood. The contribution of direct electron transfer mechanisms to overall electron transfer was investigated for the first time by restricting *S. oneidensis* cells close to or away from an anode electrode. A maximum power output of 114 mW m^{-2} was obtained when cells were retained close to the anode. This was 3.5 times more than when the cells were separated away from the anode. This result was corroborated by another study where *S. oneidensis* cells were entrapped in alginate gels. To further investigate the contribution of the c-type cytochromes forming the Mtr pathway to extracellular electron transfer, Rapid DNA Prototyping Assembly was used for the first time to assemble Mtr-pathway coding genes individually or as operons. The different constructs were overexpressed in *S. oneidensis* and heterologously expressed in *E. coli* and power production compared with the wild type strains. The best power generated was from the *mtrAB S. oneidensis* strain (144 mW m^{-2}) and from the *mtrCAB E. coli* strain (24 mW m^{-2}). Since electricity production is linked to exoelectrons forming a biofilm on the anode, ways of enhancing biofilm formation were sought. The quorum sensing molecule N (-3-oxodecanoyl)-L-homoserine lactone of different concentrations was for the first time exogenously added to MFCs and its effect on biofilm formation and power production determined. The results were compared with control experiments

without N (-3-oxodecanoyl)-L-homoserine lactone. The results indicated that power production of 184 mW m^{-2} , the highest obtained of all approaches taken in this investigation, could be obtained when 10 uM of the chemical was added compared to 56 mW m^{-2} for the control, with significant increases in biofilm density. Taken together, these results highlight the importance of using defined cocultures (e.g. for bioaugmentation of working MFCs), direct electron transfer mechanisms, overexpression of the Mtr-pathway and need to increase biofilm density on anode surfaces, for enhancing electricity recovery in microbial fuel cells.

Table of Contents

List of Figures

Chapter 1

Chapter 2

Chapter 3

Chapter 4

Chapter 5.

Chapter 7

List of Tables

Chapter 1

Chapter 2

Chapter 3

Chapter 4

Chapter 5

Acknowledgements

My PhD experience has been like a roller-coaster ride. However, despite the personal efforts put into this work, its completion would not have been successful without the direct and indirect contributions of some giants, whose shoulders I have stood on.

Firstly, I would like to express my sincerest appreciation to my Director of Studies, Dr. Godfrey Kyazze who piqued my interest in this area of research in Environmental Biotechnology and special thanks for his oversight, direction and review of my research activities since the start of the programme.

I would also like to express my profound gratitude to Professor Tajalli Kesharvarz and Prof. Mark Clements for their supervision, discussions and expert advice which enormously enhanced my progress to the completion of the PhD programme.

In appreciation, I would like to acknowledge and thank Eustace Fernando, Adelaja Seun, Priya Mani, Thomas Bridge and the University of Westminster iGEM group 2015 for their support during the research programme. In addition, my gratitude also goes to my colleagues and the technical staff at Cavendish campus especially Dr. Thakor Tandel, Neville Antonio and Dr. Zhi Song for enabling me to access research materials and some of the Laboratory facilities.

Special acknowledgement is also given to Prof. Ola Gomma for opportunity for collaboration towards finding solutions to the limitations affecting MFCs technology. I am also very grateful to Dr. Mark Odell for provision of *E. coli* Chassis; Mrs. Karima Brimah and Mr. Dinesh Shah for their comments, technical support and encouragement in the course of this programme.

Finally, I would like to express my profound thanks to Prof. Fapetu and Late Mrs. Janet Fapetu who are my wonderful parents and sponsors of my PhD programme. Also, thanks to my siblings (Tope, Samson and Joel Fapetu) and my Sisters (Aanu and Tolu Fapetu) for your wonderful love. Special thanks to Mr. & Mrs. Dosumu, Engr & Mrs. Adebayo and Mr. & Mrs. Afolaleye and all lovely well-wishers for their support in diverse ways that have contributed towards my success.

Author's Declaration

I declare that the present work was carried out in accordance with the Guidelines and Regulations of the University of Westminster.

This thesis is entirely my own work and that where any material could be construed as the work of others, it is fully cited and referenced, and/or with appropriate acknowledgement given.

Until the outcome of the current application to the University of Westminster, the work will not be submitted for any such qualification at another university or similar institution.

Signed: segunayofapetu

Dated: 11th January 2018

Segun Ayo Fapetu

This page is intentionally left blank in loving memory of my mom Mrs. Moni Janet Fapetu.

List of Abbreviations

ANOVA – Analysis of Variance

ATP – Adenosine Triphosphate

BES- Bioelectrochemical system

BOD – Biochemical Oxygen Demand

BSAI – *Bacillus stearothermophilus* 6-55 enzyme

CDSs - Protein-encoding genes

CE – Coulombic Efficiency

CEM – Cation Exchange Membrane

CFU – Colony Forming Units

CM – Direct and mediated electron transfer combined

COD – Chemical Oxygen Demand

CoTMPP – Cobalt tetramethylphenylporphyrin

DET – Direct Electron Transfer

DI – De-ionised

DNA – Deoxyribonucleic acid

E'_0 – Standard reduction potential

E^0_{emf} – Electromotive force at standard conditions

E_{andoe} – Anode potential

$E_{cathode}$ – Cathode potential

EDTA – Ethylenediaminetetraacetic acid

E_{emf} – Electromotive force

EET – Extracellular Electron Transfer

F – Faraday's constant (9.64853×10^4 $Cmol^{-1}$)

FAS – Ferrous ammonium sulphate

FMN – Riboflavin Mononucleotide

G^0_r – Gibbs free energy (joules) at standard conditions (298.15K temperature, 1 bar pressure and 1M concentrations of all chemical species).

G_r – Gibbs free energy (Joules).

HPLC – High Performance Liquid Chromatography

LB – Luria Bertani growth medium

mA – Milliampere

MacA – Macrolide export protein

MECs – Microbial Electrolysis Cells

MFCs – Microbial Fuel Cells

MM – Mediated electron transfer

Mol - Mole

MtrA – Membrane transport protein A

mV – Millivolt

mW – Milliwatt

mW m^{-2} – Milliwatt per square metre

MWCO – Molecular Weight Cut Off

NADH – Nicotiniamide Adenine Dinucleotide reduced form

NADPH – Nicotiniamide Adenine Dinucleotide Phosphate reduced form

NCBI – National Centre for Biotechnology Information

NCIMB – National Collection of Industrial, food and Marine Bacteria

NTA – Nitrilotriacetic Acid

OCV – Open Circuit Potential

ORP – Oxidation/Reduction Potential

OMC – Outer Membrane Cytochrome

PABA – p-aminobenzoic acid

PCR – Polymerase Chain Reaction

P_{max} – Maximum power generation

Pt - Platinum

R – Universal gas constant (8.314 J Mol^{-1} K^{-1})

rDNA – Ribosomal DNA

RE – Removal Efficiency

RF – RiboRiboflavin

RDP – Rapid DNA Prototyping

SD – Standard Deviation

TAE – Tris- Acetate EDTA buffer

UShA – UDP-sugar hydrolase (ushA)

Chapter 1

General Introduction

1.1 Energy use in wastewater treatment

Modernization and development are characterised by economic expansion, rapid pace of global urbanisation, high rate of population growth and rapid rise in industrialization (Wu and Tan, 2012). Water that is used in industrial processes such as for cooking, washing, cooling, heating, and extraction is inevitably changed by the process (Ng and Tjan, 2006). Industrial wastewaters are effluents produced from human activities associated with raw-materials processing and manufacturing. The wastewaters can come from chemical, pharmaceutical, electrochemical, electronics, petrochemical, breweries, and food processing industries. Industrial wastewaters have varied composition depending on the industry, type and materials processed (Karman *et al*., 2015; Ng and Tjan, 2006). Some of these wastewaters contain very high concentrations of organic compounds with chemical oxygen demand (COD) of 40-60 g L^{-1} that are easily biodegradable e.g. carbohydrate in wastewaters from cheese-producing industries (Gavala *et al*., 1999), while some contain total ammonia nitrogen above 2.5 g L^{-1} which is inhibitory to both mesophilic and thermophilic stages of anaerobic digestion processing (Sutaryo *et al*., 2014). Some wastewaters are associated with pH values beyond the range of 6-9. The total suspended solids (TSS), biological oxygen demand (BOD) and chemical oxygen demand (COD) can be in tens of thousands mg L^{-1} (Ng and Tjan, 2006); requiring BOD reduction to 400 mg L^{-1} before discharge (Goel *et al*., 2005). Hence, industrial wastewater treatment is very important and often requires treatment to remove the pollutants to protect public health and environment (Karman *et al*., 2015; Longo *et al*., 2016). The range of industrial wastewater volumes to be treated varies from factory to factory within an industry. This can range from as small as 3.6 m^3 d^{-1} (41g L^{-1} COD) from starch extracted wastewater to as large as 27240 m^3 d^{-1} (5 g L^{-1} COD) produced from paper mills (Ng and Tjan, 2006).

A significant amount of money is spent treating large volumes of wastewater because traditional methods of wastewater treatment are energy intensive and hence costly (Table 1.1).

Table 1.1: Energy needs of wastewater treatment (Logan 2008, cost of 1 kWh = ca.15 p):

Treatment method	*Energy requirement (*kWh m^{-3})	*Cost (millions of £) /year**
Trickling filter	0.12	2.3
Activated sludge	0.28 – 0.31	5.4-5.9
Membrane bioreactor	2.4	46

*For a wastewater treatment plant treating 350,000 m^3 of wastewater/day corresponding to 800,000 persons equivalents.

An example of data from Spain showed that approximately 12,800,974 m^3 of wastewaters were reported to be treated daily with a corresponding energy demand accounting for about 1% of total energy consumption of the country (Escapa *et al.,* 2014). Similar patterns of energy consumption have been reported in Germany as well as in Italy (Longo *et al*., 2016). In the USA, the United States EPA estimated 3-4% of electricity generated is spent on wastewater treatment which is approximately 110 TWh $year^{-1}$, or equivalent to 9.6 million households' annual electricity use (Logan and Rabaey, 2012; Daw *et al*., 2012).

As the number of wastewater treatment plants increases worldwide and quality requirements of wastewater treatment plants (WWTP) becomes more demanding, the issue of energy efficiency has become important. Wastewater is increasingly being considered as a sustainable resource from which energy (and other resources) can be extracted. Typical example of 1 kg of glucose contaminated wastewater corresponding to 1.06 kg of chemical oxygen demand (Harwani, 2013) can potentially generate 3.56 KWh energy (Horan *et al*., 2011). By using conventional $WWTP_s$ processes, little energy can be derived by bioconversion of glucose, as this energy is difficult to be harvested and captured within the microbial metabolism. This is eventually released as water and carbon dioxide (CO_2) that contain no useful energy (equation 1)

Equation 1: $C_6H_{12}O_6 + 6O_2 \rightarrow 6CO_2 + 6H_2O \quad \Delta G° = -2843\ kJ\ mol^{-1}$

Conventional methods such as activated sludge, membrane reactors, and anaerobic digestion to treat wastewater require high energy consumption (e.g. 0.3 KWh m^{-3} for aeration) and their adverse environmental impact have made these technologies unsuitable for sustainability as energy-efficient methods of wastewater treatment (Logan, 2008).

1.2 Capturing energy from wastewater treatment plants.

Wastewater could be used as a resource saving energy and money as wastewater contains organic matter containing stored energy in the bonds of atoms and molecules that hold the particles together. This can be oxidized by biochemical processes through bio-decomposition to generate electricity and energy-rich fuels (e.g. bio-ethanol), while at the same time cleaning up the wastewater (Guerrero-Lemus and Shephard, 2017; Logan, 2008). It is estimated that wastewater contains 9 to 10 times more energy than the energy required for its treatment (Dannys *et al*., 2016, Equation 2&3 - Harnisch *et al*., 2011). Why not recover all the energy? There is potential to make the treatment process at least self-sufficient from an energy perspective.

Equation 2: Power consumption due to aeration

$$P = 350{,}000 \left(\frac{m^3}{d}\right) \times 0.2 \left(\frac{KgBOD_5}{m^3}\right) \times 0.9 \frac{KgBOD_5\ removed}{KgBOD_5} \times 1.3 \left(\frac{KgO_2}{KgBOD_5 removed}\right) \times \frac{1\ KWh}{1.5 KgO_2} \times 3600 \frac{KJ}{KWh} \times \frac{1\ day}{96400_s} = 2275\ kW \approx 2.3\ MW$$

Equation 3: Power that can be recovered at 100% recovery could be possible

$$P = 350{,}000 \left(\frac{m^3}{d}\right) \times 0.4 \left(\frac{KgCOD}{m^3}\right) \times 14.7 \times 10^3 \frac{KJ}{KgCOD} \times \frac{1\ day}{86400_s} = 23{,}819\ kW \approx 24\ MW$$

Anaerobic digestion has been used to treat and recover energy (as biogas) from industrial wastewater but the technology is unsuitable for dilute streams (COD < 1 kg/m^3) due to external energy required (usually the source from the bioenergy

harvested) to heat up the systems for the mesophilic to thermophilic temperature required to achieve sufficient turnover/treatment. In addition, it is unsuitable for wastewater with high nitrogen-rich feedstocks due to release of ammonia-nitrogen which causes inhibition of microbial degradation processes. Recently, bioelectrochemical systems were suggested as viable ways of treating wastewater sustainably while at the same time producing electricity (Harnisch *et al*., 2011; Moestedt *et al*., 2016 ; Demirel *et al*., 2005 ; Fernando *et al*., 2012).

1.3 History of bio-electrochemical systems.

The concept that bacteria have the capabilities to transport electrons beyond their cell wall, hence, electrically interacting with their environment has been widely popular since early 1960s. NASA (National Aeronautics and Space Administration, USA) was curious about using algae and bacteria to generate electricity from waste in the closed system of a space shuttle (Ieropoulos *et al*, 2005). In 1911, M.C Potter observed electrical current production from organic compounds with the aid of platinum electrode by a fermentative culture of *Saccharomyces cerevisiae* and *Escherichia coli* in a bioelectrochemical system (Potter 1911). This work was regarded to be the first biochemical fuel cell studied where the concept of MFCs was experimentally demonstrated (Logan, 2008). In the early 1980s, the intense debate on looming energy crises and associated environmental damage occurring due to industrialization and excessive fossil fuel burning, motivated much interest to environmentally cleaner and more sustainable alternatives for energy generation and environmental remediation. Hence, research on BESs received great interest due to its promising way of environmental remediation and simultaneously electricity generation (Fernando *et al*., 2012).

1.4. Overview of bio-electrochemical systems

Bio-electrochemical systems, also called Microbial Electrochemical Technologies (METs) are rapidly developing technologies that utilize microbes capable of converting the chemical energy from biodegradable organic wastes (ranging from low strength to lignocellulosic) present in wastewater to electricity. Diverse ways of application of microorganisms in METs, either on anode or cathodes or on both anode and cathode have allowed inventions of different varieties of METs performing

distinct functions and purposes. Several types of METs (see Table 1.2) are usually identified by using variations on an MxC theme, where x denote specific application of this technology. For example, in MFCs technologies, x is replaced with F. Variations of MFCs are microbial electrolysis cells (MECs) which utilise a small external power source (typically 0.6 V) to bias the thermodynamics of the reactions occurring in the anode and cathode. MECs may be useful in terms of recovering alternative energy forms e.g. hydrogen or other chemicals (Kyazze *et al*., 2010). MECs in the form of Microbial Reverse-Electrodialysis can utilize methanogenic bacteria for methane production (Conrad, 1999) while in the form of Microbial Electrodialysis Cell can be used for desalination and hydrogen gas production (Mehanna *et al*., 2010). These innovative technologies are promising technologies that can be operated under mild conditions and can utilize inexpensive cathodes based on activated carbon catalyst (Logan *et al*., 2015).

Table 1.2: Examples of different variations of Microbial Electrochemical Technologies derivatives (adapted from Logan et al., (2015)

MxC	Full name	Comments
MDC	Microbial desalination cells	It integrates microbial fuel cell processes and electrodialysis for wastewater treatment (Saeed *et al*., 2015)
MEC	Microbial Electrolysis Cell	Typically designed for catalysing hydrogen gas production in the cathode chamber and also designed for metal reduction (Jeremiasse *et al*., 2010; Logan *et al*., 2015).
MEDCC	Microbial Electrolysis Desalination and Chemical Production Cell	Novel technology used to desalinate salty water (Chen *et al*., 2012)
MES	Microbial Electrosynthesis System	An MEC designed for production of soluble organics such as acetate (Logan *et al*., 2015)
MFC	Microbial Fuel Cell	Typically designed for electrical power production (Logan *et al*., 2015)
MxC-MBR	MFC with cathode membrane	The cathode serves a dual function of reduction and filtration of water using either MFCs or MECs (Logan *et al*., 2015)
MMC	Microbial methanogenesis cell	Typically designed for methane production from the cathode by addition of voltage. Reverse electro dialysis is placed between anode with electrogenic microorganisms and a methanogenic biocathode (Luo *et al*., 2014).
MREC	Microbial Reverse Electrodialysis electrolysis Cell	Typically used for hydrogen production (Song *et al*., 2016)
MREEC	Microbial Reverse Electrolysis and Chemical Production Cell	An MEDCC having a Reverse Electro-dialysis stack used for production of acid and bases; can be used for carbon capture, hydrogen gas production and also used for desalination.

1.5. Mode of action of microbial fuel cells.

MFCs are electrochemical devices that utilise micro-organisms such as *Shewanella, Geobacter, Rhodoferax* and yeasts predominantly found in subsurface habitats such as aquatic sediments and pristine deep aquifer and are considered candidates for bioremediation of subs-surface metal contaminated because of their ability to metabolically reduce metals (Abboud *et al*., 2005; Lai *et al*., 2007; Coates *et al*., 1996). The fundamental principle of this technology is that it comprises of two electrodes, an anode, and a cathode, in the presence of electrolyte. The two electrodes are usually separated by a proton exchange membrane and catalyses an oxidation reaction on the anode by releasing electrons, and reduction reaction by using oxygen or other electron acceptors at cathode electrode. Active biocatalyst collectively called electroactive or electrogenic bacteria can oxidize organic substrate and produce protons and electrons. The electrons produced are conveyed through the wire, while the protons are conducted through the proton exchange membrane to the cathode along with parallel reduction of oxygen to water (Chouler and Di Lorenzo, 2015 ; Rahimnejad *et al*., 2015).

This process can produce renewable bioenergy and water (or other reduced compounds) when connected to a load/resistor via an external circuit (Figure 1.1). Theoretically, MFCs has good operational stability with low cost operation compared to conventional method of treating wastewater. It can operate over a broad range of temperatures from ambient (15-35℃) to elevated temperature range (50-60℃). However, despite theoretical advances of this technology, the application of MFCs is still far from successful in real-world large-scale wastewater treatment (Liu and Cheng, 2014). The limitations of MFCs include cost (platinum often used to speed up the reactions at the cathode can be quite expensive), technical issues limiting the upscale, and factors limiting the performance of the anodic (e.g. biological limitation and processes that do not generate current such as biomass production) and cathodic electron transfer (Pham *et al*., 2006; Qu *et al*., 2012). The ideal performance of MFCs also depends on the electrochemical reactions differences occurring between the organic matter at a low potential and the final acceptor such as oxygen at a high potential. (Du *et al*., 2007).

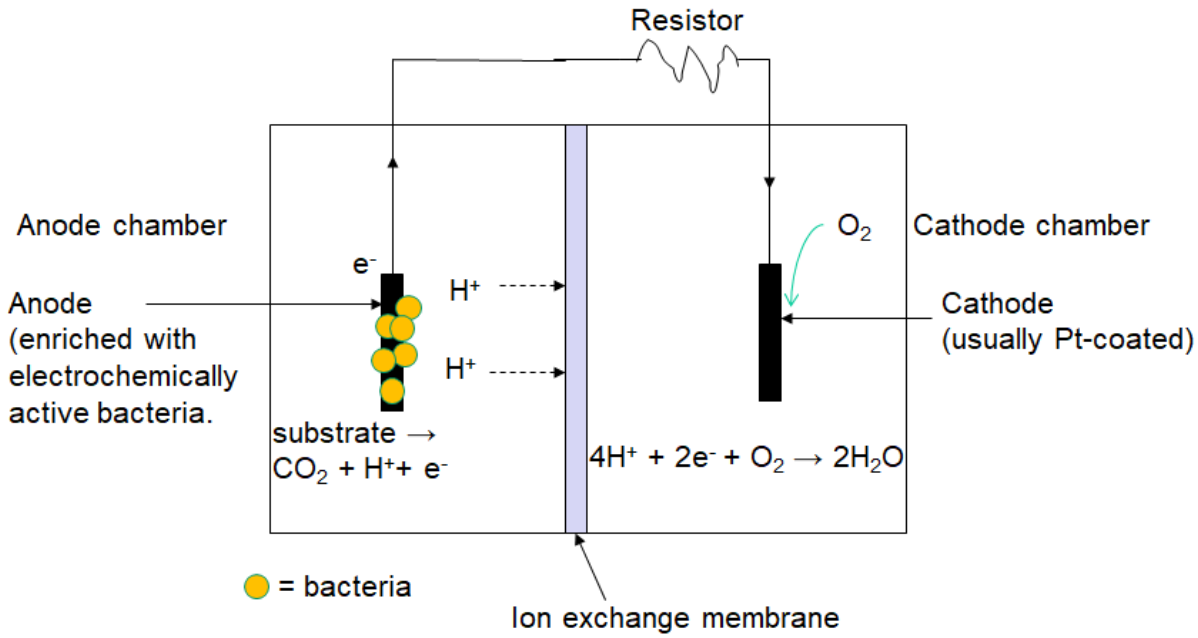

Figure 1.1. Schematic of a microbial fuel cell.

1.6. MFCs Configurations

Configuration of MFCs have been considered as an approach toward MFCs scale up. Although MFCs current and power density are relatively limited compared to chemical fuel cell or batteries, it has been reported that configuration and substrates used in MFCs (either chemically synthesized or the real wastewater) are the key factors involved in power production. Conventional MFCs configurations are operated as single-chambered, dual-chambered, and stacked MFCs (Leech 2015).

Single Chamber MFCs (an example depicted in Figure 1.2) are typical one-compartment MFC without definite cathode compartment. They are economically simple to design and are considered as the easiest to scale-up for practical application. They are constructed by putting a cathode at the open end of a tube, with the anode inside the tube. The cathode electrode has one side in contact with the liquid, while the other side is directly exposed to air for oxygen diffusion into the single chamber. The single chambered MFCs provide advantages over two-chambered MFCs because it is easy to scale-up and requires no liquid aeration, hence, saving energy and money (Leech, 2015; Logan 2008). The first application

employing a novel tubular-type single-chambered air cathode successful removed 80% of the COD and generated 26 mW m^{-2} from wastewater (Logan 2008). Problems with single chambered systems are possibility of oxygen entering the anode side which can lead to substrate loss due aerobic degradation of substrate by the oxygen diffusing through the cathode electrode (Logan *et al*., 2006; Nimje *et al*., 2012).

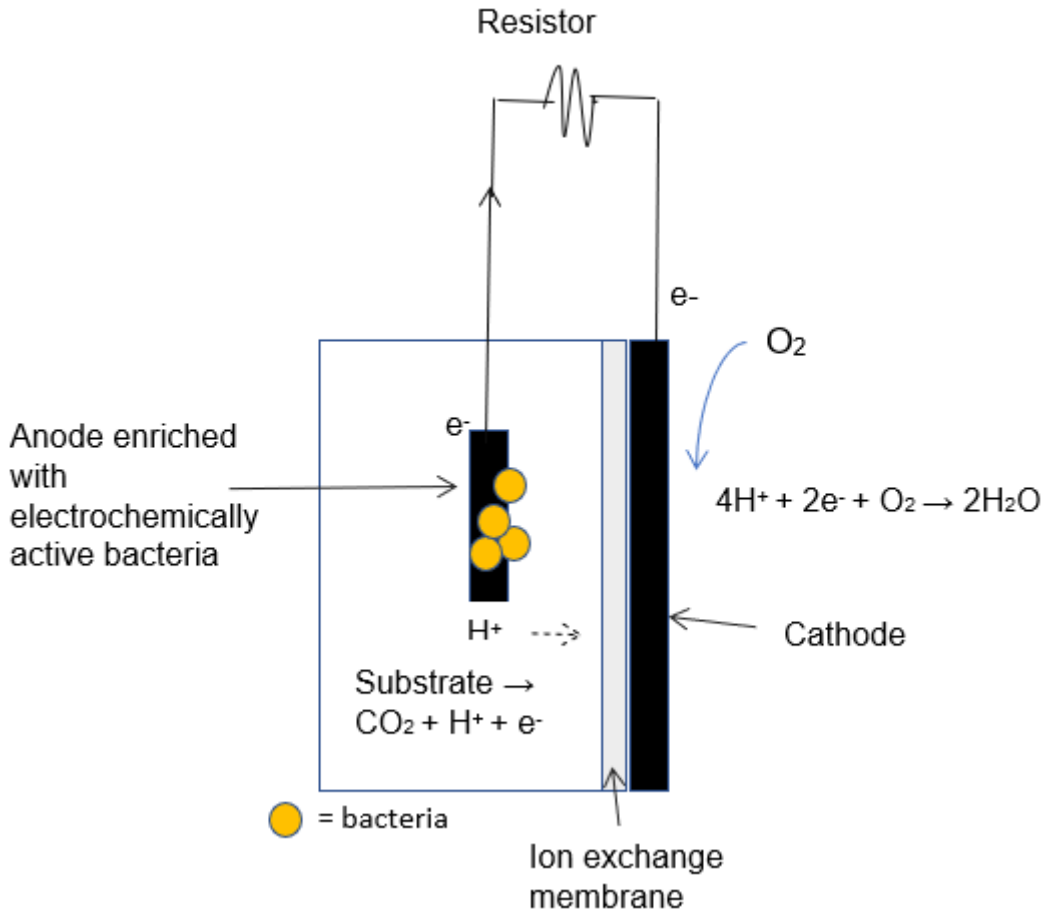

Figure 1.2. Schematic of single chamber MFCs.

Double chamber MFCs traditionally called H-type configuration (example depicted in Figure 1.3) consist of two compartments (the anode and cathode) and are widely used and inexpensive MFC design (Logan *et al*., 2006) .The anode chamber is kept oxygen free, in-order for anaerobic breakdown processes to occur. The two separate compartments are connected by putting a cation exchange membrane (made of Gel Polystyrene cross linked with divinylbenzene) in the separator (Logan *et al*., 2006; Karmakar *et al*., 2010). The cation membrane sometimes called proton exchange membrane has a structure which enables any cation to pass through. The important

properties of a proton exchange membrane (PEM) are high proton conductivity, low electronic conductivity, low fuel and oxidant permeability, and adequate electrochemical and chemical stability i.e. should have adequate good thermal and hydrolytic stability (Kraytsberg and Ein-Eli, 2014). Double chambered MFCs systems are considered acceptable for use in the laboratory for research to examine power production. (Leech 2015).

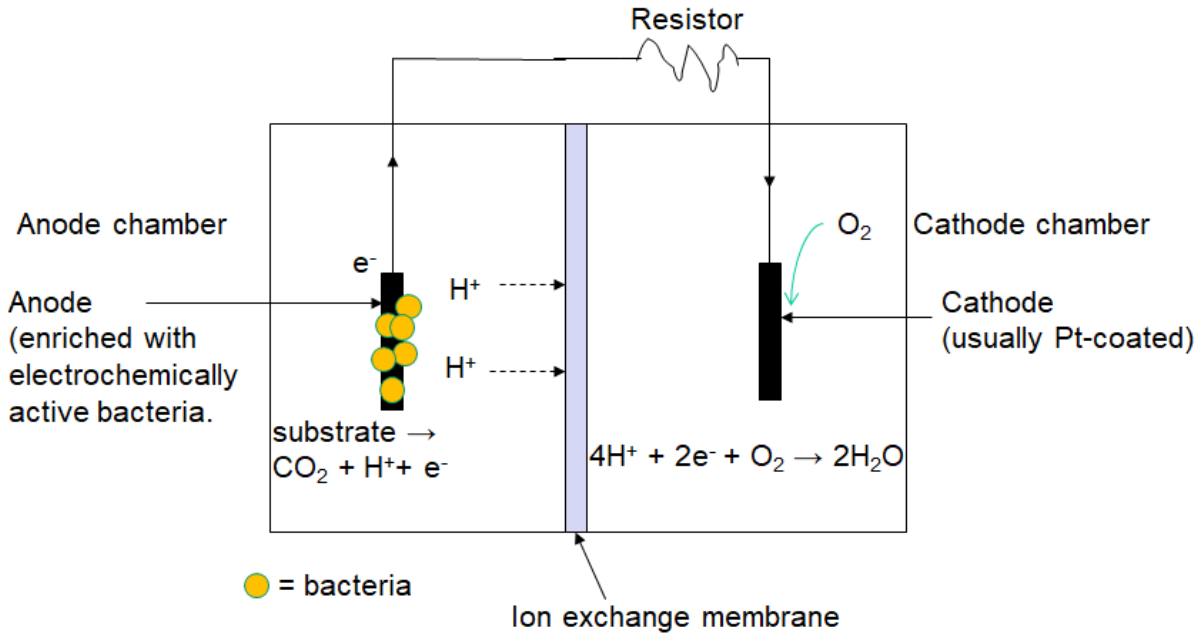

Figure 1.3. A schematic of a double chamber MFC.

Stacked MFCs consist of multiple small sized units MFCs connected together (Figure 1.4) in series or in parallel and could be used to obtain higher voltage and power output (Xinmin *et al*., 2016). Connection of 6 MFC units in series and in parallel have been reported to increase voltage (up to 2.02V) and current up to 255 mA. Although stacked MFCs can potentially generate useful energy, voltage reversal occurs during stack connection as a result of cases such as fuel starvation and insufficient oxygen at the cathode in one or more cells leading to voltage in the cell or cells abruptly reversing polarity. (Oh and Logan, 2007; Watanabe, 2008). Parameters for measuring MFCs performance are shown in Table 1.3.

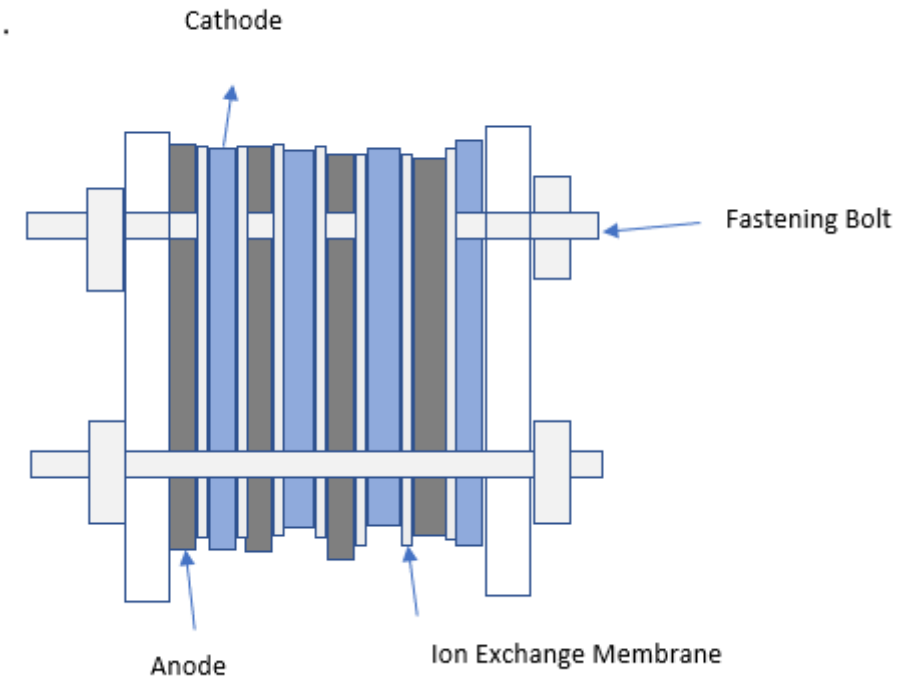

Figure 1.4. Schematic diagram of MFCs stacked in series.

Table 1.3: Parameters for evaluating MFCs Performance (Watanabe, 2008).

Parameter	Unit	Description
Effluent quality treatment efficiency (% COD removal)	% or kg m^{-3}	Concentration of organics (COD) in an effluent discharged from the anode chamber also known as COD removal efficiency estimated by dividing the COD concentration in the effluent by the influent.
Power density (per unit area of electrode)	W m^{-2}	A power output (P_{max}) is the time rate of energy transfer normalised per anode electrode surface area. It is calculated from the power curve (current versus power) and is the maximum power output that can be produced normalised by an electrode surface area.
Current density (per unit area of electrode)	A m^{-2}	This is the amount of current flow normalised per anode electrode surface area. The higher the current density the greater the flux of protons in the system.
Open-Circuit Voltage	V	A voltage measured between the anode and cathode measured in the absence of current. A difference between the total electromotive force (E.M.F; the OCV in the presence of current) and the OCV is regarded as the total potential loss.
Coulombic efficiency (CE)	%	This is the percentage of electrons recovered (coulomb) as current versus the total coulomb contained in a substrate (estimated from the total COD value). These values diminish based on other electron acceptors in the anode chamber competing for electron transfer to the anode.
Internal resistance	Ω	This is used to evaluate the total internal resistance of an MFCs and is obtained from the slope of a polarization curve (see Figure 3.2).

1.7. Fundamentals of voltage generation in MFCs

In MFCs organic substrates or feedstocks such as glucose and acetate are oxidised by microorganisms in the anode compartment to generate electrons and protons. As shown, 24 molecules of electrons are liberated per mole of glucose and 8 molecules are liberated from acetate. These electrons released are transferred to the cathode chamber where they react with chemical species with high redox potential such as oxygen or ferricyanide. Reduction by atmospheric oxygen usually used in MFCs is shown in one of the following reactions below.

$$C_6H_{12}O_6 + 6H_2O \rightarrow 24e^- + 24H^+ + 6CO_2 \ (\Delta G^0 = -1438 \text{ KJ mol-1})$$

$$C_2H_3O_2^- + 2H_2O \rightarrow 8e^- + 7H^+ + 2CO_2 \ (\Delta G^0 = -375 \text{ KJ mol-1})$$

$$O_2 + 4e^- + 4H^+ \rightarrow 2H_2O$$

To speed up the reaction in the cathode, various oxygen reduction catalysts among them platinum have been employed in MFCs. However, due to high cost of platinum, alternative cheaper catalysts have been recommended for MFCs application such as use of biomass-derived carbon material (Chouler *et al*., 2017). Those demonstrated to have low cost, high surface area, high electrical conductivity, high durability and high biocompatibility for enhanced bacteria attachment e.g. using activated carbon and activated carbon nanofibers; some others are inorganic catalysts of transition metals e.g., cobalt tetramethylphenylporphyrin (CoTMPP) and metal phthalocyanine (PC) derivatives (Schaetzle *et al*., 2009; Santoro *et al*., 2015).

For electricity to be generated in MFCs, the overall chemical reaction must be thermodynamically favourable. The Gibbs free energy (dependent on the redox potential differences ΔE of all reactions between electron donor and acceptor) can be used to measure the feasibility of MFCs to produce its maximal energy (Kracke *et al*., 2015). This is calculated as shown in equation 4.

$$\text{Equation 4: } \Delta G_r = \Delta G^0{}_r + RTIn\prod$$

Where ΔG_r is the Gibbs free energy (J) of the reaction at specific conditions; ΔG^0_r is the Gibbs free energy (J) at standard conditions (273.15 K, 1 bar pressure, 1M concentrations of all chemical species), R is the universal gas constant (8.31 J mol^{-1} K^{-1}), T (Kelvins) is the absolute temperature and ∏ is the equilibrium constant.

Gibbs free energy can also be related to the electromotive force (E_{emf}) of the system (equation 5) where E_{emf} is defined as the potential difference between the anode and cathode of an electrochemical cell (equation 5).

$$\textit{Equation 5: } Eemf = \frac{-\Delta G_r}{nF}$$

Where, n is the number of electrons transferred per reaction and F is the Faraday constant (9.65 X 10^4 $Cmol^{-1}$).

Under standard conditions, E^0_{emf} (V) is the EMF at standard conditions; shown in equation 6.

$$\textit{Equation 6: } E^0{}_{emf} = \frac{-\Delta G^0 r}{nF}$$

Therefore, from equation 4 and 5 the overall reaction can be rewritten as equation 7

$$\textit{Equation 7: } E_{emf} = E°_{emf} - (\frac{RT}{nF})\, In(\prod)$$

We get equation 8, when individual anode and cathode half cells of MFCs are considered:

$$\textit{Equation 8: } E_{emf} = E_{cathode} - E_{anode}$$

It is widely accepted that if O_2 is the TEA, the theoretical electromotive force or open circuit potential (OCV) can never exceed 1.1 V. This is illustrated by considering an MFC operating under standard conditions utilizing 5 mM acetate pH 7 as the sole electron donor in the anode and oxygen in the cathode as the sole electron acceptor at atmospheric pressure (pO_2 = 0.2) at pH7 are represented in the following reactions below:

$$2HCO_3^- + 9H^+ + 8e^- \rightarrow CH_3COO^- + 4H_2O;\ E_{anode} = -0.296\ V$$

$$O_2 + 4e^- + 4H^+ \rightarrow 2H_20;\ E_{cathode} = 0.805\ V$$

Therefore, the E_{emf} of the MFC of the reactions is represented below:

= 0.805 V – (-0.296) V = 1.106 V.

In an ideal MFC the open circuit potential would be equal to the thermodynamic E_{emf} value calculated using potentials of anode and cathode half cells. However, the real or actual cell potential is always lower than its ideal value due to various irreversible potential losses (Figure 1.5) known as overpotentials and categorised into four fundamental categories: Activation losses, ohmic losses, bacterial metabolic losses, and concentration losses. Therefore, possible measures to minimize them to achieve the ideal potential by selection of new microbes, substrates, mediators, modification of MFCs design, and a good knowledge of details of the internal losses are needed (Logan *et al.,* 2006; Logan, 2008; Rabaey and Verstraete, 2005).

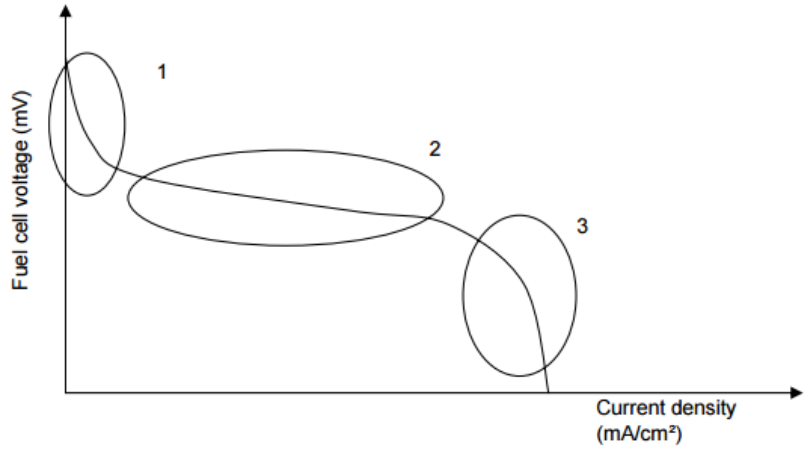

Figure 1.5: Voltage-current density profiles depicting regions of overpotentials or energy losses used for assessing factors affecting MFCs performance: Zone-1- activation losses, zone-2- ohmic losses, zone-3- concentration losses (adapted from Rabaey et al., 2005).

Ohmic losses also known as ohmic polarisation are due to ionic and electronic conduction. These are the resistances to the flow of electrons through the electrodes, external circuit, and inter-connections; it is also the resistance to the flow

of ions through the cation exchange membrane (CEM), anodic and cathodic electrolytes. Primarily, it has been shown that ohmic losses can be reduced by increasing the ionic conductivity of the electrolyte solution tolerable to bacteria and reducing electrode spacing; other ways involve using membranes with lower resistance, and thoroughly checking all contacts (Logan, 2008; Sekar and Ramasamy, 2013).

Activation losses also called activation polarization are related to activation energy needed for an oxidation/reduction reaction to occur. These could be related to compounds undergoing oxidation at the anode where microbially catalysed electron transfer occurs, or at the cathode, where electrons are coupled with a final electron acceptor. Phenomena involving adsorption and desorption of reactant species, nature of the electrode and transfer of electrons all contribute to activation polarization. Increasing the electrode surface area, adding mediator to minimise the energy barrier especially where microbes do not readily release electrons to the anode, increasing operating temperature, and enriching established biofilm on the electrode(s) are general strategies used to circumvent the adverse effect of activation losses on MFCs performance (Ren et al., 2012).

Bacterial metabolic losses are related to metabolic energy gain by bacteria during electron transport through a redox potential gradient. Bacteria transport electrons from a substrate at a low potential (e.g. acetate -0.296 V) through the electron transport chain to the final electron acceptor such as oxygen or nitrate in the cathode. In an MFC, the anode potential determines the energy gain for the bacteria. The higher the difference between the redox potential between the substrate and the anode potential, the higher the possible metabolic energy gain for the bacteria and but this however lowers maximum attainable MFC voltage. Therefore, to maximize the MFC voltage, the potential of the anode must be kept as low (negative) as possible. However, under very low anode potentials, bacteria may seek alternative terminal electron acceptors in the anolyte solution, hence, the electrons may be diverted to fermentative or methanogenic metabolic pathways (Logan et al., 2006; Ren et al., 2012).

Concentration losses also known as concentration polarization occur mainly due to inability to maintain the initial substrate concentration in the bulk fluid perpendicular to the plane of the electrode and thus, limiting current production. This occurs at high current densities due to limited mass transfer of chemicals species by simple diffusion. When sufficient mixing of the surrounding electrolyte is absent, the process of simple diffusion becomes inadequate for efficiently transporting reactants to the electrode and products away from the electrodes due to limited mass transfer of chemicals species by simple diffusion. Hence, this leads to the formation of concentration gradients of reactants and products and is a major contribution to concentration losses in MFCs. Therefore, adequate mixing of the bulk electrolyte is necessary for minimising concentration losses in MFCs. (Logan, 2008; Oliveira et al., 2013).

1.8. Background information on *Shewanella oneidensis*, *Clostridium beijerinckii*, *Geobacter sulfurreducens*, *Saccharomyces cerevisiae* and *Escherichia coli*.

1.8.1. *Shewanella oneidensis.*

S. oneidensis (MR-1) ability to reduce metals such as manganese (Wright *et al*., 2016) and hexavalent chromium makes it an important bacterium considered for bioremediation purposes (Abboud *et al*., 2005). It was firstly isolated in New York State from sediments of Lake Oneida and belongs to the phyllum proteobacteria (Kouzuma *et al*., 2015a; Venkateswaran *et al*., 1999). It mediates transfer of electrons to electrode (Kouzuma *et al*., 2015b). It has ability to adapt between low temperatures to mesophilic condition (Abboud *et al*., 2005). It is a free living facultative anaerobic bacterium with diverse respiratory capabilities (Carpentier *et al*., 2005). During aerobic respiration, MR-1 utilizes oxygen as terminal electron acceptor (Abboud *et al*., 2005). However, in an anaerobic environment MR-1 has capabilities of respiring by utilizing metals such as iron (III) oxides, fumarate and nitrate as alternative terminal electron acceptors (Carpentier *et al*., 2005; Heidelberg *et al*., 2002). It is a mesophilic bacterium and has an optimal growth temperature of 30℃. At room temperature (approximately 22℃) MR-1 has a growth doubling time of about 40 minutes. At 3℃ environmental temperature, it displayed a prolonged lag phase (100 h) with a doubling time of approximately 67 h. It develops pilus-like

structures when transited from 3℃ to 22℃ (Abboud *et al*., 2005). Its genome is made of 4,969,803 base pairs (bp). The protein-encoding reading frame (CDSs) is made up of 4,758CDSs, among which 54.4% were classified as having biological function while 22.2% has no known function matching predicted coding sequences from other organisms (known as conserved hypothetical CDSs) while 23.4% were found unique to *S. oneidensis* (Heidelberg *et al*., 2002).

Genome sequence analyses of *S. oneidensis* have been used to predict the carbon source metabolism by *S. oneidensis* (Heidelberg *et al*., 2002). *S. oneidensis* can utilize many carbon sources and prefers fermentative end products or low-molecular-weight organic acids including acetate, pyruvate, and lactate as carbon sources (Tang *et al*., 2007). It possibly possesses multiple pathways for the utilization of three- carbon carbohydrates, and utilization of amino acids as carbon and energy source is also present (Serres and Riley, 2006). The presence of a complete pentose phosphate pathway and a glycolytic pathway indicates that glucose could potentially be utilized by this organism (Heidelberg *et al*., 2002).

S. oneidensis generates ATP by substrate-level phosphorylation during anaerobic respiration. Examination of central metabolism and flux analyses by *S. oneidensis* indicated that acetate is the major product under anaerobic condition (Hunt *et al*., 2010). The general anaerobic model of *S. oneidensis* (Figure 1.6, Entner-Doudoroff glycolysis pathway) yield 2 molecules of pyruvate. However, under aerobic condition pyruvate facilitates the reduction of NAD^+ to NADH before being completely oxidized to carbon dioxide in the tricarboxylic cycle. Anaerobically, pyruvate oxidation to acetyl CoA yields formate before the pyruvate is converted to acetyl phosphate by the enzyme phosphate acetyltransferase (Pta) and to Acetate by acetate kinase (whose deletion results in the inability of *S. oneidensis* to use glucose or lactate as the electron donor. (AckA). Formate is subsequently oxidized to carbon dioxide (Hunt *et al*., 2010).

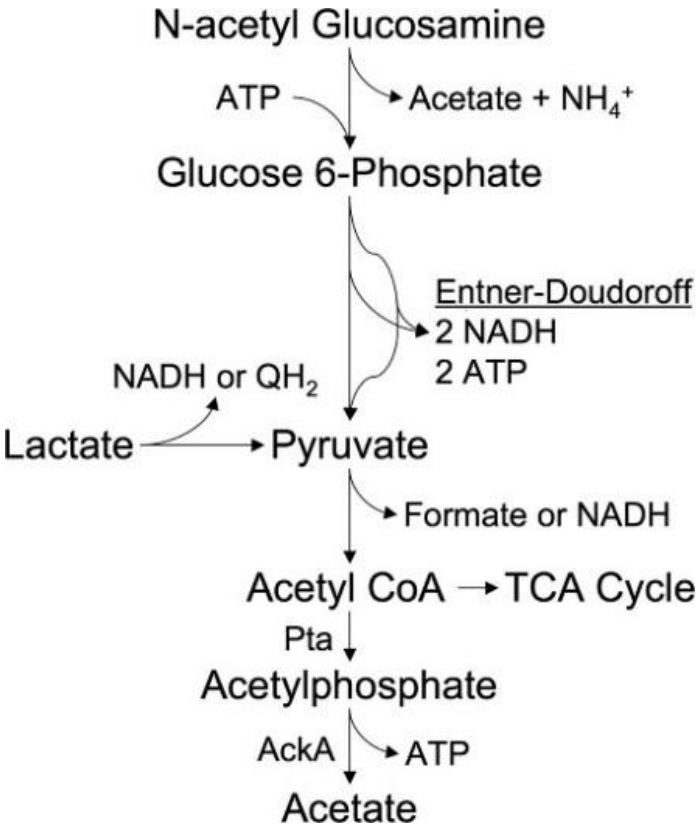

Figure 1.6: The glycolytic pathway of S. oneidensis (adapted from Hunt et al., 2010).

1.8.2. *Clostridium beijerinckii*

Clostridium beijerinckii is a primarily interesting bacterium because of its acetone-butanol-ethanol (ABE) fermentations (Noar *et al*., 2014). It is Gram-positive, saccharolytic, mesophilic, motile, rod shaped with oval sub-terminal spores and an obligately anaerobic solventogenic organism. During the growth cycle, the ABE metabolic pathway generates acidic and butyric acids which are later converted into solvents. Since the late 19th century, biobutanol (C_4H_9OH) and ethanol produced by *C. beijerinckii* have been predicted as a possible replacement for fossil fuels (Sandoval-Espinola *et al*., 2015; Visioli *et al*., 2015). The economic benefit of biobutanol production is however, dependent on the cost of fermentation substrate. Hence, using cheap renewable substrate could enhance ABE fermentation. *C. beijerinckii* was unable to utilize Cellulose abundantly present in agricultural and industrial effluent such as pulp/paper (Gomez-Flores *et al*., 2017). However, when co-cultured with *Clostridium termitidis* enhanced hydrogen production was achieved (Gomez-Flores *et al*., 2017).

1.8.3. *Escherichia coli*

Escherichia coli is an enteric (found in the intestines) rod shaped Gram-negative bacterium having a genome of 4.6 Mb. It is considered as a model organism for molecular genetic studies because it has rapid growth rate, ease of transformability and genetic manipulation. It has ability to grow on chemically defined media. During exponential phase it doubles every 20-30 minutes with overnight culture yielding 1-2 billion cells per millilitre of liquid media (Casali and Preston, 2003).

1.8.4. *Geobacter sulfurreducens*

G. sulfurreducens is a non-fermentative Gram-negative obligate anaerobic bacterium (Kracke *et al*., 2015; Caccavo *et al*., 1994) and require electron acceptors for respiration (Zacharoff *et al*., 2016). It has a rod shape and is commonly found associated with sediments of hydro-carbon contaminated environment (Caccavo *et al*., 1994). *G. sulfurreducens* is considered as a model organism for investigating electroactive bacteria (Kracke *et al*., 2015). It utilizes other organism such as fermentative organism such as *Clostridium pasteurianum* to produce metabolites for its growth. This potential to interact with fermentative organism or a facultative organism such as *E. coli* has been exploited in MFCs to enhance electricity from fermentation products (Moscoviz *et al*., 2017) or to maintain complete anaerobic condition in MFCs (Qu *et al*., 2012). Two commonly utilizable substrates by *G. sulfurreducens* is hydrogen and acetate (Coppi, 2005).

1.8.5. *Saccharomyces cerevisiae*

Saccharomyces cerevisiae is an old word terminology for beer, often called baker's yeast or brewer's yeast (Duina *et al*., 2014). It is a single-celled eukaryote, classified as a fungus or mould. It is non-pathogenic (Ostergaard *et al*., 2000) and one of the few yeast capable of growing either at aerobic or anaerobic conditions (Verduyn *et al*., 1990; Permana *et al*., 2015). It divides through a process called budding, ones every 90 minutes under optimal laboratory conditions. The optimum growth is at ambient temperature around 30^0C (Permana *et al*., 2015). They are recognized by the ability to ferment sugar to ethanol and carbon dioxide. It can ferment other sources of sugar such as grains, malts or other plant materials to produce alcoholic beverages (Duina *et al*., 2014). They are easy to grow in the laboratory and prefer

mono- and disaccharide to other carbon sources. Yeast can grow on acetate, ethanol, and D-glucose (Chu *et al*., 1981). Glucose is the primary source of energy for yeast (Chu *et al*., 1981). When yeast is grown on a mixture of glucose and other carbon sources, it exhibits diauxic growth i.e. glucose is used up first before other source of carbon are utilized. In MFCs application it requires mediators such as thionine and neutral red to transfer electrons (Permana *et al*., 2015). Sugar does not freely permeate through the cellular membrane, hence, facilitated diffusion is used for cellular uptake (Lagunas, 1993). Media glucose yeast extract is the most optimum growth medium for yeast (Fan and Xue, 2016).

1.9. Growth phases in batch cultures.

Batch culture is a closed culture system characterised by limited concentration of nutrient (Stanbury *et al*., 2013). Microbial growth culture can be categorised into four phases after inoculation into a nutrient medium. The first stage called the lag phase considered as a time of adaptation associated with no bacteria growth (Figure 1.7).

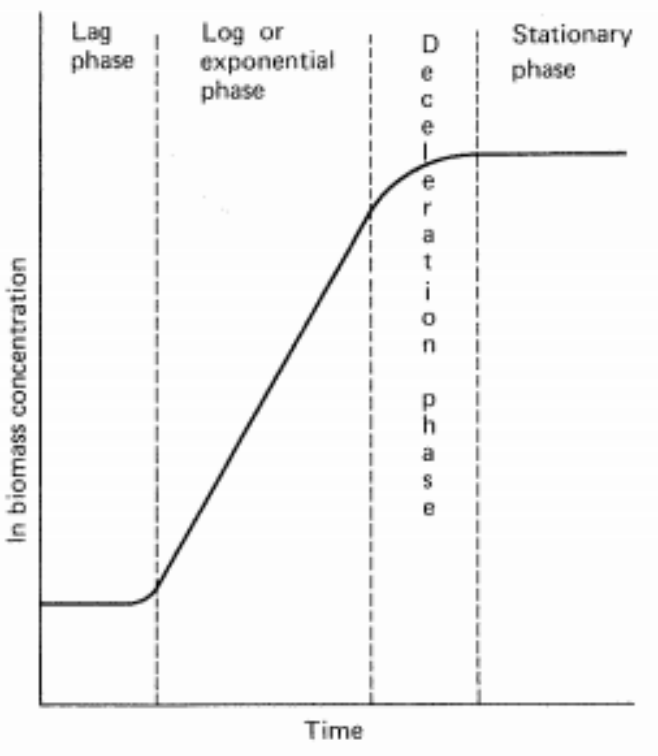

Figure 1.7: Bacteria growth phases (adapted from Stanbury et al., 2013).

The second phase called exponential phase is associated with growth with constant maximum growth rate called specific growth rate (μ) described in equation 9. At a

certain period, growth ceases and the cells enter the so called stationary phase. After a period of time the viable cells decline in a phase called the death phase. Similarly, the growth behaviour of microorganism has been associated with products formed at various stages of growth curve. During the log phase, metabolic products produced are amino acids, nucleotides, proteins, lipids, and carbohydrate which are essential for the growth of the microorganism. These products are referred to as primary products of metabolism and are of considerable economic importance. During the stationary phase, filamentous bacteria and fungi synthesized compounds with no obvious function in cell metabolism but have pharmacological properties such as antimicrobial properties and enzyme inhibitors (Stanbury *et al*., 2013).

$$\text{Equation 9: } \frac{dx}{dt} = \mu x$$

Where x is the concentration of microorganism, t is the time (in hours) and μ is the specific growth rate in hours^{-1}.

1.10. Organisation of Mtr-pathway genes in *S. oneidensis*.

The discovery of bacteria ability to take up DNA dates far back in 1928 when Griffith observed transformation in *Streptococcus pneumonia*. The transforming factor unknown until Avery and Co-workers in 1944 demonstrated the transformation principle of DNA (Lorenz and Wackernagel, 1994). Since the discovery of phage and plasmids as mobile genetic elements, there have been an advancement in molecular biology which has directly contributed enormously in many fields such as biology and biotechnology.

One common mechanism of controlling gene expression among bacteria is the organisation of genes into operons. Operons are strings or clustered genes in a common pathway or mediating a common biological function which are co-transcribed together in a single polycistronic mRNA. An example of these found in *E. coli* is the lactose operon which controls the metabolism of lactose. Linkage of genes in operon results in the production of a single mRNA whose expression level depends on the structure of the operon (Wang *et al*., 2004). In *S. oneidensis* there is evidence that showed that the four genes encoding the protein comprising OM-

cytochrome in the Mtr-pathway (*mtrC, mtrA, mtrB*) are co-transcribed as an operon. The finding is consistent with the biochemical data that *mtr* gene products form a complex (the MtrCAB complex) with 1:1:1 stoichiometry. This could be regulated by changing the promoter strengths or ribosomal strengths of the gene cluster encoding the proteins of the pathway. The transcription start site has been located upstream of *mtrC* (Kouzuma *et al*., 2015a).

1.11. Biocontainment of genetically modified organisms obtained via synthetic biology.

Biosafety has become a code of practice in microbiological and biomedical laboratories (Burnett *et al*., 2009). This discipline involves the handling of hazardous biological materials and containment of infectious microorganism from unintended proliferation in the environment (Burnett *et al*., 2009). This has become so important because the concern of potential escape of synthetically modified organism or their genes away from the realms of intended laboratory habitat into the environment could potentially cause environmental disruption (Wright *et al*., 2013; Simon and Ellington, 2016). The mechanism of escape could be by horizontal gene transfer and mutagenesis (Mandell *et al*., 2015). Effective biocontainment must protect against mutagenic drift, enviromental supplementation and horizontal gene transfer (Mandell *et al*., 2015). Biocontainment strategies reported involve strategies to make the organism inability to synthesize a vital synthetic molecule/compound (auxotroph) by altering the genetic code of synthetic organism to require specific synthetic compounds such as unnatural amino acids for growth and which can be acquired from the growth media or the environment (Torres *et al*., 2016). Another strategy involves engineering synthetic organisms with abilities to utilize exogenously supplied specific molecules/compounds or engineering particular genetic information that represses toxins expression. These are called kill switches (Simon and Ellington, 2016; Torres *et al*., 2016). Therefore, when the organism gets to the environment it expresses the toxin genes, thus killing itself (Simon and Ellington, 2016). However, the standard method of biocontainment implemented for the industrial scale production of microorganism which is the biosafety used in this present study, is by design of physical barriers (Torres *et al*., 2016) for constraining genetic modified organisms within the laboratory (Wright *et al*., 2013).

1.12. Statement of the problem

MFCs are a promising technology for electricity production (Chaturvedi and Verma, 2016; Rahimnejad *et al*., 2015; Gajda *et al*., 2015). However, the problem with MFCs is that they are still technically very far from attaining acceptable levels of power output. Several studies have been done on treatment of various wastewater types including brewery wastewater, azo-dye-containing wastewater, potato starch processing wastewater, phenol-containing wastewater etc., but electrical energy recovery from these systems was very poor, generally less than 150 W/m^3 of the anode volume (Logan, 2008; Oliviera *et al*., 2013). For example, previous attempts at treating phenol in microbial fuel cells (Luo *et al*., 2009; Song *et al*., 2014) produced a power density of only 9.1 W m^{-3}. For cost-effectiveness, the energy recovery needs to reach 1000 W m^{-3}, an energy output that would be competitive with anaerobic digesters. There is need to increase substrate turnover rate which may be dependent on biofilm thickness and/or nature of microorganisms in the anode biofilm, as well as need to increase our understanding of electron transfer processes within and from electrochemically active bacteria to anode electrodes.

1.13. Hypothesis, aims and objectives

Defined co-cultures, exogenous addition of quorum sensing molecules, and genetic engineering of *E. coli* and *S. oneidensis* with the Mtr-pathway can be used to improve electron transfer in microbial fuel cells thereby increasing the energy recovery from waste streams such as from industrial wastewater. Therefore, the overall aims were to enhance the energy (electricity) recovery from MFCs treating industrial wastewater. Hence, to achieve the overall aims, the following objectives were investigated:

(a) To enhance extracellular electron transfer in MFCs via use of co-cultures of exo-electrogens with other fermentative microorganisms as a way of improving substrate turnover rate and hence rate of electrons generated.

(b) To investigate the contribution of direct electron transfer mechanisms to electricity production in MFCs by physically retaining *S. oneidensis* cells close to or away from the anode electrode.

(c) To employ synthetic biology to overexpress the genes: *mtrA* (periplasmic membrane cytochrome), *mtrB* (outer membrane β-barrel protein) and *mtrC* (outer

membrane decaheme cytochrome) in *S. oneidensis* and heterologous expression in *E. coli* for enhanced electron transfer capabilities and hence electricity production.

(d) To enhance biofilm formation in *S. oneidensis*, thought to be directly linked to amount of electricity that can be recovered from MFCs, by exogenous addition of quorum sensing molecules.

Chapter 2

Use of co-cultures as a way of increasing substrate turn-over and hence electricity production in microbial fuel cells.

2.1. Introduction.

An alternative form of energy that can address the growing problem of fossil fuel depletion is bioenergy production. In this context, MFCs hold immense potential as green and carbon-neutral technology that directly converts organic compound into electricity. (Chouler *et al*., 2016). The electricity production in MFCs was shown to increase when glucose was replaced with its metabolic intermediates such as acetate and butyrate (Zhao *et al*., 2017). The electrical current recovery in MFCs might be enhanced by using co-cultures. Cleverly defined co-cultures might show synergistic properties that can be exploited in microbial fuel cells and for bioremediation (Bader *et al*., 2010). For example, by-products of one type of bacterium could be used as a substrate by another bacterium (Figure 2.1) hence, generating more electrons that can be harvested on electrodes. Ren *et al*., (2007) studied a co-culture MFC of *G. sulfurreducens* and *Clostridium cellulolyticum* with cellulose as a substrate and showed that while maintaining similar overall COD removal to a wastewater sludge inoculate MFC, the co-culture had significantly higher coulombic efficiency (39%) compared to 22% for the sludge inoculated MFC. Similar observations were made by Qu *et al*., (2012) who showed that a co-culture of *G. sulfurreducens* and *E. coli* improved electricity production relative to that of a pure culture of *G. sulfurreducens* in an MFC and attributed this to consumption of oxygen leaking into the anode chamber from the cathode chamber.

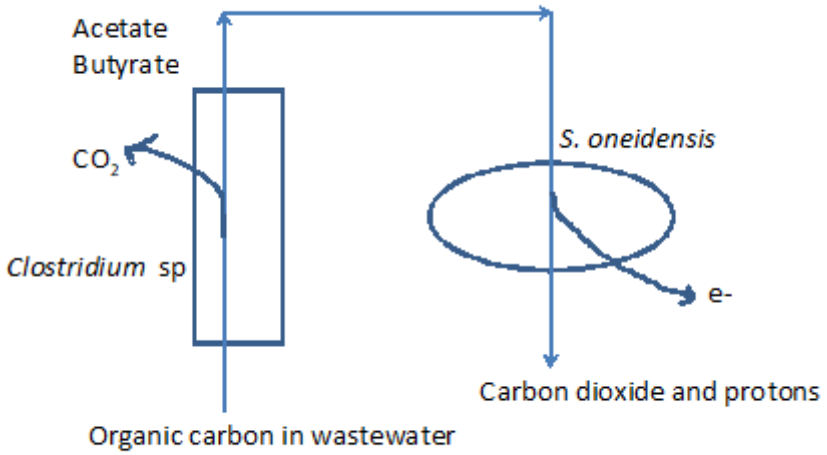

Figure 2.1. Interaction of Clostridium species and S. oneidensis during the mineralisation of organic carbon in the anode section of MFCs.

On the other hand, Bourdakos *et al*., (2013) using the same combination of microorganisms as Qu *et al*., (2012) in a membrane-less MFC found the co-culture produced less power (63 mW m^{-2}) than the pure culture of *G. sulfurreducens* (128 mW m^{-2}) attributing this to production of reduced end-products e.g. succinate thus reducing current production in the co-culture MFCs. Defined co-cultures have been used successfully in aerobic treatment of toxic water used by industry to cool machinery. Van der Gast *et al*., (2003) investigated the effectiveness of a defined consortium (composed of five non-pathogenic microbes) for treating metal working fluids (consisting of a range of oils which are rich in carbon, and water used to cool metal work pieces when they are being machined) and contrasted its performance (COD reduction) with that of undefined inocula from sludge. The defined consortium was 50% more effective than that of the undefined consortium from activated sludge. The performance of the defined consortium was more reproducible as well. However, the limitations of co-culture for real world applications is that it might be prone to virus attack, may not be applicable to widely changing substrate types or concentrations. The key questions about co-culture work in MFCs are: What informs the choice of microorganisms? How are the different nutritional requirements of the microorganisms catered for? How does the community dynamics evolve? What is the mechanism of any observed synergistic/inhibitory/additive effects? Since *S. oneidensis* prefers fermentative end products or low-molecular-weight organic acids

including acetate, pyruvate, and lactate as carbon sources. Hence, we hypothesised that by coculturing *S. oneidensis* with a fermentative organism such as *C. beijerinckii* or *S. cerevisiae* it will lead to more complete turnover of glucose in industrial wastewater initially to other metabolic intermediates such as ethanol, butyric acid, and acetic acid that can then be easily utilized by electrogenic microorganisms for electricity generation in MFCs. Previous study by Bourdakos *et al*., 2014; and Ren *et al*., 2007 have also recommended the use of defined co-culture to reduce the interaction of complex microbial communities so as to easily predict the biochemical pathways for bioelectricity production. Many MFCs have used undefined mixed cultures. Undefined mixed cultures have the following advantages: resistance to phage, robustness to changing substrates, no need for sterilisation, higher current densities than pure cultures. However, they have disadvantages such as batch to batch variability, difficult to probe roles of the different microorganisms involved with respect to electricity production as the microorganisms are unknown or simply too many and poor controllability. Defined cocultures could be used to bioaugment microbial fuel cells which are underperforming and are very useful in probing microbial interactions with a view of understanding the roles played by microorganisms in electricity production. Their limitations are susceptibility to phages and the wastewater stream may need sterilisation.

Therefore, this study, for the first time, investigated the use defined co-cultures of fermentative organism with electrogenic organism for enhancing glucose conversion and phenol remediation to electricity production in MFCs.

2.2. Materials and Methods

2.2.1. Chemicals

QIAquick PCR purification kit was purchased from Qiagen; Pierce ™ BCA Protein Assay Kit, qPCR master mix, Corning Costa 6 well plates SYBRGreen, Ficodox Plus™ mixed COD reagent, ROX dye, and TAE Buffer 50X (Tris-acetate-EDTA) for running and separation buffer were purchased from Thermofisher Scientific. Bacterial Genomic DNA Extraction Kits and Riboflavin were purchased from Sigma Aldrich; PCR Master Mix was purchase from New England Biolab. Ethanol, butyric acid, acetic acid, sulphuric acid and glucose (purity ≥ 96%) were purchased from

Sigma Aldrich (UK). All chemicals were of analytical grade and were used without further purification. The water used for making up solutions was deionised water (DI).

2.2.2. Bacterial strains, maintenance, and culture.

S. oneidensis strain 700550 and *G. sulfurreducens* strain 51573 were purchased from ATCC, *C. beijerinckii* strain 6444 was purchased from the National Collection of Industrial and Marine Bacteria (NCIMB). *S. cerevisiae* was obtained from the culture collection at the University of Westminster, Department of Life Sciences. Cryopreserved stock cultures were maintained at -80℃. Strains were first sub-cultured in Luria-Bertani broth medium (LB medium) containing (per litre) 10 g of tryptone, 5 g of yeast extract and 5 g of NaCl grown at 30^0C for 48 hours; later sub-cultured in minimal salt medium supplemented with 500 mg L^{-1} glucose. MSM contains essential salts, nitrogen, trace elements, phosphorous, vitamins and carbohydrates and supports growth of a large number of microorganisms which is important when growing cells as cocultures. MSM is also useful in increasing the conductivity of the anolyte which is useful for improving MFC performance. This last sub-cultured was used to inoculate the MFCs. Before inoculation of the MFCs, the strains were grown in LB medium supplemented with 15 g L^{-1} agar and plated for enumeration (section 2.2.6.3).

2.2.3. Investigation 1: Experimental design for using pure culture(s) and co-culture(s) of *S. oneidensis* and *C. beijerinckii* for the maximization of glucose and phenol conversion to electricity production.

The experiments involving use of pure cultures and co-cultures are schematically described in Figure 2.2 – 2.4. The first study (Figure 2.2) investigated influence of co-culture and pure cultures of *S. oneidensis* and *C. beijerinckii* on the maximization of conversion of 500 mg L^{-1} glucose-containing synthetic wastewater to power generation in MFCs.

The experiment was run for 15 days due to time limitation and was studied under strictly anaerobic-anodic conditions in two-chambered MFCs as described in section 2.2.4. The inoculum was either *S. oneidensis* or *C. beijerinckii* or both and made up of 10% (v v^{-1}) of the anode working volume (*S. oneidensis* was 3.4 x 10^9 CFU mL^{-1}, while *C. beijerinckii* was 6.8 x 10^9 CFU mL^{-1}). The power vs current density data were collected on the 3rd day when the voltage productions of the tests were in a

pseudo-steady state. The MFCs mixtures were conditioned at the start to pH7 for the co-culture and test cultures by using phosphate buffer without any adjustment throughout the experiment. The controls for the co-culture were MFCs with no microorganisms (C-closed). Another control involved the co-culture under open circuit conditions (C-open). The experiment was replicated three times and the results were expressed as means from the three runs. The temporal dynamics of the strains was also investigated to determine the interactions of the microorganisms (section 2.2.6.4).

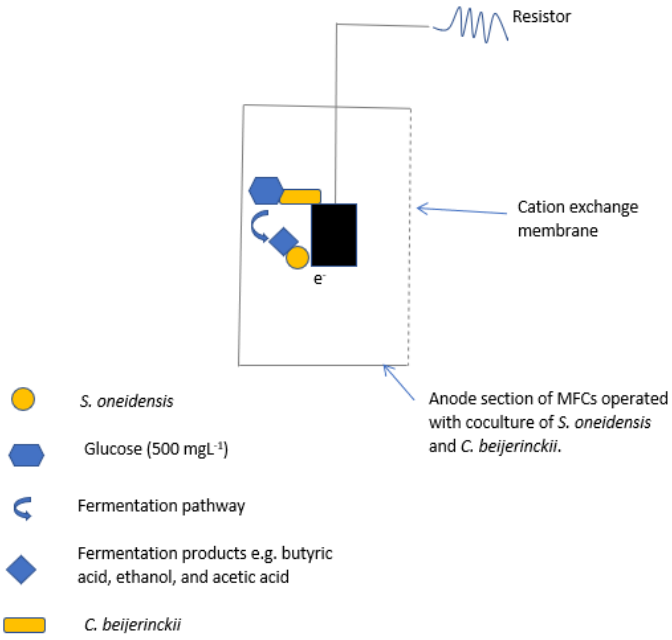

Figure 2.2. Scheme showing the anode chamber only of double-chambered MFCs used for studying co-cultures of S. oneidensis and C. beijerinckii for the maximization of conversion of 500 mg L^{-1} of glucose to electricity production.

The second study (Figure 2.3) investigated the influence of co-cultures and pure cultures of *C. beijerinckii, G. sulfurreducens* and *S. cerevisiae* on the maximization of conversion of 500 mg L^{-1} Glucose-containing synthetic wastewater (MSM) supplemented with modified Luria Bertani broth (10 g L^{-1} Tryptone and 5 g L^{-1} Yeast Extract) to power production in MFCs.

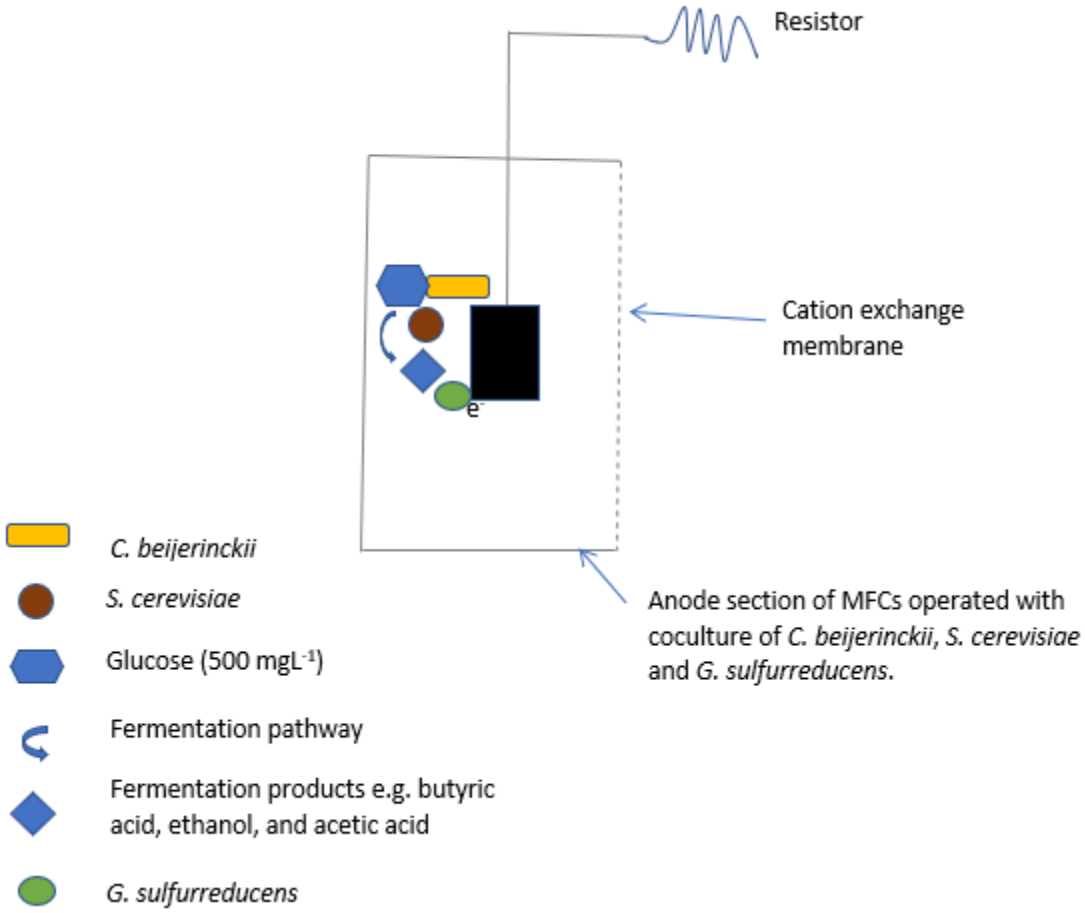

Figure 2.3. Scheme showing the anode section of double-chambered MFCs used for studying co-cultures of S. cerevisiae, C. beijerinckii and G. sulfurreducens for the maximization of conversion of 500 mg L^{-1} of glucose to electricity production.

The experiment was run for 10 days due to time limitation and studied under strictly anaerobic-anodic conditions in two-chambered MFCs as described in section 2.2.4. The inoculum was either *C. beijerinckii* or *G. sulfurreducens* or *S. cerevisiae* or each of their various possible combinations and made up of 10% (v v^{-1}) of the anode working volume (*C. beijerinckii* was 18 x 10^8 CFU, while *G. sulfurreducens* was 10 x10^8 CFU). The control for these studies were MFCs with no microorganism and the experiment was replicated three times and the results were expressed as means from their three runs. The temporal dynamics of the strains were also investigated in-order to determine the interaction of the microorganisms (section 2.2.6.4).

The third study (Figure 2.4) investigated influence of co-cultures and pure cultures of *C. beijerinckii, S. oneidensis*, and *S. cerevisiae* on the maximization of the

remediation of 500 mg L^{-1} phenol-containing synthetic wastewater (MSM) supplemented with modified Luria Bertani broth (10 g L^{-1} Tryptone and 5 g L^{-1} Yeast Extract) for power production.

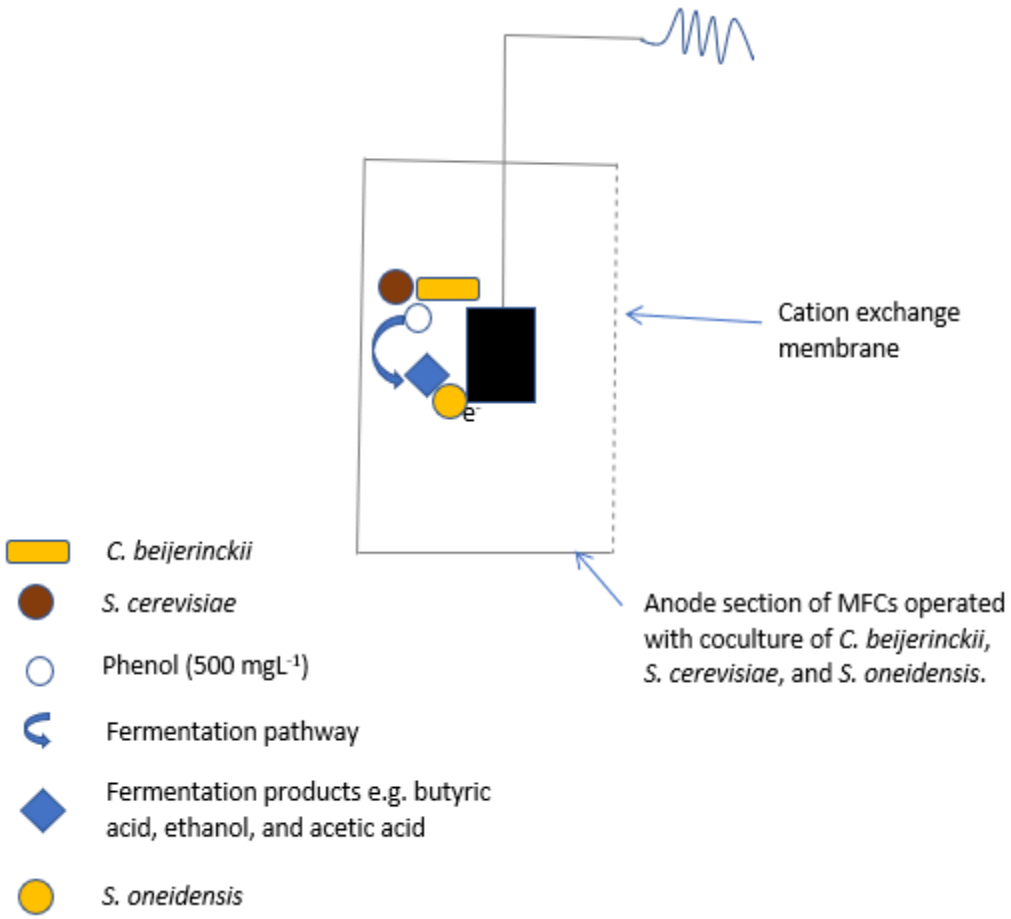

Figure 2.4. Scheme showing the anode section of double-chambered MFCs used for studying co-cultures of S. cerevisiae, C. beijerinckii, and S. oneidensis for the maximization of remediation of 500 mg L^{-1} of phenol and for electricity production.

The experiment was run for 35 days under strictly anaerobic-anodic conditions in two-chambered MFCs as described in section 2.2.4. The inoculum was either *C. beijerinckii* or *S. oneidensis* or *S. cerevisiae* or each of their various possible co-culture combinations and made up of 10% (v v^{-1}) of the anode working volume. The control was MFCs with no microorganisms. The experiment was replicated three times.

The fourth study (Figure 2.5) investigated the influence of exogenous addition of Riboflavin of varying concentrations (20, 30 and 40 µM) on the remediation of 500mg

L^{-1} phenol-containing synthetic wastewater (MSM) supplemented with modified Luria Bertani broth (10 g L^{-1} Tryptone and 5g L^{-1} Yeast Extract) using *S. oneidensis cells*.

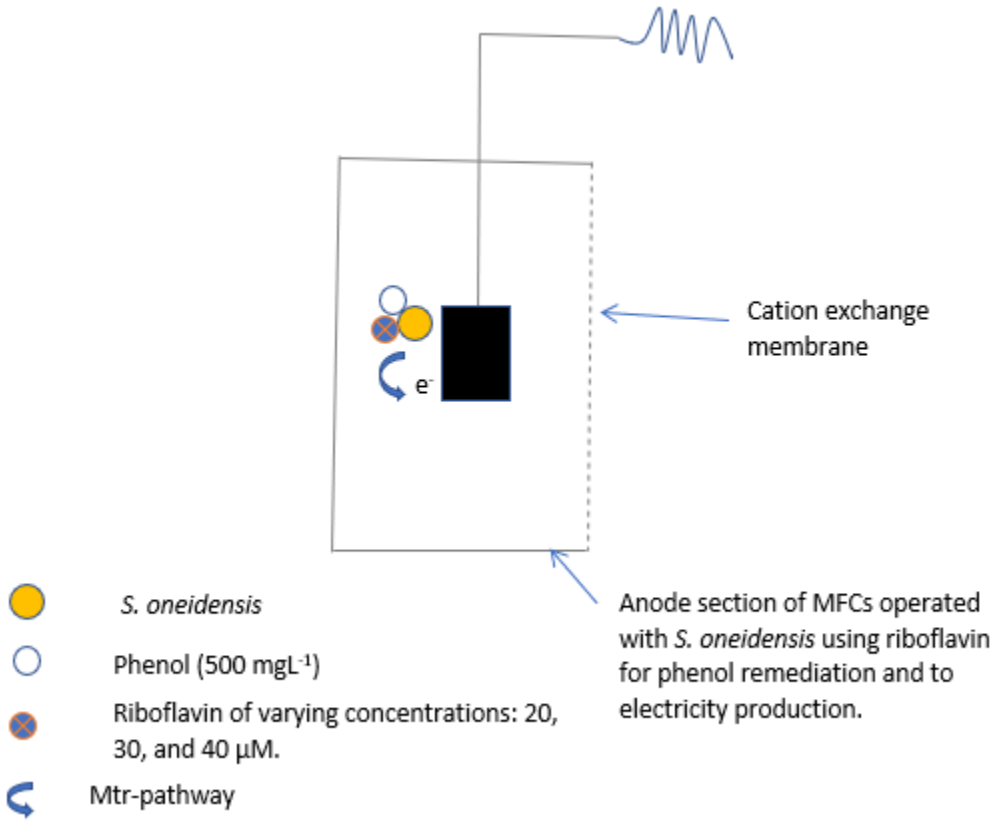

Figure 2.5. Scheme showing the experimental design for double-chambered MFCs studied using pure culture of S. oneidensis for the maximization of remediation of 500 mg L^{-1} of phenol-contaminated wastewater modified at different concentration of Riboflavin: 20, 30, and 40 µM concentrations for electricity production.

The experiment was run for 9 days due to time limitation under strictly anaerobic-anodic conditions in two-chambered MFCs as described in section 2.2.4. The control was MFCs with *S. oneidensis* with no exogenous Riboflavin addition. The experiment was replicated three times.

2.2.4. MFC setup and operation

H-type MFCs (see Figure 2.6) were constructed with two identical Duran bottles and were held together with an external metal clip. The anode and cathode compartments were separated with a cation-exchange membrane (CMI-7000,

membranes International USA). One rubber gaskets were used to ensure a seal at the anode chamber. The electrodes were constructed from carbon cloth.

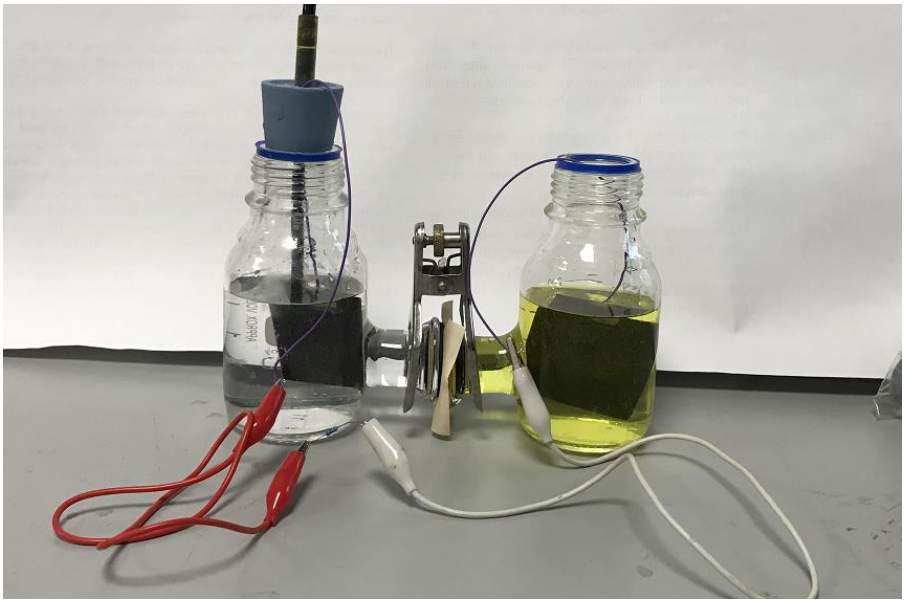

Figure 2.6. A Typical two-chambered MFC used for these investigations.

The co-culture and pure cultures experiments as described in section 2.2.3 were studied using cathodes coated with Pt catalyst layer with a loading rate of 0.5 mg cm^{-2}. Briefly, Pt powder for the cathode was mixed with carbon black powder (Sigma Aldrich, UK) to a concentration of 10% w w^{-1}. The mixture was suspended in 6.67 µLmg^{-1} nafion ionomer solution (sigma Aldrich) for every 1mg of 10% Pt/C and the suspension was applied at a uniform coating on the cathode electrodes using a paint brush. The cathode and the anode electrodes made of carbon cloth had a projected geometric surface area of 25 cm^2.

For all the experiments, electrode connections with insulated copper wires were done using lead solder. An external load of 1000 Ω was utilised for all experiments and the potential difference (voltage) across the resistors were recorded using the Picolog ADC-24 (Pico Technology, U.K.) online data logging system.

For all the experiments, anolyte Minimal Salts Medium (MSM) was used, and it was adapted from Fernando *et al.*, 2012 and modified (see Table 2.1).

Table 2.1. Components of Modified Minimal Salts Medium used in this study.

Component	Concentration (g L^{-1})
NH_4Cl	0.46
KCl	0.225
$MgSO_4.7H_2O$	0.117
NaH_2PO_4	2.5
Na_2HPO_4	4.11
$(NH_4)_2SO_4$	0.225

with addition of 1% trace elements stock solution (see table 2.2 for description of components).

Table 2.2. Components of the trace elements stock solution used in this study.

Component	Concentration (mg L^{-1})
Nitrilotriacetic acid (NTA)	1500
$MnCl_2.4H_2O$	100
$FeSO_4.7H_2O$	300
$CoCl_2.6H_2O$	170
$ZnCl_2$	170
$CuSO_4.5H_2O$	40
$AlK(SO_4)_2.12H_2O$	5
H_2BO_4	5
$NaMoO_4$	90
$NiCl_2$	120
$NaWO_4.2H_2O$	20
$NaSeO_4$	100

and 1% vitamins mix stock solution (see table 2.3 for description of components).

Table 2.3. Components of the vitamin mix stock solution used in this study.

Component	Concentration (mg L^{-1})
P-aminobenzoic acid (PABA)	50
L-ascorbic acid	100
Folic acid	50
Riboflavin	10
Nicotinic acid	100
Pantothenic acid	100
Thiamine hydrochloride	10
Biotin	100

2.2.5. Modification of anolyte minimal salts medium used for the investigation of co-culture studies.

The anolyte MSM was generally supplemented with 500 mg L^{-1} glucose for all the studies except for the phenol remediation studies.

However, the anolyte MSM for the co-cultures studies (schematically demonstrated in Figure 2.3 and Figure 2.4) was further modified with Luria Bertani broth (10 g L^{-1} Tryptone and 5 g L^{-1} Yeast Extract), trace element stock solution (x1) and vitamin stock solution (x1).

The anolyte MSM for co-cultures experiments (schematically demonstrated in Figure 2.4 and 2.5) was further modified with 500 mg L^{-1} phenol and supplemented with modified Luria Bertani broth (10 g L^{-1} Tryptone and 5 g L^{-1} Yeast Extract).

For all the studies (schematically demonstrated in Figure 2.2 – 2.5) the catholyte was 50 mM phosphate buffer solution pH 7 aerated at a rate of 100 mLminute^{-1} using an aquarium pump. During the start-up operation, the anodes were seeded with actively

growing *C. beijerinckii* (6.8 x 10^9 CFU 20 mL^{-1}) or with *S. oneidensis* (3.4 x 10^9 CFU 20 mL^{-1}) for the pure cultures while the co-culture had both pure strains in the inoculum in equal proportion by volume (Figure 2.2). Each anode of the set-ups of co-cultures studies (Figure 2.3) was seeded with the individual of the pure cultures and co-cultures of *S. oneidensis*, *C. beijerinckii*, *S. cerevisae* and *G. sulfurreducens*. Each anode of the set-ups of co-cultures studies (Figure 2.4) was seeded with the individual of the pure cultures and co-cultures of *C. beijerinckii, S. oneidensis* and *S. cerevisae*. The anode of pure culture studies (Figure 2.5) was seeded with *S. oneidensis*.

For all set-ups the volume of inoculum used was 10% v v^{-1} of the total anolyte volume. The anode chambers with the contained mixtures were stripped of dissolved oxygen by sparging nitrogen gas for 5 minutes before setup.

All experiments were replicated three times and studied at 30^0C using a temperature-controlled Stuart 160 incubator (Fisher Scientific, U.K.). Results were expressed as mean of replicates ± standard deviation

For all set-ups, the volume of inoculum used was 10% v v^{-1} of the total anolyte volume. The anode chambers with the contained mixtures were stripped of dissolved oxygen by sparging nitrogen gas for 5 minutes before setup.

2.2.6. Analytical Procedures.

2.2.6.1. COD removal

Chemical oxygen demand removal was determined by using the closed reflux titrimetric method based on the chemical biochemical oxidation of tested samples by refluxing sulphuric acid and potassium dichromate as described in the Environment Agency (UK) standard method 5220D (Westwood, 2007). Briefly, appropriately diluted 1 mL sample (so resulting COD < 500 mgL^{-1}) were used for each determination. The COD removal was calculated by the expression in Equation 10:

Equation 10: $$COD\left(\frac{mg}{L}\right) = (V_b - V_s) \times DF \times M \times 4000$$

where COD (mg L^{-1}) is the amount of dichromate reduced and represents the amount of oxygen consumed per litre of sample. This can be determined by titration with standardized iron (II) ammonium sulphate solution. V_b and V_s are ferrous ammonium sulphate (FAS) titrant volumes for the blank and the sample respectively, DF is the sample dilution factor and M is the molarity of FAS titrant.

The percentage COD removal was calculated by Equation 11:

Equation 11: Percentage removal = $$\frac{(COD_i - COD_t) \times 100}{COD_i}$$

Where COD_i and COD_t are initial and final COD values of samples at the beginning and end of the investigation respectively. The COD is a measure of the total quantity of oxygen required to oxidize all organic materials in a few hours as against BOD that measures only biologically available organic matter, which usually takes place within five days. (Di Lorenzo *et al*., 2009).

2.2.6.2. Detection of degradation products using Gas Chromatography.

Anaerobic degradation products of glucose, namely: ethanol, acetic acid, and butyric acid were identified using gas chromatography (GC) with flame ionisation detection (Appendix 1). Briefly, experimental samples (1.5 mL) for analyses were centrifuged at 15,000 g for 30 minutes using a micro-centrifuge. Thereafter, supernatant from each sample was transferred into a 2 mL vial tube and run on a Varian 3900 GC system. The mobile phase consisted of a carrier gas (helium) with a flow rate of 2 mL min^{-1}; injector temperature was 260℃. The oven was initially set at 35℃ for 5 minutes and then ramped up to 170℃ for the subsequent 10 minutes. Detector temperature was 250℃. The presence of degradation metabolites ethanol, acetic acid, and butyric acid was confirmed using the retention time of the respective standard compounds.

2.2.6.3. Quantification of *C. beijerinckii, S. oneidensis* and *G. sulfurreducens* cells in the sub-cultured medium.

The concentration of cells in the volume of sub-cultured medium, used for inoculation of the experimental systems, at the start of the co-culture investigation was determined by serially diluting the unknown concentration 10^6 times. Cells for each

strain were aseptically plated in triplicate on LB agar medium and thereafter, incubated at 30℃ for *S. oneidensis* and *G. sulfurreducens,* 37℃ for *C. beijerinckii* for 24 hours to determine colony forming units (CFU) present in the undiluted samples used for inoculation of the plates. The number of CFUs in the undiluted samples was determined by the expression in Equation 12.

$$\textit{Equation 12: } CFU(per\ mL) = \frac{N_c * D}{V}$$

where N_c is the average number of colonies counted on triplicate plates, D is the dilution factor (10^6) and V is the volume (mL) of aliquot of diluted cells added to each plate.

2.2.6.4. Relative abundance test by Real-Time PCR analysis.

Real time PCR is used to monitor the amplification of targeted DNA molecule during amplification. Therefore, real time PCR was used to target the DNA of the microorganisms in the co-culture experiment for the analysis of their relative abundance. This method was used because of the morphology similarities between *S. oneidensis, C. beijerinckii* and *G. sulfurreducens* – shape, size, and appearance on cultured plates. DNA was extracted from the known concentration sample of each of the bacteria (described in Figure 2.2 and *G. sulfurreducens* in Figure 2.3) using Bacterial Genomic DNA kits (Sigma Gen Elute^{TM}). The DNA extracts purity were checked using the A_{260}/A_{280} ratio (~1.8) to minimise PCR inhibition (by protein, RNA and reagent contaminations) and concentration determined using Nanodrop spectrophotometer. These were amplified using Primers that are specific for proteobacteria and firmicutes that specifically target the 16S rRNA genes (Fierer *et al*., 2005). The forward primer used for *C. beijerinckii* was Lgc353 with sequences: GCA GTA GGG AAT CTT CCG and its corresponding reverse primer was Eub518: ATT ACC GCG GCT GCT GG. The primer used for *S. oneidensis* or *G. sulfurreducens* was Eub 338, ACT CCT ACG GGA GGC AGC AG, and its corresponding reverse primer: Alf685, TCT ACG RAT TTC ACC YCT AC. The PCR reaction mixture (50 µL) contained the following assay mixture: 25 µL of X2 PCR master mix (New England Biolabs), 22 µL Nuclease free water, 1 µL each of Forward and Reverse primers, and 1µL of template whole genomic DNA. The PCR (Bio-Rad PCR system MJ-Mini (UK) was performed under the following conditions: initial denaturation at 95^0C for 4 minutes, followed by 30 cycles of 95^0C for 1

minutes, 0.5 minutes at the annealing temperature of 60^0C, and 72^0C for 1 minutes for the extension. Each of the samples was three replicates reaction and with appropriate set of standards. The amplified DNAs were checked on agarose gel electrophoresis. The DNA bands formed were recovered using a Genomic DNA Purification kit. The purified DNAs were diluted tenfold serially in triplicate alongside with the DNA of the tests samples. The real-time amplification of each of the standards was undertaken to determine the efficiency of the real time-PCR system (Figure 2.11). The DNA extracted from the tests samples (A_{260}/A_{280} ratio ~1.8) were run alongside the known standard DNA on qPCR. The qPCR reaction assay was conducted in strip tubes of 100 µL volume capacity each. Each 25 µL reaction contained the following assay mixture: 12.5 µL of Absolute qPCR Master Mix (ABgene), 1.25 µL of each primer (10 µM; Invitrogen), 25µL bovine serum albumin (10 mg ml^{-1}; Promega), 1.0 µL SYBRGreen dye (16000- fold dilution in H_2O), ROX dye (80-fold dilution in H_2O; ABgene) for normalization of fluorescence intensity of qPCR reporter dye, 0.5 µL nuclease free water and 5 µL of purified DNA from the samples. Real Time-PCR amplification was conducted using a Quiagen Rotor-Gene system under the following conditions: initial denaturation condition was 4 min at 95^0C, followed by 40 cycles of 95^0C for 1 min, annealing temperature at 60^0C for 0.5 min, and elongation temperature at 72^0C for 1 min according to the method of Fierer *et al*., 2005. Samples were run in triplicate, and results were quoted as cycle time vs log concentration of purified DNA. The fluorescence at a specific geometry phase was picked for all the runs and were normalised with the known starting DNA concentrations of each bacterium. The limitation about this method is that both dead and live cell's DNA will be enumerated.

2.2.6.5. Quantitation of phenolic compound using spectrophotometric method.

Quantification of residual phenol is important in-order to determine the extent of degradation of the phenol. Phenolic materials react with 4-amino antipyrine in the presence of potassium ferricyanide at a pH of 10 to form a stable reddish-brown coloured antipyrine dye. The amount of colour produced is a function of the concentration of phenolic compound. Briefly, 2 mL of Amino-antipyrine (AAP) solution (containing 2 g of 4-AAP diluted to 100 mL) and 2 mL of Potassium ferricyanide ($K_3Fe(CN)_6$) solution (containing 8 g of $K_3Fe(CN)_6$ diluted to 100 mL) were added to each set of 100 mL phenol standards 0, 50, 100, 200, 500 µg L^{-1} and

test samples adjusted to pH10 ± 2 using 2 mL aliquot buffer (containing 16.9 NH_4Cl in 143 mL concentrated NH_4OH diluted to 250 mL with distilled water), vortexed and absorbance at 510 nm taken after 15 minutes.

2.2.6.6. Quantification of *S. oneidensis* biofilm using confocal microscope.

Confocal microscope is a valuable tool for studying biofilm matrix as it allows real-time visualisation of fully hydrated specimens. It provides three-dimensional optical sectioning of fluorescently labelled sample (Schlafer and Meyer, 2017). Hence, SYPRO Ruby stain was used for the confocal microscope examination of *C. beijerinckii,* and *S. oneidensis* biofilm formation because it labels most classes of proteins including glycoproteins, phosphoproteins, lipoproteins, calcium binding protein and fibrillar protein and other proteins that are difficult to stain. This stain has been tested to stain matrix of *Pseudomonas aeruginosa* and some strain of *E. coli.* In-order to examine and quantify biofilm formation by *S. oneidensis* and *C. beijerinckii*, the cells were cultured separately on cover slips in "Corning Costa 6 Well Plates" for 2 days. The cover slips were carefully rinsed in 100 mM phosphate buffer pH 7 and thereafter placed in a fresh Corning Costa 6 well plates. SYPRO Ruby stain 200 µL was added to each of the biofilm samples on the slips without offsetting the biofilm. The samples were incubated for 30 minutes protected from light. After incubation, filter sterilized water was used to remove excess stain and the stained samples were placed into a fresh Corning Costa 6 well plates covered with 3 ml of filter sterilized water and observed under a confocal microscope.

2.2.6.7. Electrochemical monitoring.

Polarization curves for measuring power density vs current density plots were constructed using a range of external resistances from 10 Ω to 1 MΩ. The external circuit of the MFC system for each test was opened to connect various external resistances on the fourth day when the system exhibited a stable voltage across the initial 1000 Ω external resistor. The current flowing through each external load was calculated using Ohm's law (equation 13).

$$\textit{Equation 13: } I = \frac{E}{R}$$

Where E is the potential across the resistor (mV), I is the current flowing through the load (mA) and R is the external resistance (Ω).

The power generated (Equation 14) was calculated with the following expression (Fernando *et al.*, 2012).

*Equation 14: P = E*I*

Where P is the power produced (mW), E is the potential difference between anode and cathode (mV) and I is the current generated (A).

The power density and current density values were calculated by normalising power and current values to the geometric surface area of the anodic electrode (25 cm^2).

Coulombic efficiency (CE) was calculated by integrating the measured current over time based on the observed COD removal (Equation 15) by using the criteria outlined in Zhao, *et al.* 2009. CE is a measure (%) of the amount of electrons generated via substrate oxidation that are reflected as current compared to the theoretical number of electrons expected calculated using Faraday's second law of electrolysis.

Equation 15: $$CE\ (\%) = \frac{\left(M \int_0^t I\ dt\right)}{\Delta COD * FbV\ anode} \times 100$$

2.2.6.8. Statistical analysis

All experimental data indicated on the graphs are the means of triplicate experiments unless otherwise stated and the error bars represent the standard deviation of the mean (SD). Statistical analysis of data was conducted by one-way analysis of variance (ANOVA) using Prism GraphPad 5.0.

2.3. Results

2.3.1. Summary of results

The application of different co-cultures were investigated for improving MFCs performance on electricity production and wastewater remediation. The hypothesis

was that cleverly defined co-cultures could improve substrate turnover rate and hence improve electricity production. The first study involved studying a co-culture of *C. beijerinckii* and *S. oneidensis* (Table 2.4). The outcome was 87 mW m^{-2} of maximum power produced and improved substrate turnover rate to 67 ± 3% which was three-fold more than the substrate turnover rate of 20 ± 4% by *S. oneidensis* alone on 15 days of the study.

Table 2.4. Summary of results by utilization of co-cultures and pure cultures of S. oneidensis and C. beijerinckii on the substrate removal and power generation from 500 mg L^{-1} glucose.

		Co-culture:	
	S. oneidensis	*S. oneidensis* with *C. beijerinckii*	*C. beijerinckii*
Power Production (mW m^{-2})	48 ± 2	87 ± 4	60 ± 3
% COD Reduction	20 ± 4	67 ± 3	70 ± 6

The second study involved studying co-cultures of *G. sulfurreducens, C. beijerinckii* and *S. cerevisiae* (Table 2.5). The co-culture of all three strains produced the maximum power output of 80 ± 2 mW m^{-2} but with 41% substrate turnover at 15 days. The study utilized synthetic wastewater containing 500 mg L^{-1} utilized modified with Luria Bertani medium containing (g/L) tryptone – 10.0 and yeast extract – 5.0. The co-culture of all three strains produced the maximum power output of 80 ± 2 mW m^{-2} but with 41% substrate turnover at 15 days.

Table 2.5. Summary of results by utilization of co-cultures and pure cultures of C. beijerinckii, S. cerevisiae and G. sulfurreducens on substrate removal and power generation from 500 mg L^{-1} glucose.

		Co-culture:		
	C. beijerinckii	*C. beijerinckii*, *S. cerevisiae* and *G. sulfurreducens*	*G. sulfurreducens*	*S. cerevisiae*
Power Production (mWm^{-2})	74 ± 4	80 ± 2	23 ± 2	35 ± 3
% COD Reduction	40 ± 3	41 ± 3	32 ± 4	35 ± 5

The co-culture of all three strains produced the maximum power output of 80 ± 2 mW m^{-2} but with 41% substrate turnover at 15 days. The study utilized synthetic wastewater containing 500mgL^{-1} utilized modified with Luria Bertani medium containing (g/L) tryptone – 10.0 and yeast extract – 5.0.

The third study (summarised in Table 2.6) involved using a co-culture of *S. oneidensis, C. beijerinckii* and *S. cerevisiae* for remediation of wastewater containing 500 mg L^{-1} of phenol. The best outcome was from *C. beijerinckii alone* which reduced the phenol concentration to 5.2 mg ml^{-1} (99% reduction); *S. oneidensis* phenol concentration reduction was to 25 mg ml^{-1} (95% reduction) at 35 days of the study. With regards to power production, *S. oneidensis* produced 4.6 ± 0.02 mW m^{-2} while *C. beijerinckii* produced 2.7 ± 0.03 mW m^{-2} on the third day of the study.

Table 2.6. Summary of results by utilization of co-cultures and pure cultures of S. oneidensis, S. cerevisiae and C. beijerinckii on substrate removal and power generation from 500 mg L^{-1} phenol.

		Co-culture:		
	S. oneidensis	***S. oneidensis*, *S. cerevisiae* and *C. beijerinckii***	***C. beijerinckii***	***S. cerevisiae***
Power Production (mW m^{-2})	4.6 ± 0.02	2.13 ± 0.01	2.7 ± 0.03	1.85
% Phenol Reduction	95	98	99	97

Another study (summarised in Table 2.7) investigated the use of pure cultures of *S. oneidensis* with exogenous addition of varying concentrations of Riboflavin (20, 30, 40 µM). The addition of 30 µM improved maximum power production from 7.3 mW m^{-2} (control) to 54 mW m^{-2} on day 2 of the experiment while phenol concentration was reduced by 90% (30 µM Riboflavin addition) compared to 80% (control) on day 8 of the experiment.

Table 2.7. Summary of results by investigating the effect of Riboflavin on pure cultures of S. oneidensis for substrate removal and power generation from 500 mg L^{-1} phenol.

	S. oneidensis	*S. oneidensis* (20 µM)	*S. oneidensis* (30 µM)	*S. oneidensis* (40 µM)
Power Production (mW m^{-2})	7.4 ± 0.04	29 ± 1	48 ± 2	54 ± 3
% Phenol Reduction	80	75.2	90	89.2

2.3.2. Results and discussion for study involving co-culture of *C. beijerinckii* and *S. oneidensis*.

2.3.2.1. Voltage-time profiles and polarization curves of co-culture work involving C. beijerinckii and S. oneidensis.

The test of using *C. beijerinckii* and *S. oneidensis* as pure cultures and as co-culture for the maximization of 500 mg L^{-1} on voltage-time profile, polarisation, and power density curves are shown in Figures 2.6 and 2.7. What is striking in Figure 2.7 is the similarities in the voltage time profile between the co-culture and the individual strains. The open circuit control gave the maximum potential difference as expected, as under open circuit conditions there is infinite resistance meaning no electron flow and hence no electrochemical losses.

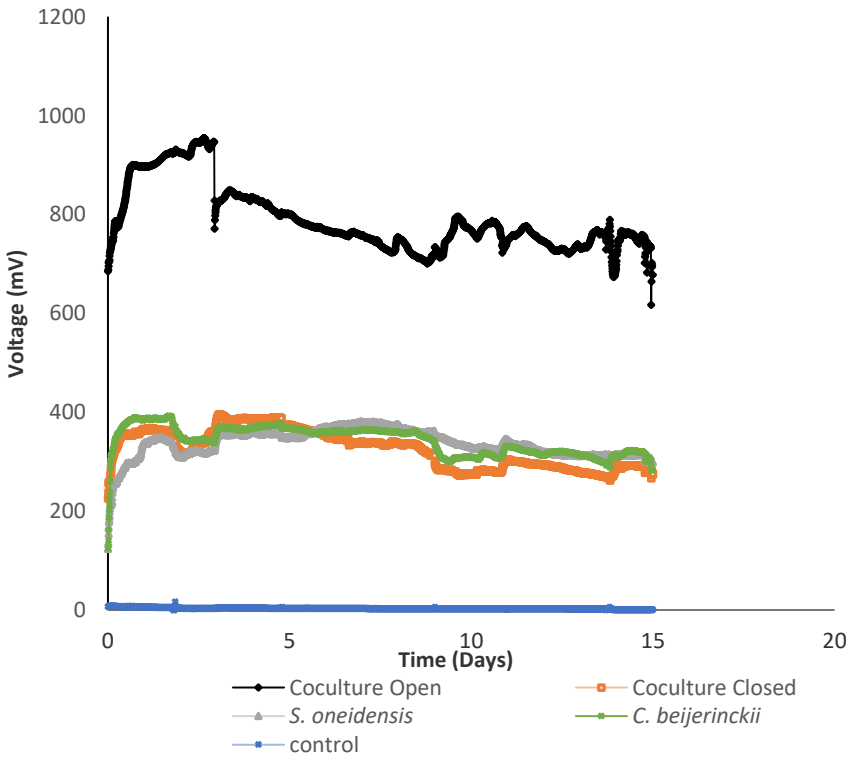

Figure 2.7. Voltage time profiles for the co-culture experiment investigated using 1000Ω resistor for 14.5 days. Co-culture open result represents the ideal behaviour of the co-culture while the co-culture closed represents the real potential of the tested co-culture which behave similarly with other tested studies except the control with no microorganism.

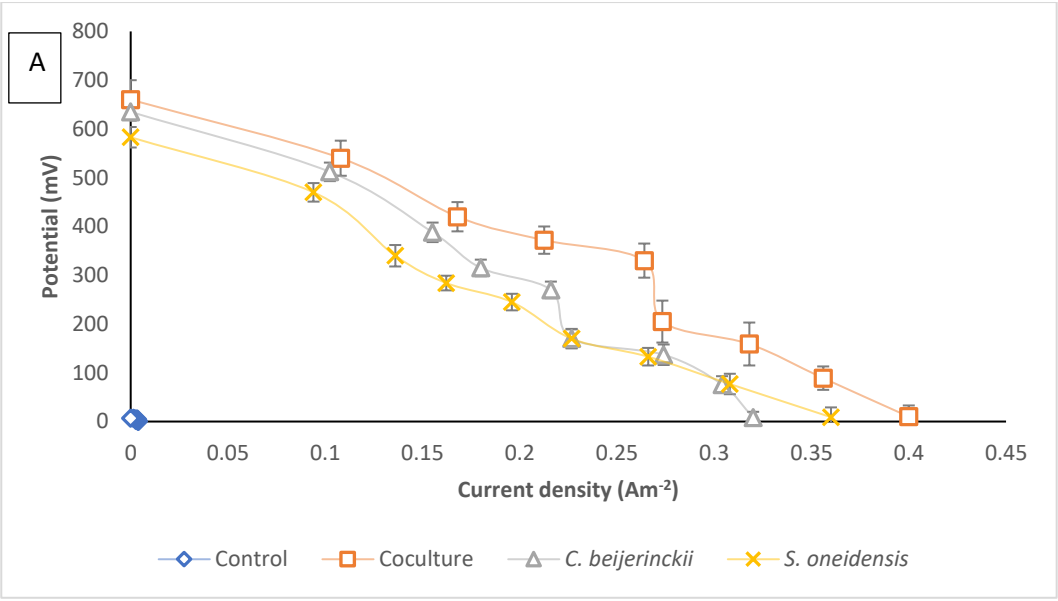

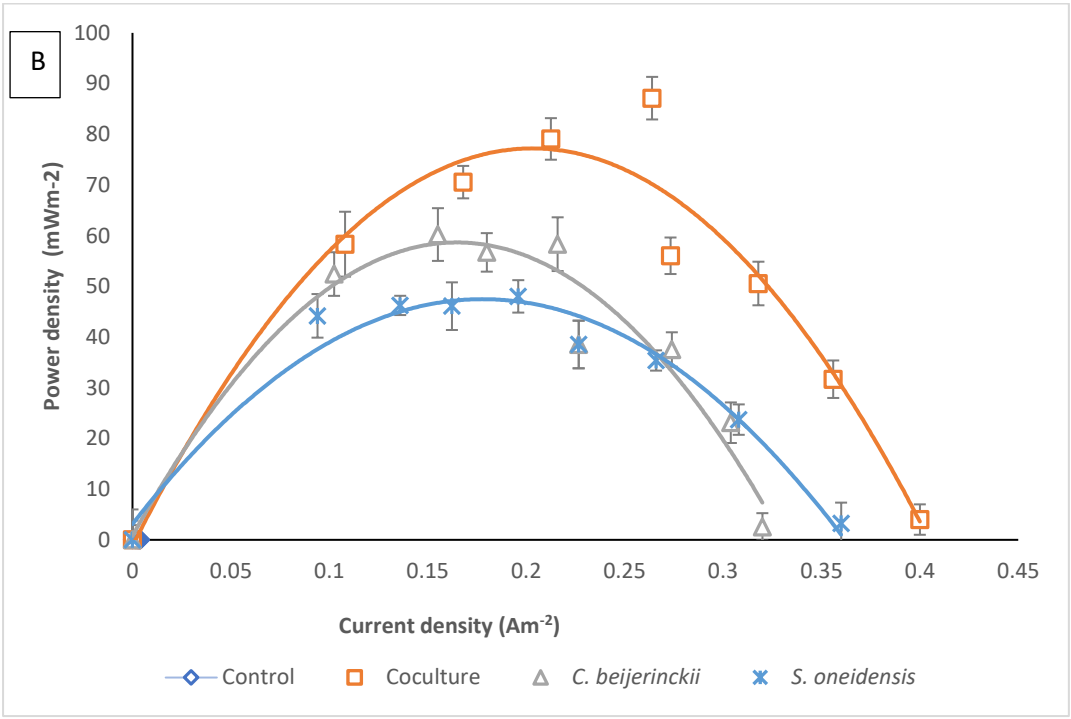

Figure 2.8. (A) Polarization curves (showing how voltage can be maintained as a function of current production) for the co-culture experiment involving C. beijerinckii and S. oneidensis investigated with wastewater containing 500 mg L^{-1} glucose; (B) Comparison of MFC performance (power density vs current density) obtained by varying the external circuit resistance (10Ω-50,000Ω). Control curves are too small to be seen on the graphs. The error bars represent standard deviation of the mean (n=3).

Power density measurements (Figure 2.8B), showed that the maximum power density that stands out was recorded by the co-culture and gave 87±4 mW m^{-2}; the pure culture of *C. beijerinckii* gave 60±3 mW m^{-2} while *S. oneidensis* gave 48±2 mW m^{-2}.

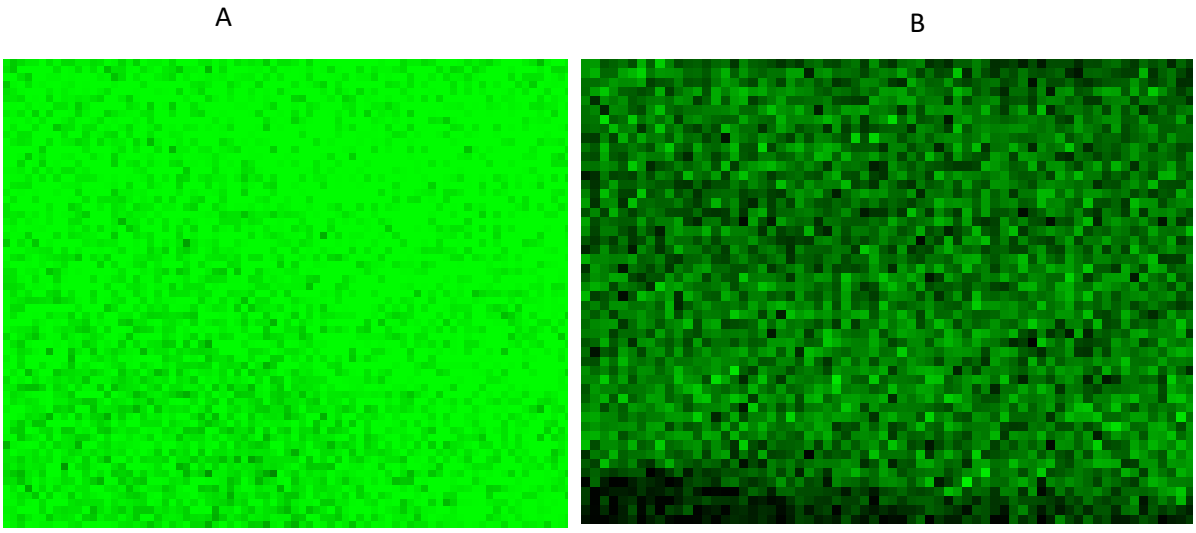

Figure 2.9. Confocal microscope analysis of C. beijerinckii biofilm (A) showing more denser cells in the background than S. oneidensis biofilm (B) grown under non-MFCs condition, on microscope slide in six well plates using MSM medium containing 500 mg L^{-1} glucose grown at 30℃ for 2 days under complete anaerobic conditions.

2.3.2.2. COD degradation and coulombic efficiency (CE).

Table 2.8 gives a comparison of substrate degradation (as glucose and as COD) and CE on day 15 of the investigation. What can be seen clearly is the high COD reduction (67%) by C-closed compared to 20% by *S. oneidensis* but was similar ($p>0.05$) to the COD reduction by *C. beijerinckii*. However, in comparison to *C. beijerinckii* the CE for C-closed was much higher (10%) compared to 0.7% for *C. beijerinckii*. The degradation of glucose was similar in all test runs. The highest CE (35%) was obtained from *S. oneidensis* although it gave a low substrate degradation of 20%.

Table 2.8: Comparison of substrate degradation and electron recovery at 360 h of the investigation. Values are means of triplicate experiments ± standard deviation. NA = not applicable.

	S. oneidensis	***C. beijerinckii***	**C-closed**	**C-open**
COD degradation (%)	20 ± 4	70 ± 6	67 ± 3	20 ± 5
Glucose degradation (%)	86 ± 6	79 ± 5	82 ± 4	86 ± 4
Coulombic efficiency (%)	35 ± 1	0.7 ± 0.5	10 ± 2	NA

2.3.2.3. Relative abundance of S. oneidensis and C. beijerinckii in C-closed and C-open systems.

The relative abundance (%) of microorganisms calculated as the ratio between the measured copy numbers for each group-specific quantitative PCR (q-PCR) assay to all the bacteria in the co-culture assay and is presented in Figure 2.10. The result of efficiency of the real-time PCR for specific amplification of target genes is presented in Figure 2.11. What is interesting in the Figure 2.10 is that there is no significant difference in the relative abundance at the end of investigation between the two strains co-cultured under closed circuit condition (*S. oneidensis* approximately recorded 50.1 ± 1% while *C. beijerinckii* approximately was 49.9 ± 2%). However, in comparison to the starting inoculum, the relative abundance of *S. oneidensis* was markedly increased by 23% while *C. beijerinckii* was reduced by 17.1%. In the open circuit MFC (MFC left disconnected from 1000Ω resistor), the relative abundance of *S. oneidensis* was 36±1% while *C. beijerinckii* was 64±3% at the end of the investigation. However, in comparison to the starting inoculum, there was little significant changes on the relative abundance of *S. oneidensis* and was increased by 3% while *C. beijerinckii* was decreased by 3%.

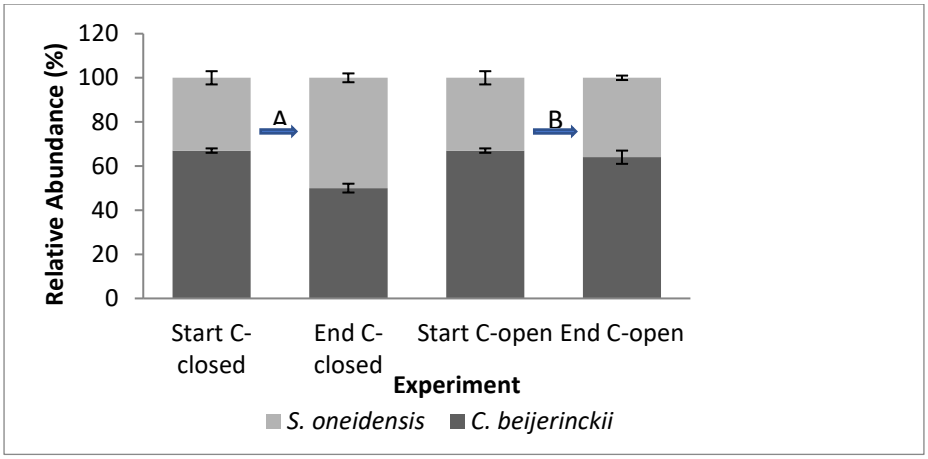

Figure 2.10. Relative abundance analyses at the start and end of the investigation for the two target organisms in the co-culture experiment. (A) Comparison of relative abundance tests at start and end for the C-closed MFCs. (B) Comparison of relative abundance tests at start and end for the C-open MFCs. The bars represent standard deviation of the mean (n=3).

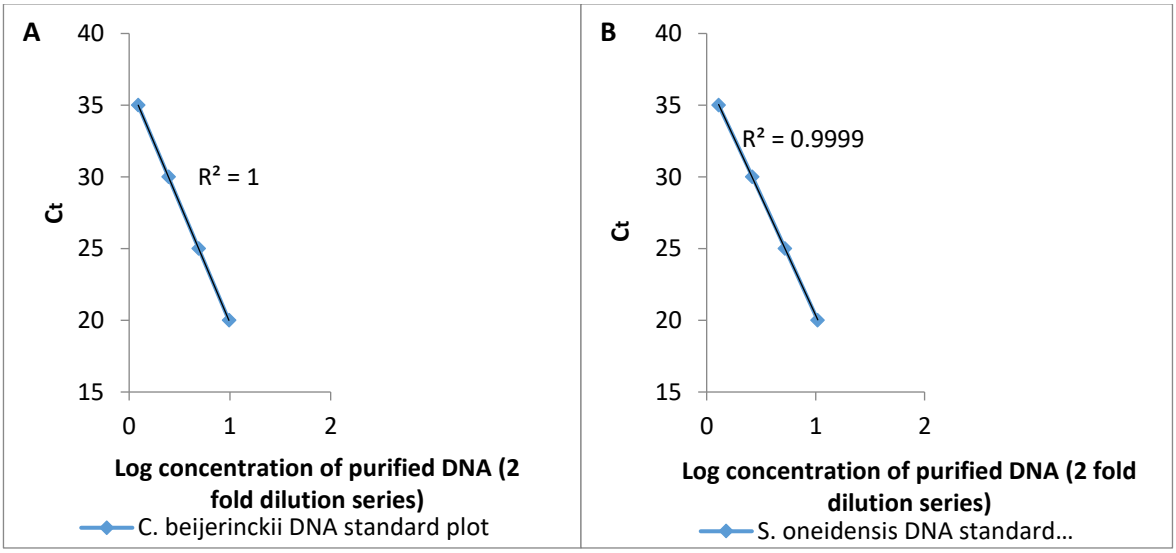

Figure 2.11: Standard calibration curves for determining the efficiency of the real time-PCR assay; graphs show Ct values (correlation of fluorescence to amplified product) for known DNA concentrations (x10 dilution fold series) of (A) C. beijerinckii and (B) S. oneidensis.

2.3.2.4. Metabolites of glucose utilization.

Glucose was widely metabolised across all tests (Table 2.9). The products of metabolism upon analysis were ethanol, butyric acid, and acetic acid. What is striking in the table is higher concentrations of metabolites produced by *C. beijerinckii* compared to other tests. What can also be clearly seen is that metabolite concentrations in the C-open MFCs were generally higher than in C-closed MFCs. Ethanol was not detected from all the tests at the end of the study.

Table 2.9. Comparison of glucose degradation, maximum power generation and fermentation products at the 72 h and 360 h of the investigation. ND = not detected; G = Glucose. Values are means of triplicate experiments ± standard deviation.

			Fermentation Products (mg/ml)					
			Acetic Acid		Butyric Acid		Ethanol	
Test	*G* (%)	P_{max} (mW m^{-2})	*72h*	*360h*	*72h*	*360h*	*72h*	*360h*
S. oneidensis	86 ± 6	48	50	187	0.818	0.996	ND	ND
C. beijerinckii	79 ± 5	60	422	307	95	233	153	ND
Co-culture (Closed)	82 ± 4	87	178	237	0.880	82	ND	ND
Co-culture (Open)	86 ± 4	ND	231	226	0.923	105	ND	ND

2.3.3. Results and Discussion for study involving co-culture of *C. beijerinckii*, *G. sulfurreducens* and *S. cerevisiae*.

2.3.3.1. Voltage-time profiles and polarization curves of co-culture work involving *C. beijerinckii, G. sulfurreducens* and *S. cerevisiae.*

The test of using pure cultures and co-cultures of *C. beijerinckii*, *G. sulfurreducens* and *S. cerevisiae* on maximization of 500 mg L^{-1} glucose on voltage-time profile for this study is shown in Figure 2.12. It reveals, that the peak voltage produced was 404 mV produced by the pure culture of *C. beijerinckii*. What is interesting in the chart is that the co-cultures: (1) *C. beijerinckii, S. cerevisiae* and *G. sulfurreducens*

(2) *G. sulfurreducens* and *C. beijerinckii which* produced 371mV and 362 mV respectively.

The least maximum voltage was 89 mV produced by the co-culture of *S. cerevisiae* and *C. beijerinckii*.

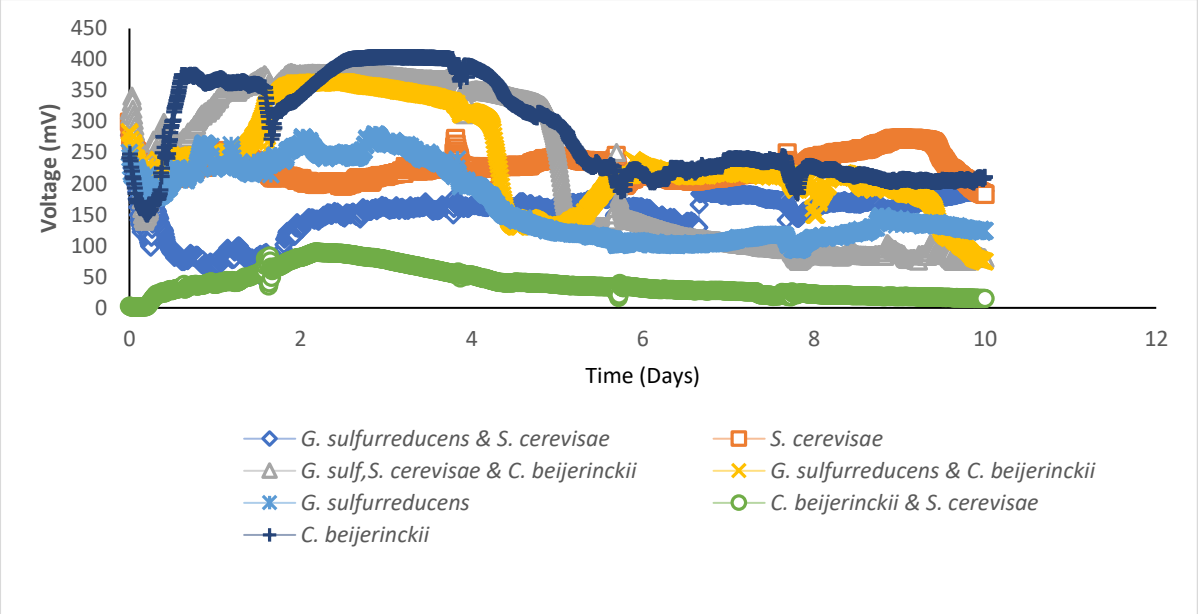

Figure 2.12. Voltage-time profile for pure cultures and co-cultures of G. sulfurreducens, C. beijerinckii and Saccharomyces cerevisiae investigated using synthesized wastewater containing 500 mg L^{-1} glucose.

As shown in Figure 2.13B reveals that the maximum power produced was 80±2mW m^{-2} produced by the co-culture of *C. beijerinckii, S. cerevisiae* and *G. sulfurreducens* slightly higher than 74±4 mW m^{-2} produced by *C. beijerinckii*. What is interesting in the chart is the power produced by the co-culture of *C. beijerinckii* and *S. cerevisiae* (less than 1 mW m^{-2}).

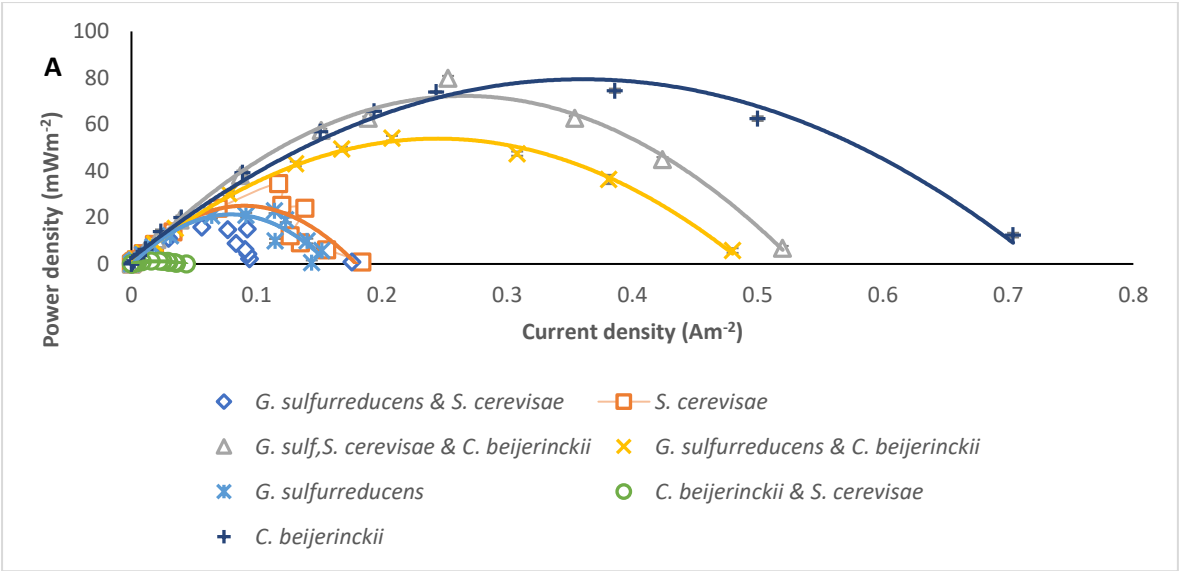

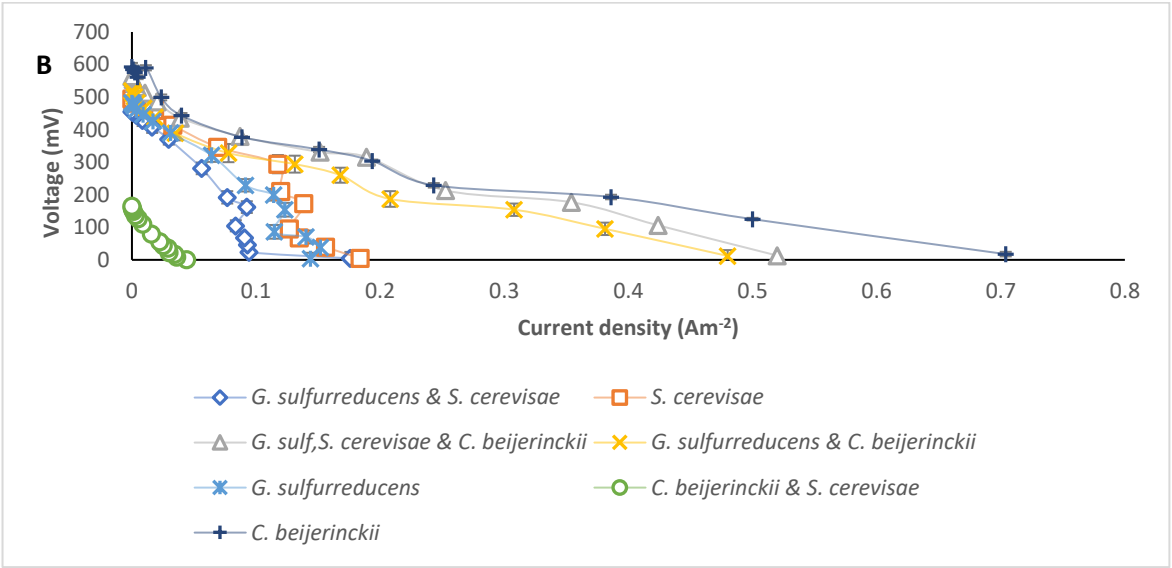

Figure 2.13. (A) Comparison of MFC performance (power density vs current density) obtained by varying the external circuit resistance (10Ω – 50,000Ω); (B) Polarization curves for the co-culture experiment. Control curves are too small to be seen clearly on the graph.

2.3.3.2. COD degradation and coulombic efficiency.

Comparison of total substrate reduction expressed as COD (%) and coulombic efficiency as CE (%) is shown in Table 2.10. What can be seen clearly is the peak COD reduction of 55% recorded by the co-cultures throughout the studies, except for the co-culture involving the three strains. What is interesting is that pure cultures of *G. sulfurreducens* produced the least COD reduction of 32%.

Table 2.10. Comparison of substrate degradation (COD%) and coulombic efficiency (CE%) between tests.

Tests	COD (%)	CE (%)
C. beijerinckii + S. cerevisae	55 ± 2	1
S. cerevisae	35 ± 5	7 ± 0.1
G. sulfurreducens	32 ± 4	8 ± 0.1
G. sulfurreducens + S. cerevisae	55 ± 3	4
C. beijerinckii	40 ± 3	13 ± 0.3
G. sulfurreducens + C. beijerinckii	55 ± 4	6 ± 0.1
C. beijerinckii + S. cerevisae + G. sulfurreducens	41 ± 3	8 ± 0.2

2.3.3.3. Relative abundance of co-culture of *G. sulfurreducens and C. beijerinckii.*

The result on comparison of relative abundance test for coculture of *C. beijerinckii* and *G. sulfurreducens* is shown in Table 2.11.

Table 2.11. Comparison of relative abundance of the two target organisms in the co-culture tests at start and end of the investigation.

	Co-culture	
	G. sulfurreducens	***C. beijerinckii***
% composition at Start	36	64
% composition at Day 10	62	38

The result indicated that co-culture of *C. beijerinckii* reduced from 64% and *G. sulfurreducens* increased from 36% at the start of the studies to 38% and 62% respectively at the end of the studies.

2.3.3.4. Products of metabolism.

As shown very high concentrations of ethanol, acetic acid and butyric acid were produced at the Day 2 of the studies. However, at Day 10 of the study what can be seen clearly is that they were insignificantly detected for the tests involving pure culture of *C. beijerinckii*, and similarly stands out where it was utilized as co-culture. From the metabolites detected only acetic acid was utilized for power production in the co-culture involving the three organisms.

Table 2.12. Comparison of fermentation products produced at Day 2 and Day 10 of the investigation between pure cultures and co-cultures studied.

	Fermentation Products (mg/ml)					
	Ethanol		***Acetic Acid***		***Butyric Acid***	
Tests	***48h***	***240h***	***48h***	***240h***	***48h***	***240h***
G. s	**593**	**489**	**4105**	**5482**	**4153**	**6634**
G. s + C. b + S. c	**618**	**618**	**3395**	**8**	**6054**	**6054**
G. s + C. b	**773**	**ND**	**3894**	**ND**	**4555**	**ND**
C. b	**952**	**0.73**	**5378**	**ND**	**5662**	**ND**
C. b + S. c	**161**	**ND**	**4468**	**2912**	**4919**	**6371**
S. c	**2471**	**ND**	**5523**	**1963**	**3715**	**2979**
G. s + S. c	**112**	**227**	**5080**	**4187**	**4827**	**4827**

2.3.3.5. Discussion.

Specific application of microorganisms in biotechnology involves the use of pure culture to reduce contaminants and avoid the longer down-times during sterilization (Pandhal and Noirel, 2014). However, in most cases, co-culturing of microorganisms provide more advantages such as improving on efficiency of complex biochemical processes than using pure culture (Pandhal and Noirel, 2014) and often produce more electricity production than pure culture or undefined mixed culture in MFCs (Table 2.13). Co-cultures is also employed as bio-augmentations in real world practical applications for example for the bioremediation of highly contaminated oilfield soils (Qiao et al., 2014; Mrozik and Piotrowska-Seget, 2010).Bio-augmentations is defined as a technique for improvement of degradative capacity of contaminated soil by introduction of specific competent strains or consortia of microorganisms (Mrozik and Piotrowska-Seget, 2010). Microbes are ubiquitous and inevitably live in communities in the environment (Kouzuma *et al*., 2015a). They secrete varieties of metabolites for the growth of other organisms (Kouzuma *et al*., 2015b). However, on the flipside, interactions between organisms in co-culture could enhance or inhibit the activities of other organisms (Bader *et al*., 2010).

The aim of the first coculture experiment was to maximise the turnover rate of glucose as a substrate for electricity production in microbial fuel cells. Hence, the influence of the use of co-culture of *S. oneidensis* and *C. beijerinckii* on the maximization of substrate was investigated and compared to using their pure cultures. The resulting performances are compared in terms of the substrate utilization, power, and polarization curves (produced form polarization experiments). Figure 2.7 indicates similar potential differences in the MFC utilising pure and co-culture under closed circuit conditions. However, there were differences in power production; these differences could be because of possible differences in electrochemical losses – activation and polarisation losses required for an oxidation/reduction reaction to occur during electron transfer (Mansoorian *et al*., 2014)

Table 2.8 indicates that the co-culture enhanced COD reduction which was not statistically significantly different ($p>0.05$) from that of *C. beijerinckii* but differed significantly with the COD reduction from *S. oneidensis*. Clostridia are fermentative organisms and they have been shown under MFC conditions to convert fermentation end products into alcohols e.g. butanol (Finch *et al*., 2011). In the co-culture, *S. oneidensis* can utilise the end products of *C. beijerinckii* releasing carbon dioxide (Rosenbaum *et al*., 2011). This could explain the similar COD reduction for *C. beijerinckii* and the co-culture. The low COD reduction in the case of *S. oneidensis* could be explained in terms of high biomass production and/or accumulation of unknown intermediates (see Appendix 3) which are not broken down. The COD utilization in the open circuit was lower than that was used in the closed circuit condition and consistent with previous report (Qu *et al*., 2012)

Figure 2.8B suggests that more power production can be achieved by using the co-culture rather than using pure cultures which some previous investigations also supported (Read *et al*., 2010; Ren *et al*., 2007 and Qu *et al*., 2012). Although the power produced is higher than the pure culture, the result was less than the sum of the individual strains perhaps because *C. beijerinckii's* performance could have been inhibited by redox active molecules secreted by *S. oneidensis*. A study using the same approach as this study by studying the co-culture of *C. cellulolyticum* and *G. sulfurreducens* recorded maximum power of 143 mW m^{-2} from carboxylmethyl cellulose (Ren *et al*., 2007) but it is difficult to make a strict comparison in terms of the maximum power generated with this study (87 mW m^{-2}) because of differences in the nature of strains co-cultured and the substrate used for the study. One possible explanation why the MFC system operated with pure culture of *S. oneidensis* generated low power density when compared with *C. beijerinckii* is the low amounts of substrate utilized by *S. oneidensis* (20% of the total COD content of the substrate) which is almost 3 fold less compared to the total substrate consumed by *C. beijerinckii* and therefore indicated it is a poorly fermentative organism. This observation can be correlated with the study reported by Biffinger *et al.*, 2008, that glucose is not utilised effectively by *S. oneidensis* under strictly anaerobic conditions or that conditioning with nutrients such as lactate is needed for timely utilization of glucose (Howard *et al.*, 2012). Coulombic efficiency results (Table 2.8) suggest that *S. oneidensis* contributed most electrons transferred by the co-culture. The low CE

for the co-culture suggests the relationship between *S. oneidensis* and *C. beijerinckii* was an inhibitory one with *C. beijerinckii* inhibiting the electron transfer abilities of *S. oneidensis* perhaps through biofilm formation (Qureshi, *et al.* 2005) which could also explain the result of the power production (Zhang *et al.,* 2013; Baranitharan *et al*., 2015). Although *S.oneidensis* and *C. beijerinckii* have similar doubling time 40 and 38 minutes respectively (Abboud *et al*., 2005; Liyanage *et al*., 2000) the relative abundance test result suggested *S. oneidensis* is more predominant (3% increase) at closed circuit condition; it is consistent with the observation made by Qu *et al*., 2012 but inconsistent with open circuit condition.

The aim of the second coculture experiment was to enhance the turnover rate of 500mg L^{-1} glucose to electricity production by employing the use of more complex co-culture involving *G. sulfurreducens*, *C. beijerinckii* and *S. cerevisiae*. The result in Figure 2.12 and 2.13 demonstrated that cocultures are needed for the improvement of voltage and power production in MFCs from wastewater contaminated with level of 500mg L^{-1} glucose. However, it is difficult to make a strict comparison between this study that produced 80 mW m^{-2} from glucose with studies by Ren *et al*., 2007 that produced 143 mW m^{-2} and 59.2 mW m^{-2} from carboxymethyl cellulose and MN301 cellulose respectively or with the study by Bourdakos *et al*., 2014 using acetate, because of differences in the nature of strains that were studied and the substrate used for the study. Table 2.12 suggests that *C. beijerinckii* improved conversion of fermentation products to electricity when co-cultured with the other microorganisms than when used as a pure culture. *S. cerevisiae* was associated with situations where high levels of fermentation products were produced.

Table 2.13. Comparison of power production produced by cocultures and mixed cultures

Coculture	Rationale	Power density	Reference
C. beijerinckii and *S. oneidensis*	Improvement of glucose turnover rate and hence rate of electron generation	87 mW m^{-2} produced by the coculture compared with 48 mW m^{-2} produced by *S. oneidensis*	This study
C. beijerinckii, S. cerevisiae and *G. sulfurreducens*	Improvement of glucose turnover rate and hence rate of electron generation	80 mW m^{-2} produced by the coculture compared with 23 mW m^{-2} produced by *G. sulfurreducens*	This study
Geobacter sulfurreducens and *Escherichia coli*	Using *E. coli* as a facultative organism for consumption oxygen leaking into a single chamber reactor	63 mW/m^3 produced by the coculture, limited by succinate produced by *E. coli* compared to 128 mW m^{-2} produced by pure culture of *G. sulfurreducens*	Bourdakos *et al*., 2014
Klebsiella pneumonia and *Lipomyces starkeyi*	*In situ* production of redox mediator by *K. pneumonia*	12.87 W m^{-3} (3-6 fold increase over control)	Islam *et al*
Clostridium cellulolyticum and *Geobacter sulfurreducens*	*In situ* electricity production directly from cellulose	143 mW m^{-2} and 59.2 mW m^{-2} produced comparable to none by the control from 1 g L^{-1} carboxymethyl cellulose and MN301 cellulose respectively.	Ren *et al*., 2007
Mixed culture	*In situ* electricity production directly from cellulose	42.2 mW m^{-2} and 33.7 mW m^{-2} produced from 2 g L^{-1} carboxymethyl cellulose and from MN301 cellulose respectively	Ren *et al*., 2007

2.3.4. Results and Discussion for study involving co-culture of *S. oneidensis, C. beijerinckii* and *S. cerevisiae* from wastewater contaminated with 500 mg L^{-1} phenol.

2.3.4.1. Power production and polarization curves of co-culture work involving *S. oneidensis, C. beijerinckii* and *S. cerevisiae* from 500 mg L^{-1} phenol contaminated water.

The test of using pure cultures and co-cultures of *S. oneidensis*, *C. beijerinckii* and *S. cerevisiae* for improving simultaneous remediation of 500 mg L^{-1} phenol contaminated wastewater for power density and polarization curves is shown in Figure 2.14. The peak power recorded was 4.6 ± 0.02 mW m^{-2} produced by the pure culture of *S. oneidensis* closely similar to 4.25 mW m^{-2} produced by co-culture of *C. beijerinckii* and *S. cerevisiae* and also closely similar to the case of co-culture of *C. beijerinckii* and *S. oneidensis* produced 4.09 mW m^{-2}. Pure culture of *C. beijerinckii* produced 2.7 ± 0.03 mW m^{-2}, co-culture of *S. oneidensis, C. beijerinckii* and *S. cerevisiae* produced 2.13 ± 0.01 mW m^{-2}, co-culture of *S. oneidensis* and *S. cerevisiae* produced 1.9 mW m^{-2}, pure culture of *S. cerevisiae* produced 1.85 mW m^{-2}.

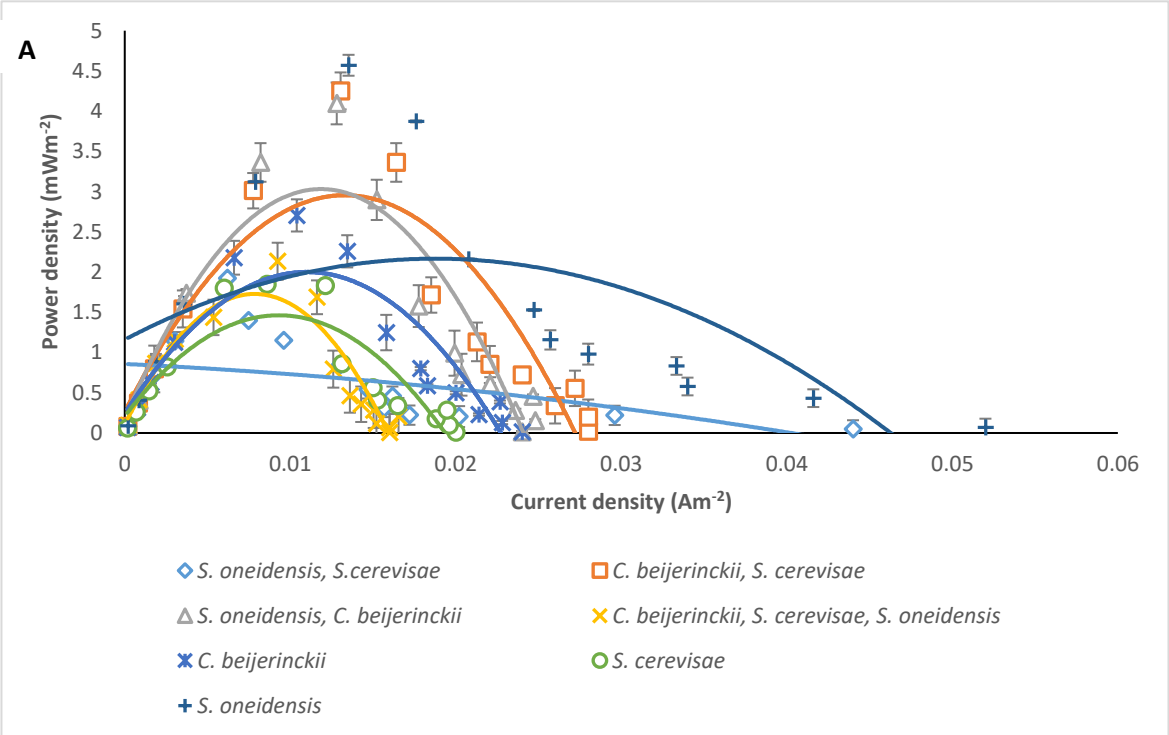

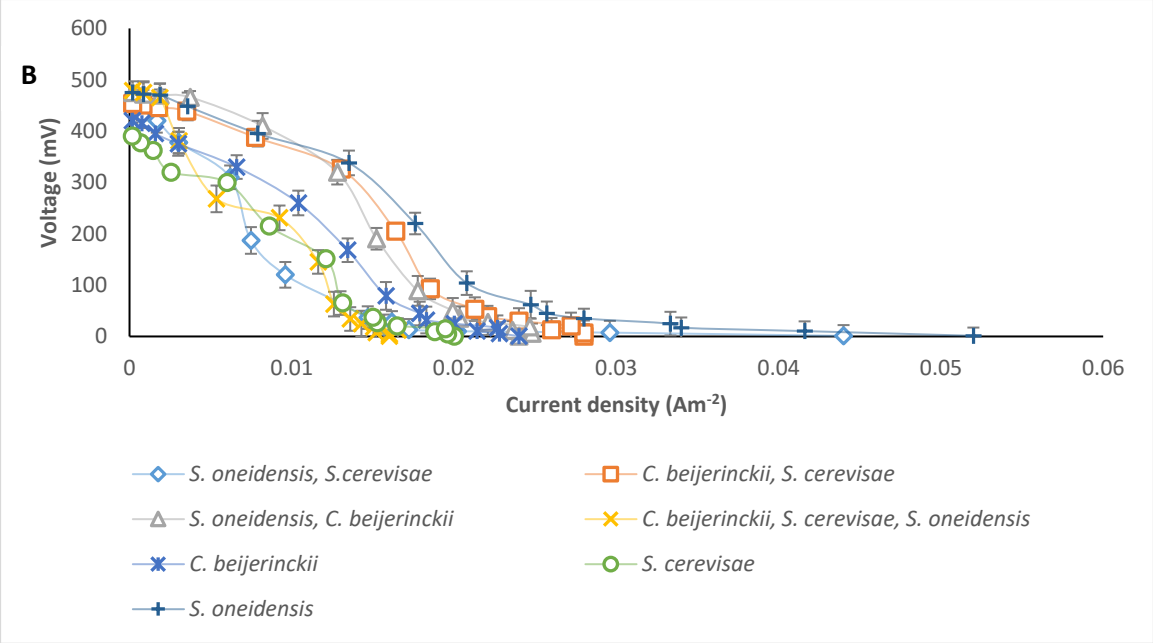

Figure 2.14. (A) Comparison of MFC performance (power density vs current density) obtained by varying the external circuit resistance (10 Ω – 50,000 Ω); (B) Polarization curves for the co-culture experiment. Control curves are too small to be seen clearly on the graph. The bars represent standard deviation of the mean (n=3).

2.3.4.2. Comparison of 500 mg L^{-1} phenol remediation used as substrate in tested systems in MFCs.

The result on remediation of phenol studies (Figure 2.15) at 35 days showed that

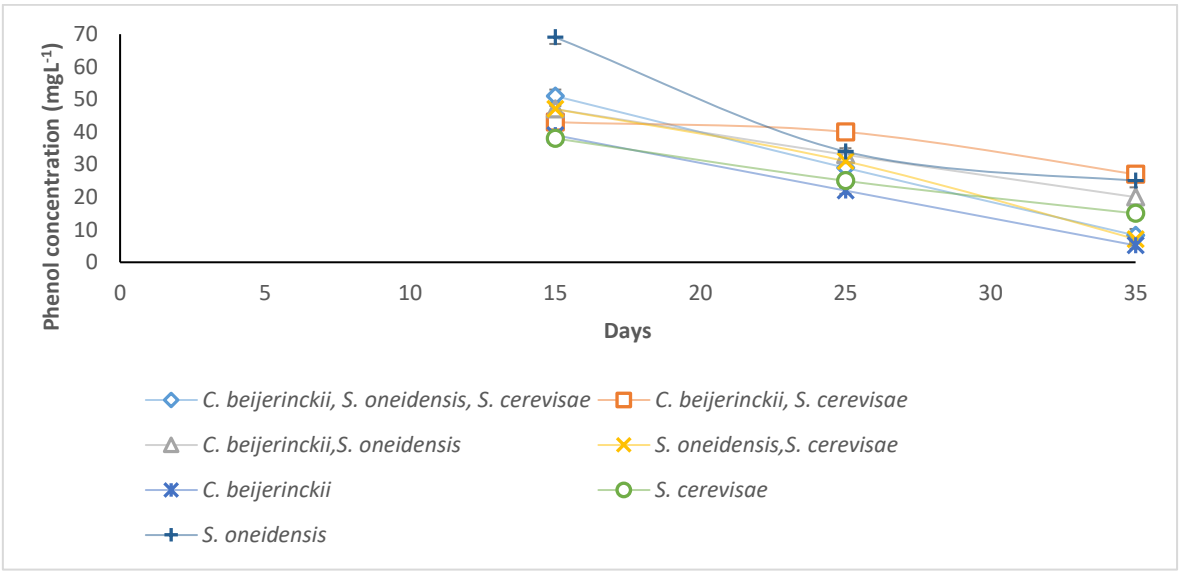

Figure 2.15. Phenol degradation by the pure culture and co-cultures of S. oneidensis, C. beijerinckii and S. cerevisiae studied for 35 days.

C. beijerinckii achieved 99% reduction compared to 97% by the pure culture of *S. cerevisiae* and 95% by the pure culture of *S. oneidensis*. The best result of co-culture was 99% by *S. oneidensis* and *S. cerevisiae*; 98% by co-culture of *S. oneidensis, C. beijerinckii* and *S. cerevisiae*.

2.3.5. Results and Discussion for study involving exogenous addition of riboflavin.

2.3.5.1. Effect of Riboflavin on voltage-time profile and Power production by *S. oneidensis* from remediation of 500 mg L-1 phenol contaminated wastewater.

Riboflavin is a redox mediator widely used for enhancing energy production and bioremediation in MFCs. In order to the test the effect on the voltage output of *S. oneidensis* during the remediation of 500 mg L^{-1} of phenol; varying concentrations 20, 30 and 40 µM were tested. The effect on voltage-time profile is shown in Figure 2.16 showing varying degrees of stationary voltage between 341 to 352 mV occurring at 0 days to 4 days of the studies before gradual decline. The pure culture with exogenous addition of 40 µM concentration had a prolonged stationary phase before gradual decline after 4 days. Voltage was observed to increase after a gradual decline from exogenous addition of 20 µM and 30 µM Riboflavin concentrations.

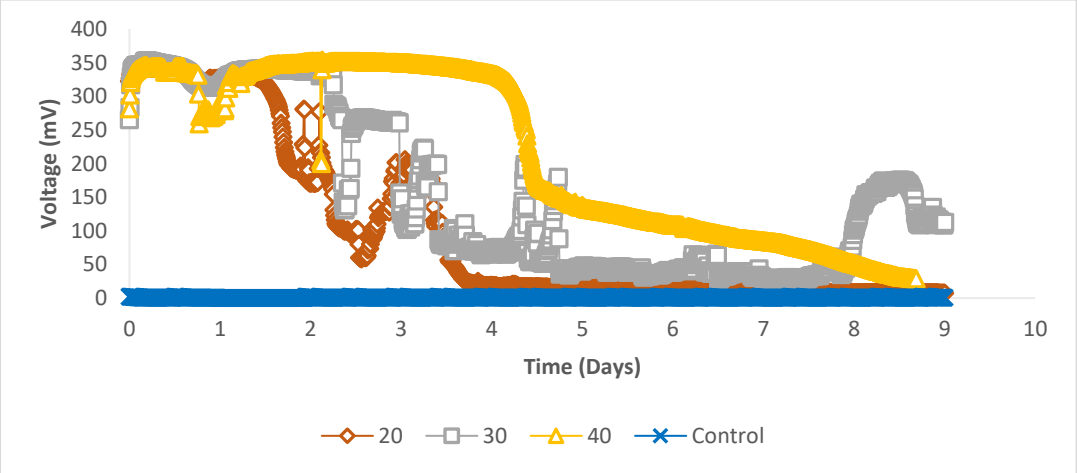

Figure 2.16. Voltage-time profiles of pure cultures of S. oneidensis utilizing phenol containing wastewater in the presence of 20, 30, 40 µM Riboflavin exogenously added.

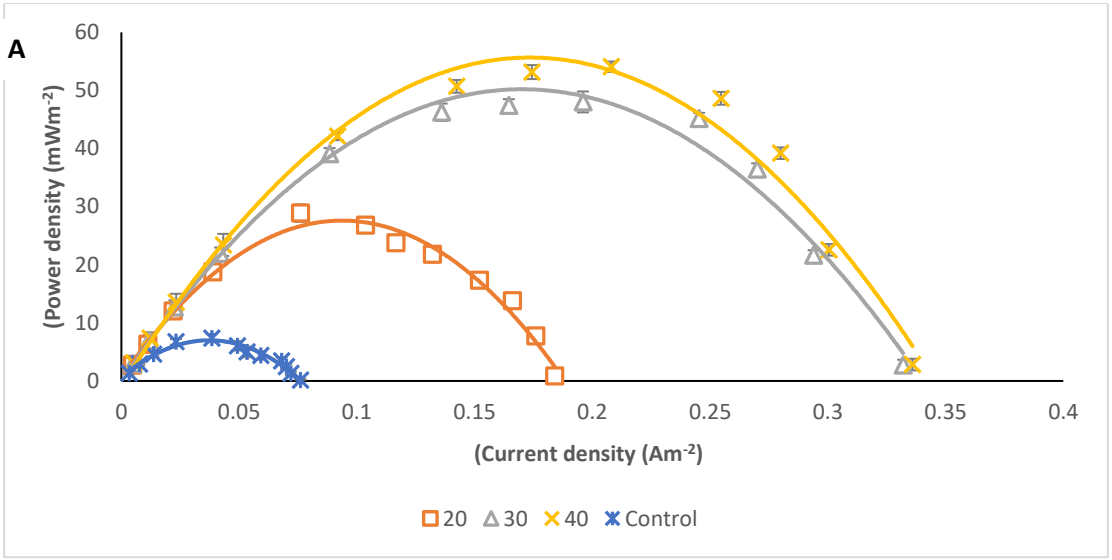

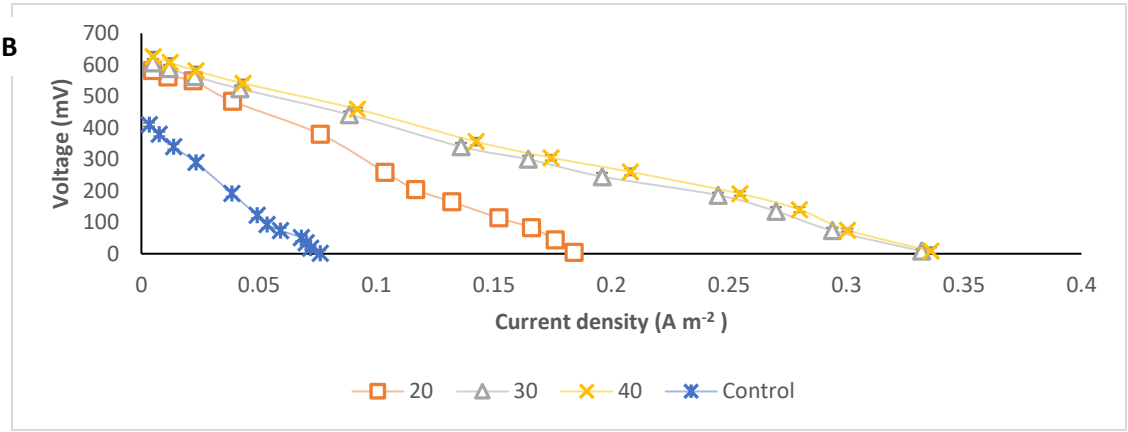

Figure 2.17. (A) Comparison of MFC performance (power density vs current density) obtained by varying the external circuit resistance (10Ω – 50,000Ω); (B) Polarization curves for the pure culture experiment. Control curves are too small to be seen clearly on the graph. The error bars represent the standard deviation of the mean (n=3).

As observed from the results on power generation presented in Figure 2.17, what is striking is that power recorded increases as the Riboflavin concentration increases. The peak power produced was 54 ± 3 mW m^{-2} by 40 µM Riboflavin, followed by 48 ± 2 mW m^{-2} using 30 µM Riboflavin. At 20 µM concentration, the power was 29 ± 1 mW m^{-2} while the control with no Riboflavin was 7.4 ± 0.04 mW m^{-2}.

2.3.5.2. Comparison of 500mgL-1 phenol remediation used as substrate for pure culture of S. oneidensis using Riboflavin of different concentration tested in MFCs system.

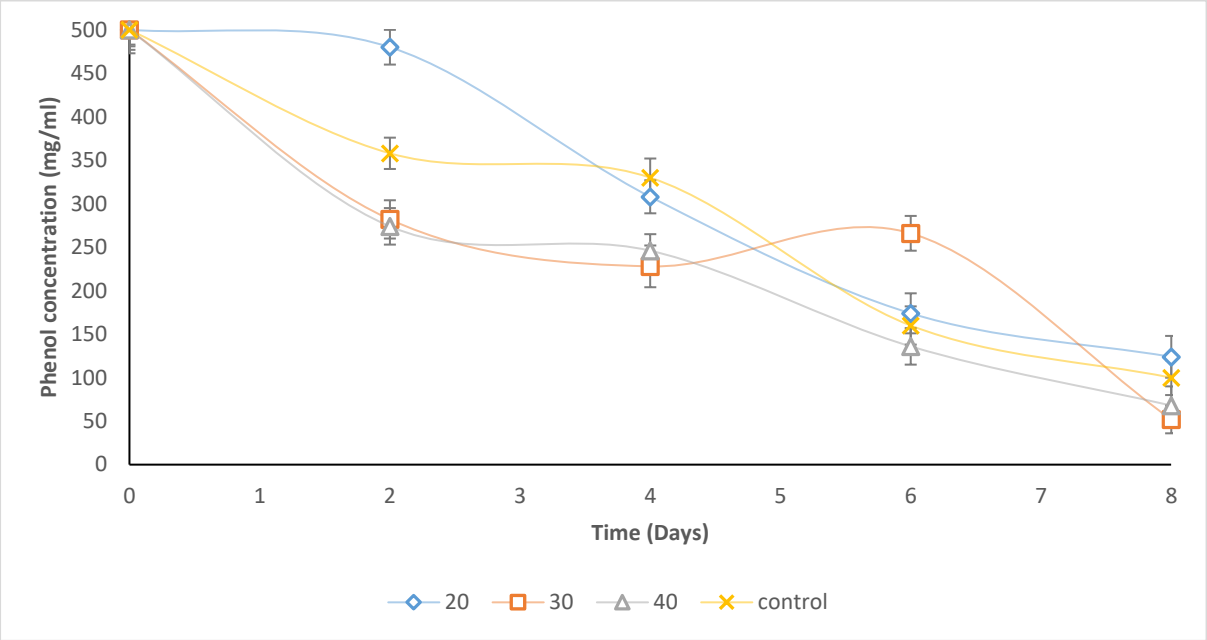

Figure 2.18. Phenol degradation by the pure culture of S. oneidensis studied utilizing 20, 30, and 40 µM exogenous addition of Riboflavin concentrations.

The result on phenol remediation studied for 8 days is represented in Figure 2.18. What Figure 2.18 reveals is that exogenous addition of 30 µM riboflavin produced the best reduction effect (52 mg L^{-1}). Other results 20, 40 and control on phenol reductions were 124, 68 and 100 mg L^{-1} respectively.

2.3.5.3. Discussion.

The aim of the experiment was to reduce 500 mg L^{-1} phenol-contaminated wastewater in MFCs using co-cultures and pure cultures of *S. oneidensis*, *C. beijerinckii* and *S. cerevisiae* to dischargeable level of 5 mgL^{-}1 the maximum permissible limit for phenolic concentrations in industrial effluent before discharging into municipal sewers and surface waters (Pant *et al*., 2010; Singh and Srivastava, 2002). Phenol is one of the most commonly found aromatic compounds in wastewater that concentration above 500mg L^{-1} produce inhibitory effects to aquatic life and give objectionable taste to drinking waters even at low concentrations (Tian

et al., 2017). Few studies: Al-Shehri, 2015, Friman *et al*., 2013; Haiping *et al*., 2008; Jiang *et al*., 2012; Luo *et al*., 2009; Song *et al*., 2014 have studied phenol degradation in MFC; these works often require supplementation of glucose with phenol for these studies. The results of the preliminary study in Figure 2.18 suggests that pure culture of *S. oneidensis* could potentially be utilized for the bioremediation of phenol-contaminated wastewater at a level of 500 mg L^{-1} without the need for coculturing with either *C. beijerinckii* or S. *cerevisiae* in MFCs. Hence, motivated another study investigating use of Riboflavin molecules which has been used for improving power production from petroleum hydrocarbons (Adelaja *et al*., 2015; (Zhai *et al*., 2016)). The result suggested that, increasing the concentration of Riboflavin to 40 µM enhanced power generation to 54 mW m^{-2} (Figure 2.17) more than the preliminary work of this study of 1.85 mW m^{-2} (Figure 2.14). Hence, suggesting that increasing concentration of riboflavin to optimal level, results to increasing the power generation; this is consistent with previous work using Riboflavin such as Pandit *et al*., 2014 and Sun *et al*., 2013, and in the study when glucose was supplemented with phenol for electricity production (Jiang *et al*., 2012) . The pure culture of *S. oneidensis* using 30 µM concentrations of Riboflavin in this study (Figure 2.18) gave the best phenol removal. Recent work comparing the effect of five redox mediators showed that 30 µM of RiboRiboflavin enhanced power generation (Al-Shehri, 2015).

2.4. Concluding remarks.

The use of fermentative bacteria for the maximization of glucose or phenol conversion to simpler bioprocessing products that are easily utilizable for bioelectricity production by *S. oneidensis* was demonstrated. This approach represents the model way of recovering bioenergy from wastewater contaminated with glucose that is not preferred as a primary source of substrate for electricity production by *S. oneidensis*. The result of the first study involving *S. oneidensis* and *C. beijerinckii* corroborates the result of the second studies using *C.* beijerinckii, *G. sulfurreducens* and *S. cerevisiae* on the influence on power and COD utilization. By using *C. beijerinckii* with *S. oneidensis* %COD utilized was increased from 20% to 67% while electricity was increased from 48 mW m^{-2} to 87 mW m^{-2}. By coculturing *C. beijerinckii* and *S. cerevisiae* with *G. sulfurreducens*, COD utilization was increased from 32% to 41% while power was increased from 23 mWm^{-2} to 80 mWm^{-2}. The

improved electricity production by the co-cultures was as a result of fermentation products made available for metabolism by the electroactive bacteria *S. oneidensis* or *G. sulfurreducens* i.e. syntrophy . This work further demonstrated that pure culture of *S. oneidensis* can potentially be used to recover energy from wastewater contaminated with phenol, while pure cultures of *C. beijerinckii* strain 6444 can be used to remediate phenol wastewater by using coculture modifications employed in this study. Exogenous supplementation of Riboflavin to phenol wastewater to a concentration level at 30 µM concentration can be used to improve the remediation of phenol wastewater, while Riboflavin concentration at a level of 40 µM can be used to improve the electricity recovery while at the same time remediating phenol wastewater in MFCs system.

Chapter 3

Contribution of direct electron transfer mechanisms to overall electron transfer in MFCs utilising *S. oneidensis* as biocatalyst.

3.1. Introduction

Three possible mechanisms utilized by electrochemically active bacteria for electron transfer to anodes have been suggested (Figure 3.1): directly using a cascade of membrane proteins and/or conduction by nanowires, and mediated electron transfer.

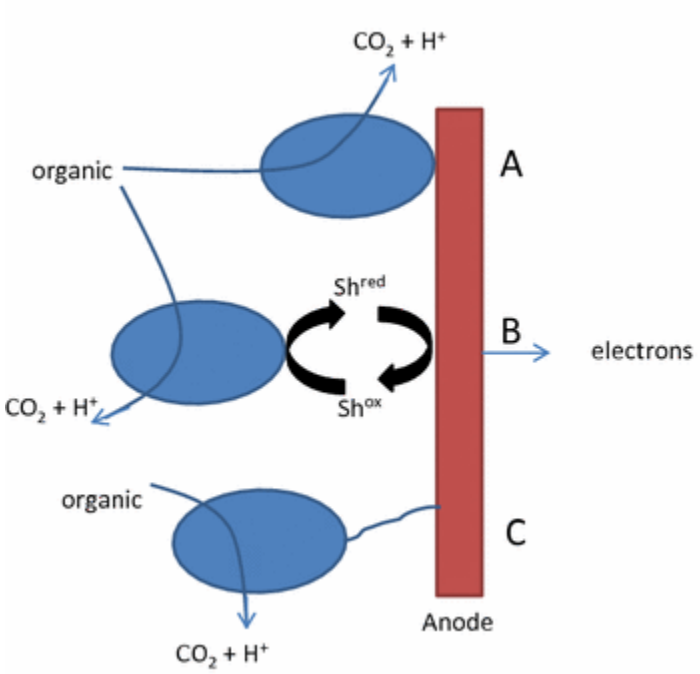

Figure 3.1. Hypothetical extracellular electron transfer (EET) pathways at an anode: A – direct electron transfer via membrane bound cytochromes in direct contact with the anode; B – direct electron transfer via conductive nanowires (pili); C – mediated electron transfer using redox shuttles

Dissimilatory metal reducing bacteria like *S. oneidensis* and *G. sulfurreducens* are reported to conduct direct electron transfer by using membrane-bound c-type cytochromes for transferring respiratory electrons to solid electrodes. This

mechanism transfers electrons directly via contact with a solid electrode and does not use diffusional redox mediators (Wrighton *et al.*, 2011).

Mediated electron transfer is thought to be involved through the use of various natural, synthetic electron shuttle, or soluble endogenous redox-active molecules. These include using endogenous compounds such as quinones, Riboflavin mononucleotide (FMN), and phenazines produced and used by bacteria; or using other synthetic exogenous compounds such as neutral red and methylene blue to shuttle electrons from the electron transport chain to solid electrodes (Okamoto *et al*., 2012). In addition to the above mechanisms, electrons could also be transported to the electrode surfaces by using pilus-like appendages containing c-type cytochromes. These are termed bacterial nanowires and are utilized by both *S. oneidensis* and *G. sulfurreducens* for distant transfer of electrons directly to electrode surfaces (Wrighton *et al.,* 2011).

Low extracellular electron transfer efficiency between electroactive bacteria and anodes remains one of the major bottlenecks in the practical application of microbial fuel cells. Assuming more than one electron transfer mechanism is operating in a given microorganism, it would be useful if the relative contribution of these mechanisms to electron transfer could be quantified. Efforts could then be geared towards improving the efficiency of that mechanism if its contribution is found to be relatively large by comparison to other mechanisms.

Electrochemically active bacteria such as *Shewanella* form biofilms during growth and it has been demonstrated that the power output of MFCs was directly dependent on biofilm growth and composition (Okamoto *et al.*, 2012). However, it is not clear what contribution is made by the different electron transfer mechanisms to electricity production or whether aiding biofilm formation for example by adding quorum sensing molecules can improve electricity production.

Microbial electron transport involves transferring electrons from a low potential energy donor to an acceptor (more positive redox potential) known as redox processes. Microorganisms use this process to adapt to different environmental conditions for metabolism and for energy gains. To achieve this process some microorganisms such as *S. oneidensis* have developed enormous varieties of electron transport chains for the establishment of motive force that drive ATP

synthesis. Some of these systems (that couple electron from donor such as NADH to an acceptor such as H^+, Oxygen, nitrate and fumarate) include primary dehydrogenases, membrane-localised multiprotein complexes (cytochrome), quinones (lipophilic molecules), flavines, heme (catalytic cofactors), iron-sulfur or copper ions (Kracke *et al*., 2015). This study therefore investigated the contribution of direct electron transfer mechanisms to electricity production, for the first time by physically retaining *S. oneidensis* cells close to or away from the anode electrode using a dialysis membrane as well as immobilising the cells in alginate beads.

3.2. Materials and Methods

3.2.1 Chemicals

Dialysis membrane tubing (12000 Dalton MWCO), Sodium pyruvate and other chemicals listed in section 2.2.1 (purity ≥ 96%) were purchased from Sigma Aldrich (UK). All chemicals were of analytical grade and were used without further purification.

3.2.2. Bacterial strains, maintenance, and culture.

S. oneidensis strain used is as described in section 2.2.2. The strain was first sub-cultured in Luria-Bertani broth medium (LB medium) containing (per litre) 10 g of tryptone, 5 g of yeast extract and 5 g of NaCl at 30^{o}C for 48 hours; followed by sub-culturing in minimal salt medium containing sodium pyruvate.

3.2.3. Experimental design.

The experiment design investigating the contribution of direct electron transfer mechanism to electricity production was studied due to time limitation for 11 days under strictly anaerobic-anodic conditions in a two-chambered MFC. The inoculum was made up of 10% (v v^{-1}) of the anode working volume (3.4 x 10^9 CFU - target cell density). *S. oneidensis* cells were retained close to or physically separated from the anode electrode using a dialysis membrane (MWCO 12,000 Da pore size, Figure 3.2). This pore size is small enough to prevent cells from going through but large enough to allow movement of proteins, redox shuttles, or metabolites. The control

was an MFC with an anode having a dialysis membrane but no enclosed microorganisms. All experiments were conducted in triplicate.

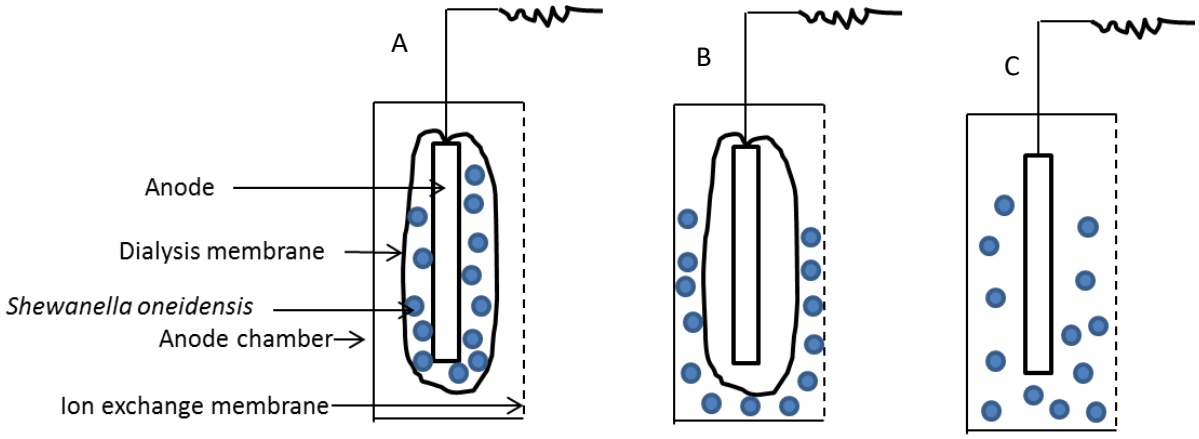

Figure 3.2. Schematic of the setup (anode chambers only) for investigating the contribution of direct electron transfer mechanism to microbial electricity production: A – Direct electron transfer; B – Mediated electron transfer; C – Combination of both mechanisms, A and B (Not drawn to scale).

Another experiment involved immobilising *S. oneidensis* cells in the anode chamber in alginate beads as a way of separating them from the anode. Beads were prepared by mixing equal volumes (20 ml) of *S. oneidensis* cells (density 3.4 x 10^9 CFU) with sodium alginate (4%) and releasing drops of the mixture using a Pasteur pipette into calcium chloride solution (20 g L^{-1}) to entrap the cells. Controls involved cells inoculated into the anolyte without restriction (meaning electrons could be transferred by direct and mediated electron transfer mechanisms) as well as anodes without microorganisms. The experiment was conducted in triplicate.

3.2.4. MFCs Setup and Operation.

The MFCs setup and operation is as described in section 2.2.4, except with some modifications. The cathodes contained no Pt catalyst layer (as the catholyte was ferricyanide - details below) and the electrodes had a geometric surface area of 25 cm^2. Potassium ferricyanide was used as catholyte.

The performance of the MFCs was investigated with respect to electrochemical performance (i.e. voltage outputs, maximum power generation and coulombic efficiency, section 3.2.3) and degradation performance (substrate's degradation rate

and COD removal efficiency, section 3.2.3). The inoculum used was 10% v/v of the total anolyte volume. The anode chambers with the contained mixtures were stripped of dissolved oxygen by sparging nitrogen gas for 5 minutes before setup.

All experiments were replicated three times and studied at 30°C using a temperature-controlled Stuart 160 incubator (Fisher Scientific, U.K.). Results were expressed as mean of replicates ± standard deviation.

3.2.5. Modification of anolyte minimal salts medium used for the investigation of contribution of direct electron transfer mechanism.

The anolyte MSM for the investigation of the contribution of direct electron transfer mechanism to electricity production was supplemented with 500 mg L^{-1} casein hydrolysate and 2.2 g L^{-1} sodium pyruvate as the primary carbon source was used in this study because it is a more reduced, and can easily be utilized by *S. oneidensis* without the need for coculturing with a fermentative bacterium. Also supplemented were trace element stock solution (x1) and vitamin stock solution (x1).

The catholyte used was 50mM phosphate buffer pH 7 containing 0.1 M potassium ferricyanide, without aeration. During the start-up operation, actively growing *S. oneidensis* (3.4 x 10^9 CFU -10% v v^{-1} of the total anolyte volume) cells were retained close to the anode using a dialysis sack to enable direct electron exchange; *S. oneidensis* cells were also separated from the anode using a dialysis sack meaning electron exchange could occur via redox shuttles i.e. mediated electron transfer mechanism. The final set up did not have a dialysis sack meaning both mechanisms of electron transfer would operate (combined studies) – Figure 3.2C.

For all set ups the volume of inoculum used was 10% v v^{-1} of the total anolyte volume. The anode chambers with the contained mixtures were stripped of dissolved oxygen by sparging nitrogen gas for 5 minutes before setup.

All experiments were replicated three times and studied at 30°C using a temperature controlled Stuart 160 incubator (Fisher Scientific, U.K.). Results were expressed as mean of replicates ± standard deviation.

3.3. Results

3.3.1. Summary of Results

Investigation of the contribution of direct electron transfer mechanism on electricity production was studied by physically retaining *S. oneidensis* cells close to or away from the anode electrode using a dialysis membrane. The summary of the outcome of this study (Table 3.1) indicated a maximum power output of 114±6 mW m^{-2} when cells were retained close to the anode, 3.5 times more than when the cells were separated from the anode. Without the membrane (utilization of mediated and direct mechanisms) the maximum power output was 129±6 mW m^{-2}, a result that has been corroborated by another experiment where *S. oneidensis* cells were immobilised by entrapment in alginate gels. This work has been published in Biotechnology Letter (Appendix 4).

Table 3.1. Summarization of results involving the contribution of direct electron transfer to overall electricity production.

	Direct Mechanism	Combined Mechanism	Mediated mechanism
Power Production (mW m^{-2})	114 ± 6	129 ± 6	32 ± 8
% COD Reduction	21 ± 2	57±3	46 ± 3

3.3.2. Voltage-time profiles and polarization curves.

The voltage-time profile, polarisation, and power density curves for the contribution of direct electron transfer mechanism to electricity production are shown in Figure 3.3 and Figure 3.4. MFCs utilising the direct mechanism of electron transfer (DM) generated the highest voltage throughout the study. The maximum voltage generated under 1000 Ω was by DM. MFCs utilising DM, mediated electron transfer mechanism (MM) and those utilising both mechanisms (CM) were 586 ± 5 mV, 400 ± 6 mV and 470 ± 6 mV respectively. At day 8 there was exponential increase in voltage production by CM after a gradual reduction of voltage to 157± 3 mV.

Similarly, DM produced the highest average voltage of 485 ± 7 mV, followed by CM of 323 ± 5 mV and the least was generated by MM of 317 ± 6 mV.

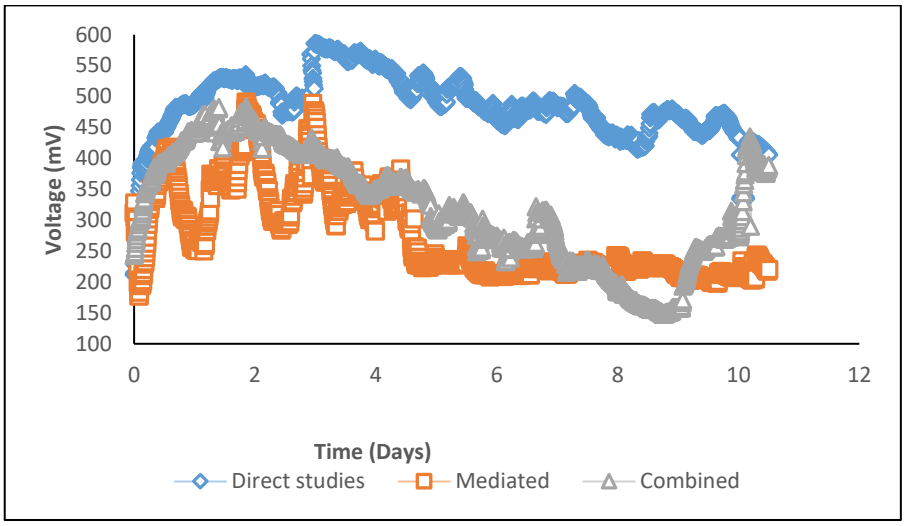

Figure 3.3. Voltage time profiles for the contribution of direct mechanism to electricity production by S. oneidensis. The direct mechanism gave the highest potential difference while at day 8 there was an increase in voltage production by combined mechanism after voltage decreased to a minimum value of 157mV.

Power density tests were conducted on the second day when all the MFCs were in their pseudo-steady-state conditions. As shown in Figure 3.3B, the CM system generated the highest maximum power density of 129 ± 6 mW m^{-2}; DM study generated 114 ± 6 mW m^{-2} while MM produced the least maximum power density of 32± 8 mW m^{-2}.

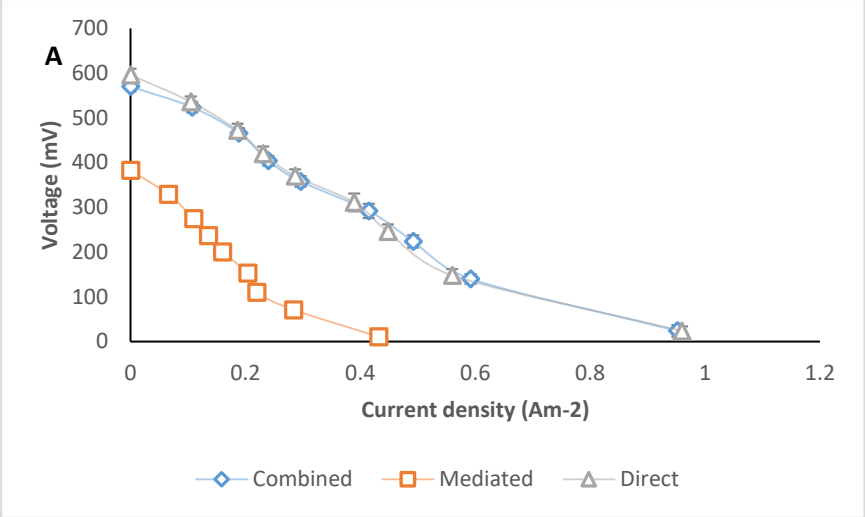

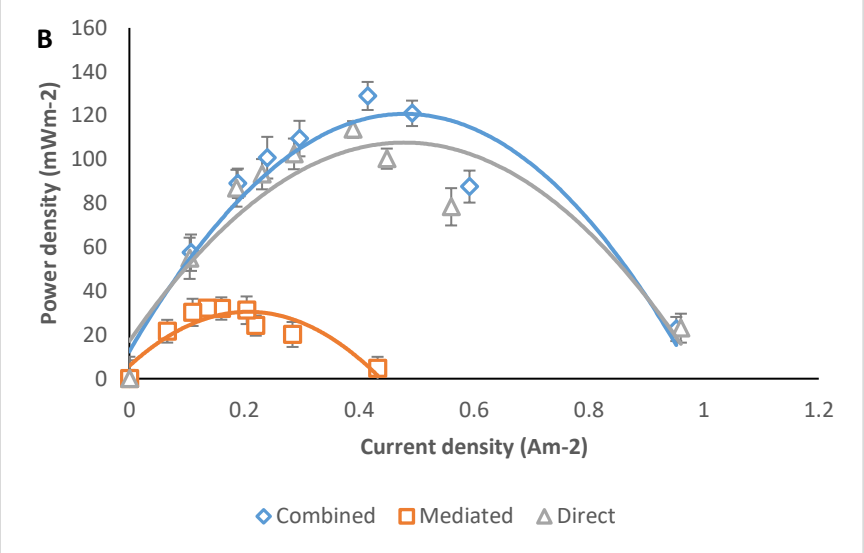

Figure 3.4. (A) Polarization curves and (B) power density curves for the experiment involving the contribution of DET mechanism to electricity generation. Error bars indicated standard deviation where n=3.

The voltage-time profile, polarisation, and power density curves for the contribution of mediated electron transfer mechanism to electricity production are shown in Figures 3.5 and 3.6 respectively. MFCs utilising the mediated mechanism of electron transfer (MET) generated the highest voltage throughout the study. The maximum voltage generated under 1000 Ω by MET and other mechanisms CM were 445 ± 6 mV and 395±5 mV respectively. At day 10.4 there was exponential increase in voltage production by CM after a gradual reduction of voltage to 239 ± 4 mV. Similarly, MET produced the highest average voltage of 347 ± 4 mV and for CM was 267± 6 mV.

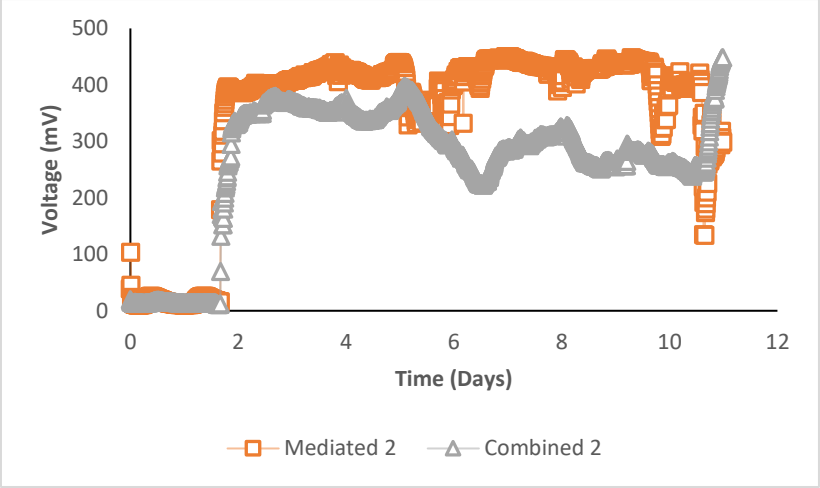

Figure 3.5. Voltage time profile for the contribution of mediated electron transfer mechanism to electricity production by immobilised S. oneidensis cells.

As shown in Figure 3.5B, the CM system generated maximum power density of 105 ± 4 mW m^{-2} while MET produced a maximum power density of 36 ± 6 mW m^{-2}.

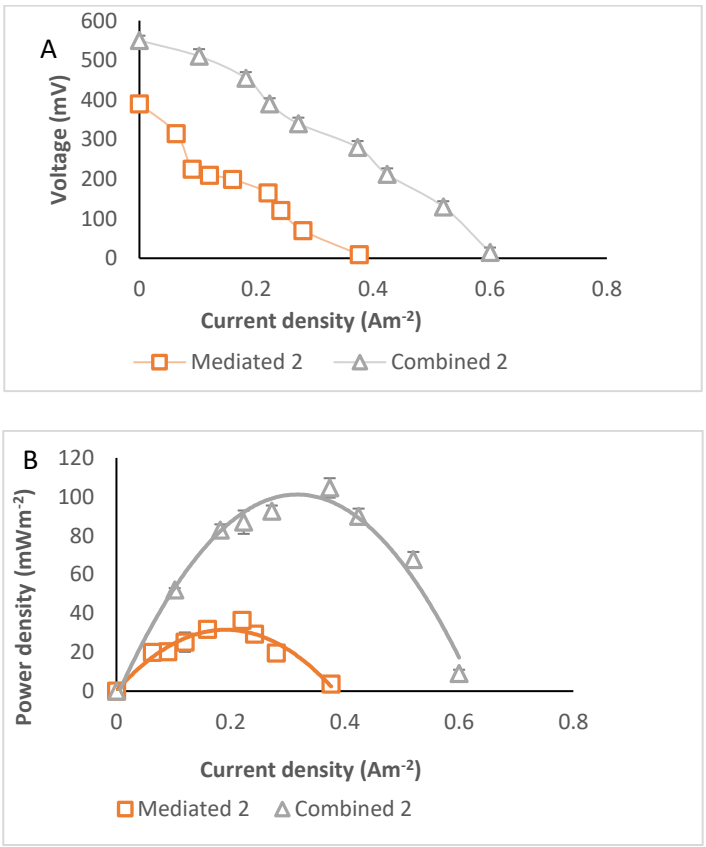

Figure 3.6. (A) Polarization curves and (B) power density curves for the experiment involving the contribution of mediated electron transfer to electricity generation by immobilised S. oneidensis cells.

3.3.3. COD degradation and coulombic efficiency.

Table 3.2 shows the comparison of substrate degradation as COD and amount of electron recovery on day 11 of the investigation. The CM gave the highest substrate utilization of 57 ± 3% which was more than 2-fold higher than DM which gave 21 ± 2%. However, with regards to coulombic efficiency, DM gave 36 ± 1% and was 4-fold higher than CM of 9 ± 1%. MM gave 46 ± 3%COD reduction with a CE of 11 ± 2%.

Table 3.2. Comparison of substrate degradation and electron recovery at 11 days of investigation for contribution of mechanisms of electron transfer processes by S. oneidensis. Values are means of triplicate experiments ± standard deviation.

	Combined	**Direct**	**Mediated**
COD degradation (%)	57 ± 3	21 ± 2	46 ± 3
Coulombic efficiency (%)	9 ± 1	36 ± 1	11 ± 2

Values are means of triplicate experiments ± standard deviation.

3.3.4. Metabolites of substrate degradation.

Acetic acid and butyric acid were the main degradation products with acetic acid produced in larger amounts than butyric acid across the systems (Table 3.3).

Table 3.3. Fermentation end products from the degradation of sodium pyruvate in the experiment investigating the contribution of DET to electricity production. Values are means of triplicate experiments ± standard deviation.

	Acetic acid (mg ml $^{-1}$)	Butyric acid (mg ml^{-1})
Test		
Combined	236 ± 4	41 ± 2
Mediated	311 ± 5	171 ± 4
Direct	301 ± 4	199 ± 3

3.3.5. COD degradation and coulombic efficiency.

Table 3.4 shows the comparison of substrate degradation as COD and amount of electron recovery on day 11 of the investigation. The CM system gave the highest substrate utilization of 43 ± 2% with a coulombic efficiency (CE) of 13 ± 2% whereas MET gave 36 ± 3% COD reduction with a CE of 20 ± 4%.

Table 3.4. Comparison of substrate degradation and electron recovery at 11 days of investigation for contribution of mediated mechanisms of electron transfer processes by S. oneidensis.

	Combined	Mediated
COD degradation (%)	43 ± 2	36 ± 3
Coulombic efficiency (%)	13 ± 2	20 ± 4

3.4. Discussion.

Microbial fuel cell is a promising technology for sustainable wastewater treatment. The concept is possible due to extracellular electron transfer passed on from electrogenic organism via different mechanisms to catalyse anodic reactions for current production (Choi and Sang, 2016). There are three known mechanisms through which extracellular electron transfer in *Shewanella* might occur; these are direct electron transfer and transfer using redox shuttles (Oram and Jeuken, 2016). However, the contribution of electron transfer mechanisms utilized by *S. oneidensis* for electricity production in MFCs remain controversial (Jiang *et al*., 2010). The experiment aimed to investigate the contribution of direct electron transfer mechanism to electricity production in microbial fuel cells utilising *Shewanella* as biocatalyst. This mechanism is thought to involve four key proteins – CymA, MtrA, MtrB and MtrC (Figure 3.6) – which form a conduit for electron transfer from the quinone pool to the outside of the cell. Other direct electron transfer pathways e.g. the MtrFDE pathway has also been suggested (Kracke *et al.,* 2015). Conductive appendages (pili) might also be involved.

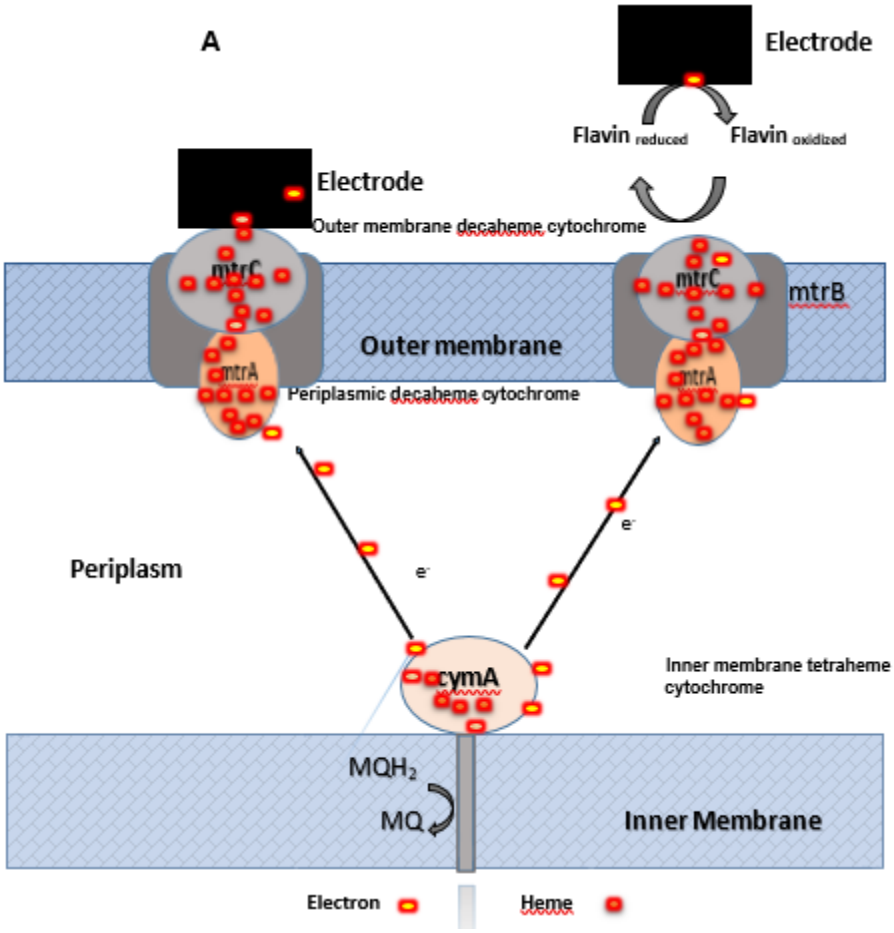

Figure 3.7. Proposed extracellular electron transfer (EET) pathways in S. oneidensis MR-1 involved in direct EET pathway – A, and mediated EET – B. MQH_2 is the reduced form of menaquinone; MQ, oxidized form of menaquinone.

The experiment aimed to investigate the contribution of direct electron transfer mechanism respond for charge transport at the microbe/electrode interface for electricity production in microbial fuel cells. This work employed the use of dialysis which has MWCO 12,000 Da pore size that can entrap *S. oneidensis* cells close to the electrode for microbe-electrode direct electron transfer, and synthesis of sodium alginate beads to control *S. oneidensis* cells from having physical contact with the electrode surfaces whereby the only possible means of electron transfer to electrode is by mediated electron transfer process. Transport. The results indicated that in the case where a dialysis membrane was used (Figure 3.4) DET makes a significant contribution, $\frac{\left[\frac{(114+129)}{2}\right]-32}{\left[\frac{(114+129)}{2}\right]}$ = 74%, to overall electricity production. When cells are

retained close to the anode, direct electron transfer was assumed to be the main mechanism but this does not stop mediated electron transfer from operating hence the averaging of the two maximum power density values 114 and 129 mW m^{-2}. When cells were immobilised in alginate beads (Figure 3.6) the corresponding contribution was $\frac{(105-36)}{105} = 66\%$. This contribution is antithetical to previous work that electron transfer occurs predominantly by mediated electron transfer (Jiang *et al*., 2010). The results are however, in direct contrast to the work of Kotloski and Gralnick (2013) who showed that direct electron transfer accounted for ca. 25% of *Shewanella's* ability to reduce insoluble substrates. They showed this by generating mutants of *Shewanella* that could no longer secrete redox shuttles (flavins) and characterising the mutants for reduction of Fe^{3+} in comparison with wild type strains. The reduced electron transfer in the riboflavin-deficient mutant in this case could also have been due to reduced cell growth rate reducing substrate turnover rate as riboflavin is necessary for growth.

Table 3.4 indicates that DET gives more CE than other mechanisms possibly because retaining the cells close to the anode helps to overcome resistances to electron transport from bacteria to the anode by the formation of cells on the anode as a biofilm and by direct contact of cells to the anode via cytochromes (Mohan *et al*., 2008). In the case of CM and MM, the observed diminished CE can possibly be due to diversion of electrons for biomass growth (Zhuang *et al*., 2012).

Table 3.4 indicated a strikingly low concentration of butyric acid production by CM which could be explained by Figure 3.3 at day 8, when the voltage increased after a gradual decline suggesting a metabolic shift. Butyrate could have been reused as substrate as was also observed by Finch *et al*., 2011

The less COD reduction observed by DET as shown in Table 3.4 can be due to the diffusion limitation of substrate across the dialysis membrane limiting the availability of substrate that can be readily consumed.

3.5. Concluding remarks

The outcome of this investigation revealed the importance of direct electron transfer mechanism utilized by *S. oneidensis* for electricity production in MFCs. The

investigation found that 66-74% of the electrons transferred could be attributed to the cells being in close proximity with the anode electrode suggesting that avenues for improving direct electron transfer in *Shewanella* spp (or heterologous expression in other hosts) should be given more priority in investigations to improve electricity production from microbial fuel cells. This has been attempted in Chapter 4 involving synthetic biology.

Chapter 4

Enhancing electricity production in MFCs by overexpression of *mtrAB* in *S. oneidensis* and heterologous expression of *mtrCAB* in *E. coli*

4.1. Introduction

S. oneidensis has been extensively studied in MFCs. Its potential in MFCs application is based on its anaerobic respiratory pathway (Mtr-pathway) which the proteins form a complex and has been associated with great environmental impact in reduction of iron and manganese oxide (Belchik *et al*., 2011; Cheng *et al*., 2013). The Mtr-pathway of *S. oneidensis* is the best understood among the Disimilatory Metal Reducing Bacteria (DMRB) and comprises of c-type cytochrome that shuttle electrons from the cytoplasmic (an inner membrane oxidizing enzyme) towards the outside of the cell during anaerobic growth. When *S. oneidensis* is grown under metal or electrode respiring conditions, reduction equivalents (Figure 4.1) from the oxidation of organic compounds are transferred from the entry point of the menaquinol pool to the cytoplasmic membrane-bound tetraheme cytochrome c *cymA*, to the periplasmic decaheme cytochrome c *mtrA* and finally to the outer membrane beta-barrel protein encoded by the gene *mtrB*, which plays an additional role for proper localisation and insertion of the outer membrane deacheme oxides cytochrome c (the *mtrC*) involved in direct electron transfer extracellularly to metal and electrodes. These proteins complexes are known as mtrCAB pathway (Jensen *et al*., 2016; Tai *et al*., 2010). While heterologous expression of the Mtr-pathway in *E. coli* has been studied with regard to metal oxide reduction (Jensen *et al*., 2010), the role of the genes in direct electron transfer in an MFC environment has not been reported. Further, the overexpression of the Mtr-pathway in *S. oneidensis* itself has not been reported.

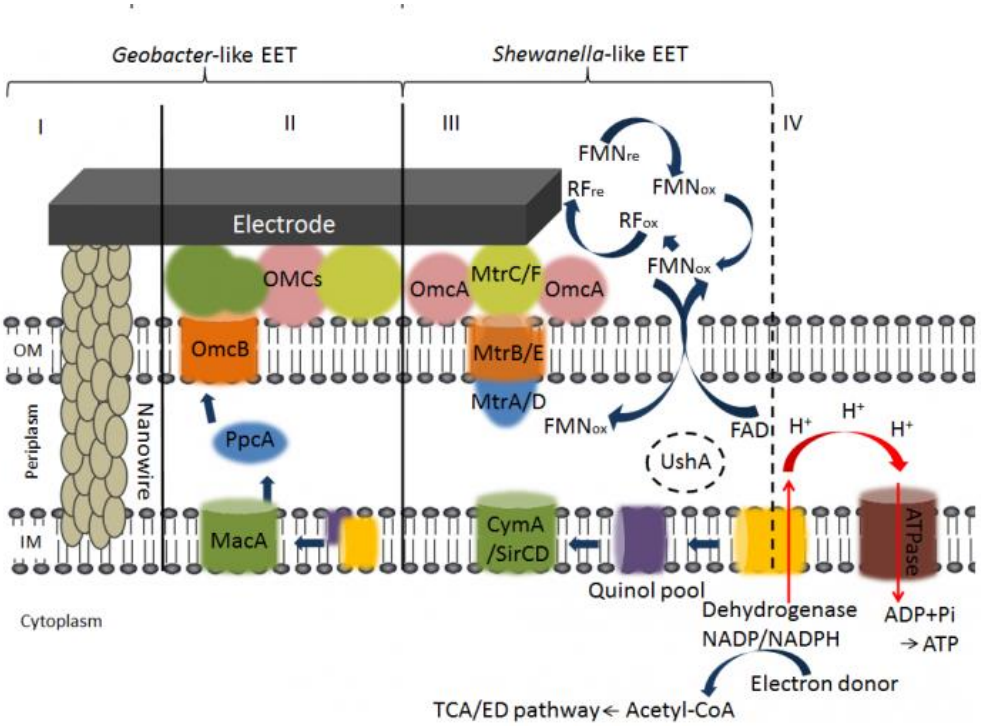

Figure 4.1. Hypothetical extracellular electron transfer (EET) pathways at an anode: I. via conductive nanowires; II. Direct electron transfer via outer membrane cytochromes (OMCs); III. Complex electron transfer via OMCs and redox mediators, e.g. Riboflavins; IV. Connection to motive force formation and ATP generation.

Next generation sequencing has provided genomic sequence data for *S. oneidensis* Mtr-pathway genes (see appendix 5-7 for nucleotide sequences coding for *mtrCAB* pathway). Bacterial genes that function or interact together are often clustered together in bacterial genome and have minimal effect on gene expression.

The molecular weight of mtrCAB protein, elucidated using biochemical and molecular biology techniques and using homologue crystal structure, showed that MtrC is made up of 69-KDa while mtrA is made of 32-KDa, while mtrB is made up of 72-KDa. These proteins when co-purified from *S. oneidensis* are predicted to form 1:1:1 complex. Several studies have been conducted to understand the roles played by the expression of genes involved in the mtrCAB pathway e.g. in metal reduction. Deletion of the *mtrC* gene was shown to improve chromium reduction in *S. oneidensis* (Belchik *et al*., 2011). Heterologous expression of the *mtrCAB* pathway in *E. coli* strain BL21(DE_3) using plasmids under the regulation of a strong promoter displayed limited control of *mtrCAB* expression, impaired cell growth compared to the wild type and this was attributed to problems in mis-regulation of the post

translational modification of *mtrCAB* conduit (Figure 4.2) due to excessive production of signal sequence-containing polypeptides secretions that could overload the Sec translocon system, hence, resulting in the aggregation of polypeptide in the cytoplasm (Goldbeck *et al*., 2013).

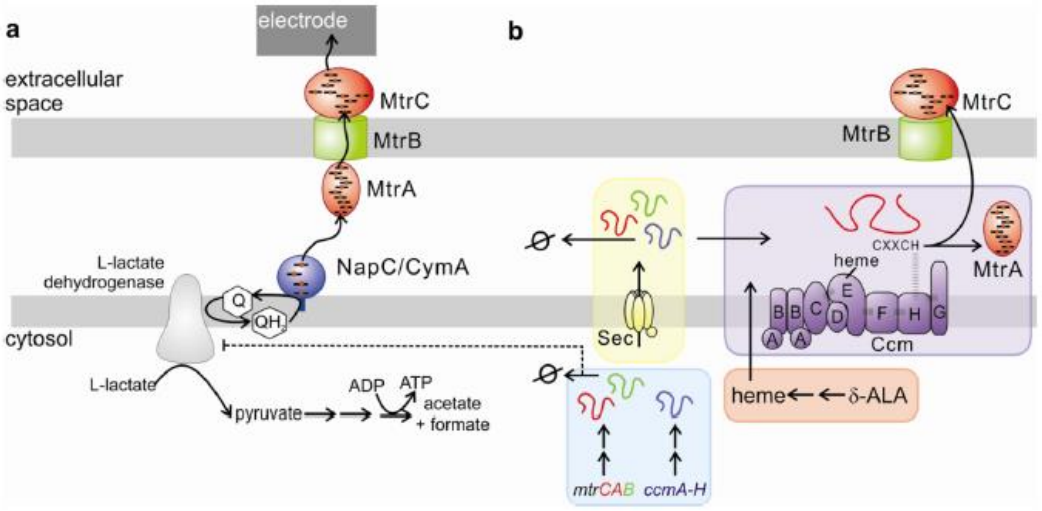

Figure 4.2. Schematic diagram of mis-regulation of post-translational modification of mtrCAB gene adapted from Goldbeck et al., 2013.

iGEM teams from Bielefeld University, Germany <http://2013.igem.org/Team:Bielefeld-Germany/Project/MFC> and York University, UK < http://2013.igem.org/Team:York_UK> have made genetic constructs and attempted to express the *mtrABC* operon in *E. coli* but they failed to show that the genes were expressed citing possible problems with regard to expression regulation, heme loading, correct folding and localisation of the cytochromes. It could also be that the proteins expressed were toxic to *E. coli* cells.

MtrCAB studies using promoters with strong activity by Goldbeck *et al*., 2013 reported reduced cell growth when *E. coli* was transformed with the *mtrCAB* operon but extracellular electron transfer (EET) was improved. However, over expression of *mtrC* and *mtrA* studied in three electrode microbial electrochemical system by increasing promoter strength did not significantly improve current production in *E. coli* compared to cells with fewer morphological changes (having *mtrCAB* conduit) which generated highest current (Goldbeck *et al*., 2013) and engineering of *mtrCAB*

pathway in *E. coli,* improved the reduction of metal ions and solid metal oxides approximately 8 fold and 4 fold faster than its parental strain (Jensen *et al*., 2010). Hence, there could therefore be the potential of using synthetic biology approach to engineer *S. oneidensis* for increasing electron transfer pathways and hence, improve electricity production in MFCs.

The whole structure and function of an organism is controlled or determined by its DNA (Barabasi and Oltvai, 2004). Before the advent of gene cloning, classical random mutagenesis approach has been used to identify genes functions. This involves studying mutant that either lack genes or express an altered version of the genes, hence, determining the cellular processes that have been disrupted or compromised (Hughes et al., 2000). Today numerous genome projects have added nucleotide sequences to the public data bases such as in National Centre for Biotechnology Information. Several techniques have been used for cloning such as Gateway Recombination Cloning, TOPO Cloning and Gibson Assembly. However, the challenge with these methods are limited numbers of fragments that can be cloned or often requiring the creation of site directed mutagenesis (this is an invitro method of creating specific mutation in a known sequence) in-order to by-pass illegal restriction sites (such as EcoR1, Xba1) existing within the gene to be cloned. This may affect gene function or create mutant genes (Wong et al., 2007). However, one recent method that can be used for cloning multiple fragments involves the use of Rapid DNA Prototyping (RDP) Assembly method. This method overcomes the problem, by bypassing the need for conducting site directed mutagenesis within the gene of interest and can be used to synthesize nucleotide sequence of genes between 125 to 3000 bp of known specific functions into functional parts called gBlocks (double-stranded sequence-verified genomic blocks) which are further standardized into formats that can be assembled for rapid prototyping of circuits from DNA regulatory elements. This can be used to build biological systems of pre-existing functions or new functions (http://synbiota-tinker-studio.wikidot.com/compliance-manual). RDP assembly method starts with an anchor and ends with a cap (Figure 4.5).

For the first time, this study employed the use of synthetic biology (an application driven-field with engineering approach to the redesign of existing or new complex biological systems from well characterised and usable DNA parts and circuits) by

using a new cloning strategy - Rapid DNA Prototyping (RDP) technology. This method bypasses traditional methods of molecular cloning which rely on the presence of restriction sites. Methods such as Golden gate assembly in both vector and insert methods are constrained to cloning of one or two inserts at a time (Roth *et al*., 2014). However, this new method is mostly similar to Gibson assembly method for modular assembly of bio brick libraries. One foundation principle of RDP technology is that a standard DNA part can be used to predict the combinations of DNA parts when assembled into larger genetic circuits (Figure 4.5). Each RDP part is defined by a promoter, RBS, coding region and terminator. A magnetic anchor is used to assemble series of RDP parts to form an expression plasmid system (http://synbiota-tinker-studio.wikidot.com/dna-assembly).

4.2. Materials and Methods

4.2.1. Chemicals

QIAquick PCR purification kit was purchased from Qiagen; gBlocks Gene Fragment of sequence verified *mtrA*, *mtrB* and *mtrC* were chemically synthesized from Integrated DNA Technology (IDT); the RDP kit was provided by Synbiota; Nebuilder Hifi DNA Assembly Master Mix was provided by New England Biolabs. Pierce ™ BCA Protein Assay Kit was purchased from Thermofisher Scientific; TAE Buffer 50X (Tris-acetate-EDTA) for running and separation buffer was purchased from Thermofisher Scientific. Chloramphenicol antibiotics, ethanol, butyric acid, acetic acid, sulphuric acid and glucose (purity ≥ 96%) were purchased from Sigma Aldrich (UK). All chemicals were of analytical grade and were used without further purification. Ficodox Plus™ mixed COD reagent was purchased from Fisher Scientific (UK), Riboflavin (Sigma Aldrich). The water used for making up solutions was deionised water (DI).

4.2.2. Bacterial strains, maintenance, and culture

S. oneidensis strain 700550 was purchased from ATCC. Top10 chemically competent *E. coli* cells that allow stable replication of high-copy number plasmids at a transformation efficiency of 1 x 10^9 CFU μg^{-1} plasmid DNA were generously provided by Dr. Mark Odell at the University of Westminster. Cryopreserved stock cultures section 4.2.11, were maintained at -80℃. Strains were first sub-cultured in

Luria-Bertani broth medium (LB medium/Chloramphenicol (25 µg mL^{-1})) containing (per litre) 10 g of tryptone, 5 g of yeast extract and 5 g of NaCl grown at 30^{o}C for 48 hours; later sub-cultured in minimal salt medium (MSM, required for increased solution conductivity for proton transfer during MFC operation) supplemented with 500 mg L^{-1} glucose and adjusted to 25 µg ml^{-1} chloramphenicol concentration. This last subculture was used to inoculate the MFCs. Before inoculation of the MFCs, the strains were grown in LB medium supplemented with 15 g L^{-1} agar containing 25 µg ml^{-1} chloramphenicol concentration and plated for enumeration.

4.2.3. Investigation 3: Experimental design.

The experimental design for heterologous expression of Mtr-pathway in *E. coli* due to time limitation was studied for 10.4 days and for overexpression in *S. oneidensis* studied for 15.5 days in two chambered MFCs, schematically described in (Figure 4.3). The inoculum studied were *E. coli* (Top 10) for the first experiment and *S. oneidensis* cells for the second experiment. Both were modified with individual construct of gene: *mtrA* or *mtrB* or *mtrC* or *mtrAB* or *mtrBC* or *mtrCAB* of the Mtr-pathway by following promega instruction protocol on transformation. The genes were expressed individually and as operons. The anode MFCs consisted of 10% (v/v) anode working volume of each inoculum. The inoculum used for control experiments for both studies were wild type *E. coli* and wild *S. oneidensis* respectively. The experiments were replicated in triplicate and tested for influence on power generation, COD removal and growth rate.

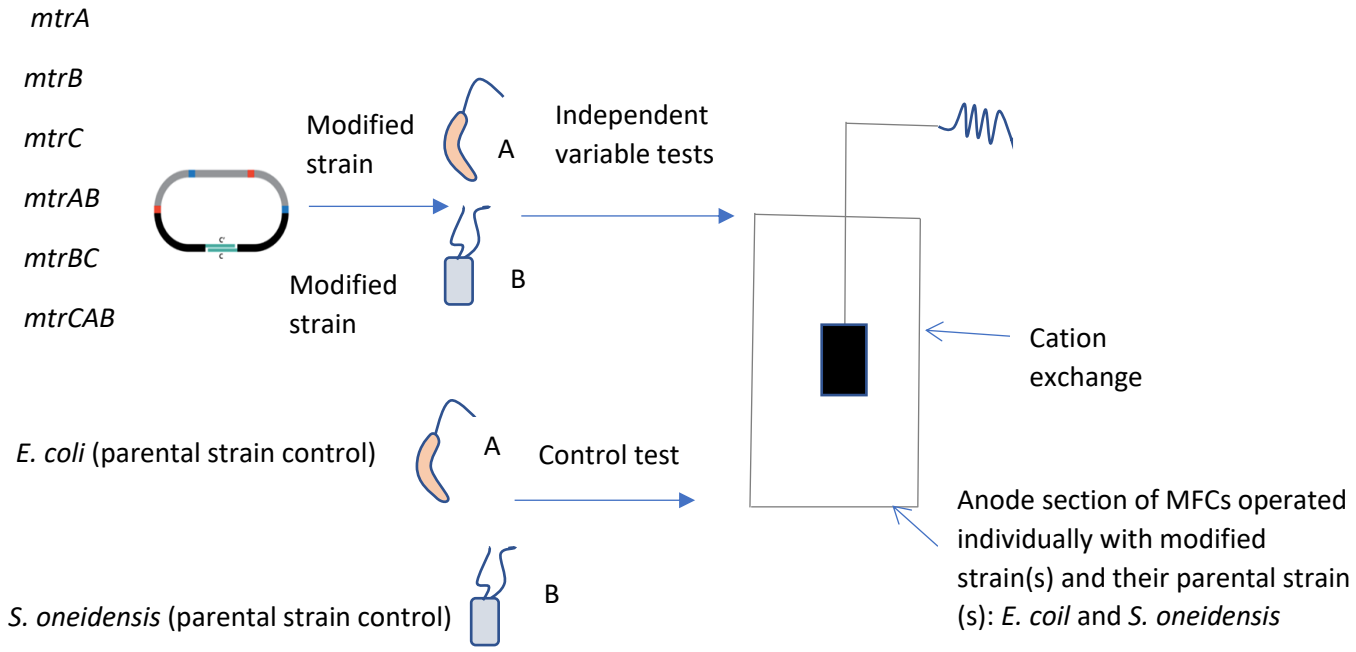

Figure 4.3. Schematic diagram of experimental design for tests (A) modified E. coli *and its parental strain, (B) modified S. oneidensis and its parental strain for the understanding of the genes involved in Mtr-pathway for electricity production in MFCs.*

4.2.4. MFCs Setup and Operation.

The MFCs setup and operation is as described in section 2.2.4. The cathodes contained no Pt catalyst layer (as the catholyte was ferricyanide - details below) and the electrodes had a geometric surface area of 50 cm^2.

For all set ups the volume of inoculum used was 10% v/v of the total anolyte volume. The anode chambers with the contained mixtures were stripped of dissolved oxygen by sparging nitrogen gas for 5 minutes before setup.

All experiments were replicated three times and studied at 30^0C using a temperature-controlled Stuart 160 incubator (Fisher Scientific, U.K.). Results were expressed as mean of replicates ± standard deviation

For all set ups, the volume of inoculum used was 10% v/v of the total anolyte volume. The anode chambers with the contained mixtures were stripped of dissolved oxygen by sparging nitrogen gas for 5 minutes before setup.

4.2.5. Modification of anolyte minimal salts medium used for the investigation of heterologous expression and overexpression of Mtr-pathway in *E. coli* and *S. oneidensis* respectively for bioelectricity production.

The anolyte MSM for the investigation of heterologous expression in *E. coli* and overexpression of Mtr-pathway *S. oneidensis* for bioelectricity production was supplemented with 500 mg L^{-1} glucose and 500 mg L^{-1} casein hydrolysate, trace element stock solution (1%) and vitamin stock solution (1%).

The catholyte used was 50 mM (pH 7) phosphate buffer containing 0.1M potassium ferricyanide, without aeration.

4.2.6. Gblocks RDP Primer design.

Primers used for amplification of the gBlocks were designed using Gentle-beta Synbiota software. It amplified the gBlocks into Rapid DNA Prototyping (RDP see Table 4.1) format. The primers used in this study and their relevant features are represented in Table 4.1:

Table 4.1. Primer used for amplification of cytochromes protein coding genes: mtrA, mtrB and mtrC (the prefix tcagtcagtcagtcag sequence represents X' format overhang attached to the primer sequence, while the prefix tcagtcagtcagtcag sequence represents z' formant overhang attached to the primer sequence).

Primer	Sequence 5'– 3' (RDP X-Z' format)
mtrA	tcagtcagtcagtcagGGTCTCAGATGAAGAACTGCCTAAAAATGAAAAACCT (Forward). ctgactgactgactgaGGTCTCTGCCGCGCTGTAATAGCTTGCCAGATGG (Reverse)
MtrB	tcagtcagtcagtcagGGTCTCAGATGAAATTTAAACTCAATTTGATCACTCT (Forward). ctgactgactgactgaGGTCTCTGCCGAGTTTGTAACTCATGCTCAGCATCAGC (Reverse)
mtrC	tcagtcagtcagtcagGGTCTCAGATGATGAACGCACAAAAATCAAAAATCGCA (Forward). ctgactgactgactgaGGTCTCTGCCGAGTTTCACTTTAGTGTGATCTGCAACTGT (Reverse)

4.2.7. Resuspension and Isothermal assembly of gBlock gene fragments (IDT).

gBlock tubes of *mtrA* (synthesized as one fragment from IDT (integrated DNA technology)), *mtrB* and *mtrC* (synthesized as two fragments from IDT) were centrifuged for 3-5 seconds at 3000 g to ensure the gene fragments were pelleted to the bottom of the tube. Thereafter, TE buffer was added to the gBlocks and vortexed to make a final concentration of 10 ng μL^{-1}. The gBlocks of *mtrB* and *mtrC* were

made into a single fragment using NEBuilder Hifi DNA assembly reaction protocol. Briefly, reactions consisting of 10 µl of NEBuilder Hifi DNA Assembly master mix, 6 µl of deionised water and 2 µl each of the two fragments of *mtrB1* and *mtr*B2 gBlocks (0.12 pmols each) and *mtrC1* and *mtrC2* gBlocks (0.06 pmols each) were incubated at 55℃ for 15 minutes to make a single fragment of *mtrB* gene and *mtrC* gene.

4.2.8. PCR amplification of gBlocks fragments.

Gentle generated primers were synthesized from IDT and used to amplify the gBlock fragments. This step creates the RDP ends to a standardized DNA parts. For this study, RDP X' – Z' orientation was selected because of complementarity to the genetic element parts in the Synbiota RDP™ plate kit (e.g. anchor, promoter, ribosome and cap) required for creating expression plasmid. The laboratory procedure involved, firstly, making the genetic blocks into single fragments of *mtrA, mtrB* and *mtrC* by using NEBuilder hifi DNA assembly reaction protocol (https://www.neb.com/protocols/2014/11/26/nebuilder-hifi-dna-assembly-reaction-protocol). The PCR amplification reactions included 4 µl of template DNA, 2 µl forward and reverse primer each and 92 µl of High fidelity master mix (X1). The PCR conditions included initial denaturation at 95℃ for 3 mins followed by 30 cycles of denaturation step at 95℃ at 30 secs, annealing step at 55℃ for 40 secs, extension step at 72℃ for 1 minute and final extensions at 72℃ for 10 mins. Amplified PCR products were firstly examined by nanodropping technique and checked on 0.6% agarose gel electrophoresis.

4.2.9. Analysis of amplified PCR products on agarose.

Agarose gel electrophoresis was used to separate amplified DNA samples. Agarose 0.5% (used for fragments of 200bp to about 20 Kb) was melted by heating in a microwave in 50 mL XTAE buffer (40 mM Tris-acetate, 1 mM EDTA and agarose/buffer mixture). Before the polymerization (non-covalently association and formation of network of polymeric molecules and pore size determines gel's molecular sieving properties) 1 µL Sybrgreen (binds double stranded DNA molecules by intercalating between the DNA bases in electrophoretic gel and fluorescent under

UV illumination) per 50 mL gel was used to pre-impregnate the gel. Gel loading buffer 6X (containing Ficoll which creates brighter and tighter bands, SDS for sharper bands, EDTA to chelate magnesium (up to 10 mM) for deactivating metal-dependent enzyme, a combination of two dyes: Dye 1 (red) and Dye 2 (blue). The two dyes separate upon gel electrophoresis. The red band is similar to bromophenol blue is the major indicator as a tracking dye on agarose) was added to the PCR products before applied to the gel. For identification of the fragments sizes, a 1kb ladder (BioLabs) with known fragment sizes and concentrations were used. The 50 mL gels were run at 100 V for 45 minutes. After electrophoresis has completed the gel were viewed under Ultraviolet visualizer (see Figure 4.4 to view the gel).

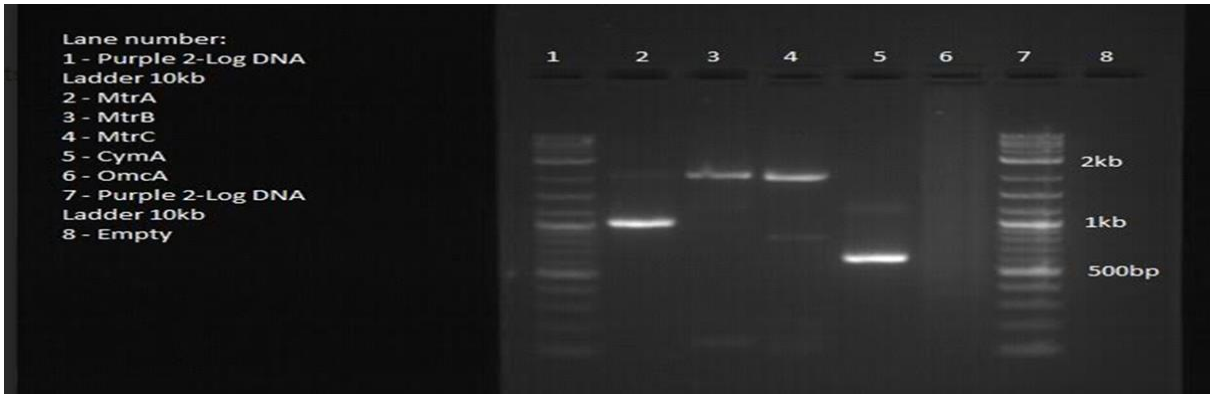

Figure 4.4. Gel image of agarose separation of mtrA, mtrB, mtrC … amplified genes viewed under UV visualization.

4.2.10. Digestion of amplified PCR products with BsaI Enzyme and assembly of RDP parts.

This procedure cleans up the PCR products by using QIAquick PCR purification kit before digestion with BsaI enzyme to create RDP sticky ends corresponding to the 5'- 3' direction of the amplicons. Briefly, 10 µl of NEB cutsmart buffer and 2 ul of BsaI-HF endonuclease (40 units) were added to the cleaned-up DNA (75 µl), then mixed and centrifuged briefly to pull down any splashes and bubbles. The mixtures were incubated at 37℃ for 1h. After incubation, the BsaI enzyme was inactivated by DNA clean up. Concentration of parts created was measured using Nano Drop in ng ul^{-1} and converted to pm ul^{-1} by using the close approximation: 1 pm ul^{-1} = 670 ng ul^{-1}

divided by the length of the part (kb). For the RDP assembly (Figure 4.5), the PCR parts were adjusted to a concentration of 0.04 pm ul^{-1} per reaction for a total of 0.2 pm in 5 ul RDP part.

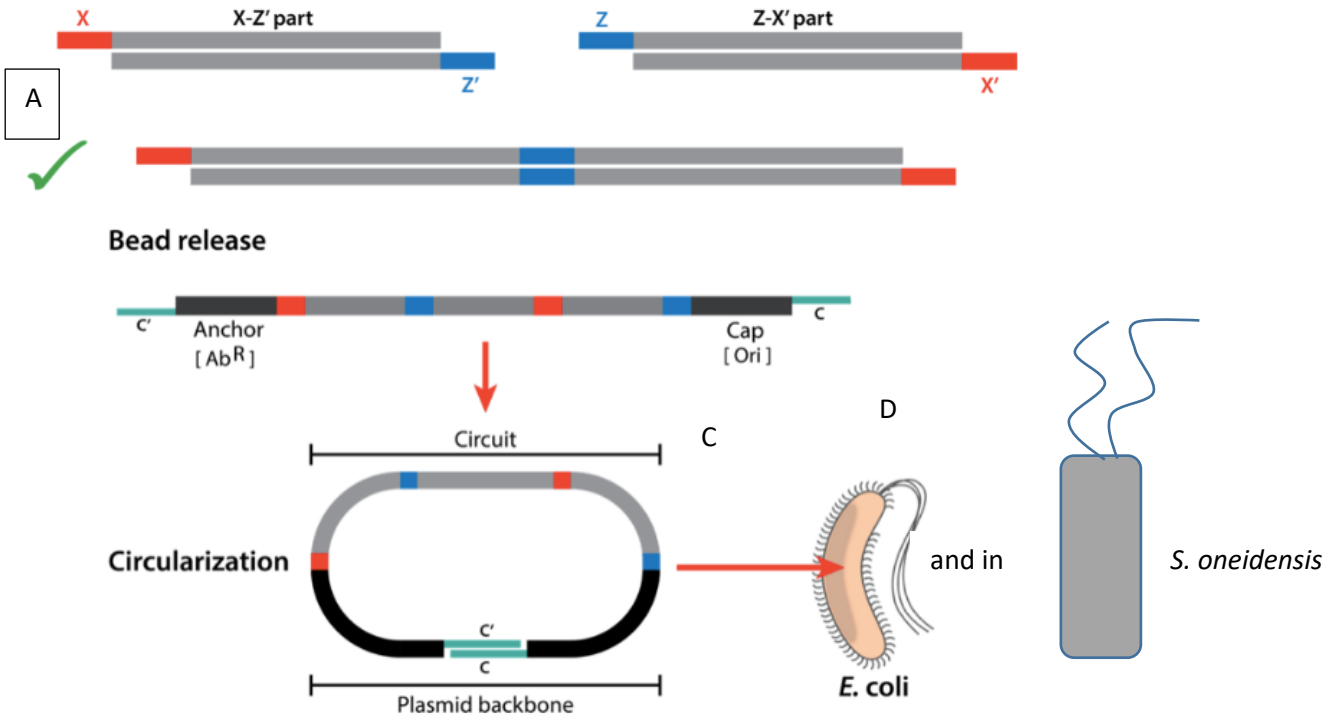

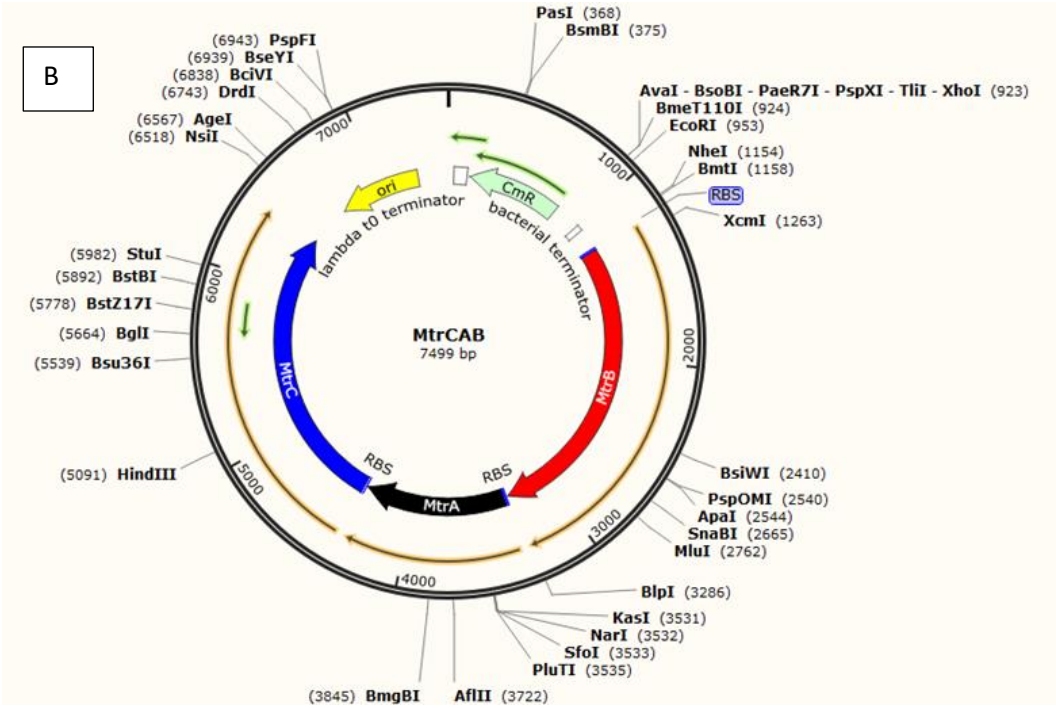

Figure 4.5. Schematic flow diagram of the RDP assembly procedure including transformation into E. coli and S. oneidensis); B - an example of RDP plasmid of *mtrCAB* construct designed using snap gene software.

RDP parts needed (Figure 4.6) for constructions of the assembly were firstly identified and organised from the RDP kit. The standardized genetic elements engineered into different constructs included the following (http://synbiota-tinker-studio.wikidot.com/dna-assembly):

- Fixed-level strong Promoter with short name x-Pr.3-z' (produces mRNA at a fixed rate.
- Strong Ribosomal Binding Site with the short name z-Rbs.3-x' (region when translated to mRNA acts as a binding site for ribosome to initiate translation.
- Anchor, chloramphenicol resistance with the short name dA18-ChlrR-x' (the chloramphenicol resistance marker composing of native fixed promoter, native ribosomal binding site, an engineered coding sequence (chloramphenicol acetyltransferase) and the TO forward terminator.
- Cap, high copy origin with short name z-Ori.3-dT18 (plasmid containing high copy Ori pMB1 exists at ~200-300 copies per cell.
- A periplasmic decaheme cytochrome DNA (created) with short name x-mtrA-z'
- An outer membrane decaheme cytochrome DNA (created) with short name x-mtrC-z'
- An outer membrane β-barrel DNA (created) with short name x-mtrB-z' (code for outer membrane β-barrel protein).

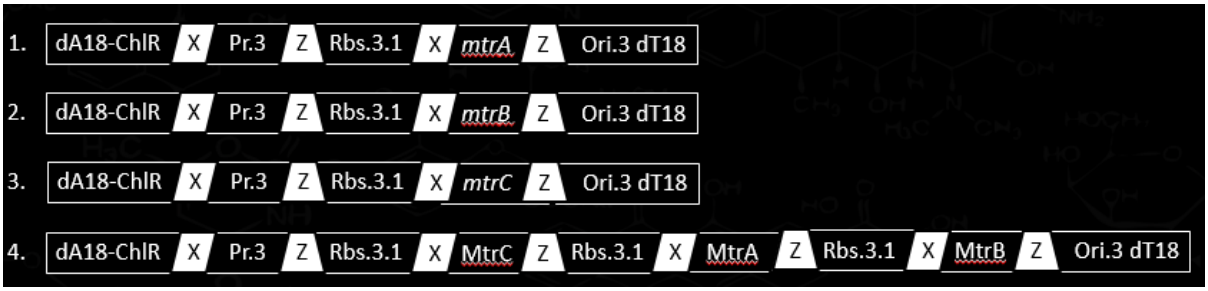

Figure 4.6. Synbiota RDP assembly of the cytochromes protein coding genes: mtrA, mtrB and mtrC parts and other genetic elements into constructs.

4.2.11. Making competent *S. oneidensis* cells and their transformation.

S. oneidensis cells were made competent by following the method used by Hanahan, 1985. Briefly, *S. oneidensis* cells were inoculated into 5 ml SOC medium and grown overnight in a shaker at 30℃. Thereafter, the cells were subcultured in Luria-Bertani medium (20 g L^{-1}) and grown at 30℃ until optical density (600 nm) reached ~0.5. The cells were pelleted by centrifuging at 5000 g at 4℃ using Thermo Fisher Centrifuge. Pelleted cells were suspended in transformation buffer1 (8 ml TB1 pH 6.4). The TB1 solution contained KCl 7.4 g L^{-1}, KCH_3COO 30 ml of 1M (pH7.5), $CaCl_2.2H_2O$ 1.5 g L^{-1} and $C_3H_8O_3$ 150 g L^{-1}. The solution was adjusted to pH 6.4 with 0.2 M acetic acid. The suspended cells were placed on ice for 15 minutes and then spun down as above. Thoroughly the pelleted cells were suspended in transformation buffer 2 solution (4 ml, TB2) containing KCl 0.74 g L^{-1}, $CaCl_2.2H_2O$ 11 g L^{-1} and Glycerol 150 g L^{-1} and 0.5 M MOPS (20 ml) for 2 hours on ice. Aliquot competent *S. oneidensis* cells were stored immediately at -70ºC.

The transformation of *S. oneidensis* with plasmid constructs was done using Promega instruction protocol on transformation. Briefly, frozen chemically competent *S. oneidensis* cells (from -70℃) were placed on ice until thawed. Pipette tips maintained at 4℃ were used to transfer cells by distributing the thawed cells into chilled sterile 17 x 100mm polypropylene culture tubes (100ul each). 10 ng of the plasmid constructs were added to 100ul of competent cells and placed on ice for 10 minutes. The tubes with mixtures were heat-shocked for 50 seconds at 40ºC in a water bath. The tube was transferred to ice without shaking and after 2 minutes 900ul of cold (4 ºC) SOC medium was added to the transformation reactions and incubated at 30ºC for 60 minutes with shaking (225 rpm). The cells (10 ul each) were confirmed for transformation by plating on LB/Chloramphenicol plates (25 µg mL^{-1}) grown overnight at 30℃. Efficiency of transformation of *S. oneidensis* (in CFU formed per microgram DNA) was calculated using the following equation 16:

Equation 16: $$\frac{cfu\ on\ plate}{ng\ of\ competent\ Cells\ DNA\ plated} \times \frac{1\ X\ 10^3\ ng}{\mu g}$$

4.2.12. Determination of total protein content of anodic broth from MFCs utilizing overexpression of *S. oneidensis* mtr-pathway.

The total protein content was estimated by using Thermos Scientific Pierce Bicinchoninic Acid Reagent (BCA) Protein Assay for the colorimetric detection and quantitation of the total protein. This method combines well- known reduction of Cu^{+2} from the BCA reagent to Cu^{+1} (cuprous cation) by protein in an alkaline medium (the biuret reaction) and colorimetrically detected. Briefly the water-soluble complex exhibits a strong absorbance at 562 nm. Briefly, a series of dilutions of known concentrations of Bovine Serum Albumin (2 mg mL^{-1}, BSA) were prepared to prepare a set of protein standards (appendix 2). The concentration of the standards were µg mL^{-1} (250; 125; 50; 25; 5; 0) and assayed alongside with the unknown(s) samples extracted by using physical disruption using protein extraction kit. Thereafter 0.1mL of each standard and unknown samples triplicate were added to 2 ml of BCA (20 – 2,000 ug mL^{-1}). The mixture was allowed to incubate at 37℃ for 30 minutes. The absorbances of all the samples were measured using a spectrophotometer at 562 nm after 10 minutes.

4.3. Results

4.3.1. Summary

Synthetic biology was employed in this study to overexpress the genes: *mtrA* (periplasmic membrane cytochrome), *mtrB* (outer membrane β-barrel protein) and *mtrC* (outer membrane decaheme cytochrome C) involved in the Mtr-pathway for understanding and enhancing extracellular electron transfer in *S. oneidensis* and heterologous expression in *E. coli*. The genes were expressed individually or as operons and the effect on electricity production and substrate utilisation determined. The best outcome regarding power generation was from the *mtrAB S. oneidensis* strain which produced 144 ± 4 mW m^{-2}; this was 3 fold higher than the wild type (48

± 2 mW m^{-2}). Regarding *E. coli*, the best power was obtained from the *mtrCAB* strain which produced 25 ± 0.7 mW m^{-2} compared to 1 ± 0.01 mW m^{-2} by the wild type. The *mtrAB S. oneidensis* strain utilised 36% of the substrate compared to 30% utilized by the wild type. The *mtrCAB E. coli* strain utilised 27% of the substrate compared to 73% utilized by the wild type *E. coli.*

Table 4.2. Summary of results (A) modified E. coli and its parental strain, (B) modified S. oneidensis and its parental strain for the understanding of the genes involved in Mtr-pathway for enhancing electricity production in MFCs.

A	*E. coli*	*mtrA*	*mtrB*	*mtrC*	*mtrCAB*	*mtrAB*
Power Production (mW m^{-2})	1 ± 0.01	8.15 ± 0.02	4.7 ± 0.01	2.5 ± 0.02	25 ± 0.7	7.1
%COD Reduction	73 ± 2	3 ± 1	45 ± 3	24 ± 1	27 ± 2	21 ± 2

B	*S. oneidensis*	*mtrA*	*mtrB*	*mtrC*	*mtrCAB*	*mtrAB*
Power Production (mW m^{-2})	48 ± 2	77 ± 2	nil	65 ± 3	78 ±3	144 ± 4
% COD Reduction	30 ± 1	76 ± 3	39 ± 2	88 ± 2	94 ± 2	36 ± 1

4.3.2. Voltage-time profiles and polarization curves.

The overexpression and heterologous expression of Mtr-pathway on voltage-time profile, polarisation, and power density curves are shown in Figures 4.7 & 4.8 respectively. What is striking from the figure is that S. *oneidensis mtrAB* strain gave the highest maximum voltage of 530 mV. This was followed by *mtrBC* strain (491 mV), *mtrA* strain (489 mV), *mtrCAB* strain (454 mV), *mtrC* strain (434 mV), the wild

type (376 mV) and finally *mtrB* (16 mV). The voltage produced by E. coli was observed to decline after a stable voltage from the first to the second day of the studies (Figure 4.7B).

Regarding power production, what stands out in Figure 4.8A is that *mtrAB S. oneidensis* strain gave the best maximum power production while *mtrB* strain gave the least power. The power generated by *mtrAB* strain was 144 ± 4 mW m^{-2} (3-fold more than what was produced by wild type). There were similar power densities for *S. oneidensis mtrCAB, mtrA*, *mtrBC* strain produced 78 ± 3 mW m^{-2}, 77 ± 2 mW m^{-2}, 74 ± 5 mW m^{-2} respectively.

What is interesting by the studies involving heterologous of Mtr-pathway in *E. coli* (Figure 4.8B) was that the maximum power produced was by *mtrCAB E. coli* strain which produced 25±0.7 mW m^{-2} while it stands out that *mtrAB* strain produced 7.1 mW m^{-2}. The highest power of 25 ± 0.07 mW m^{-2} produced by *mtrCAB E. coli* strain was 25-fold of that produced by the wild type (1 ± 0.01 mW m^{-2})

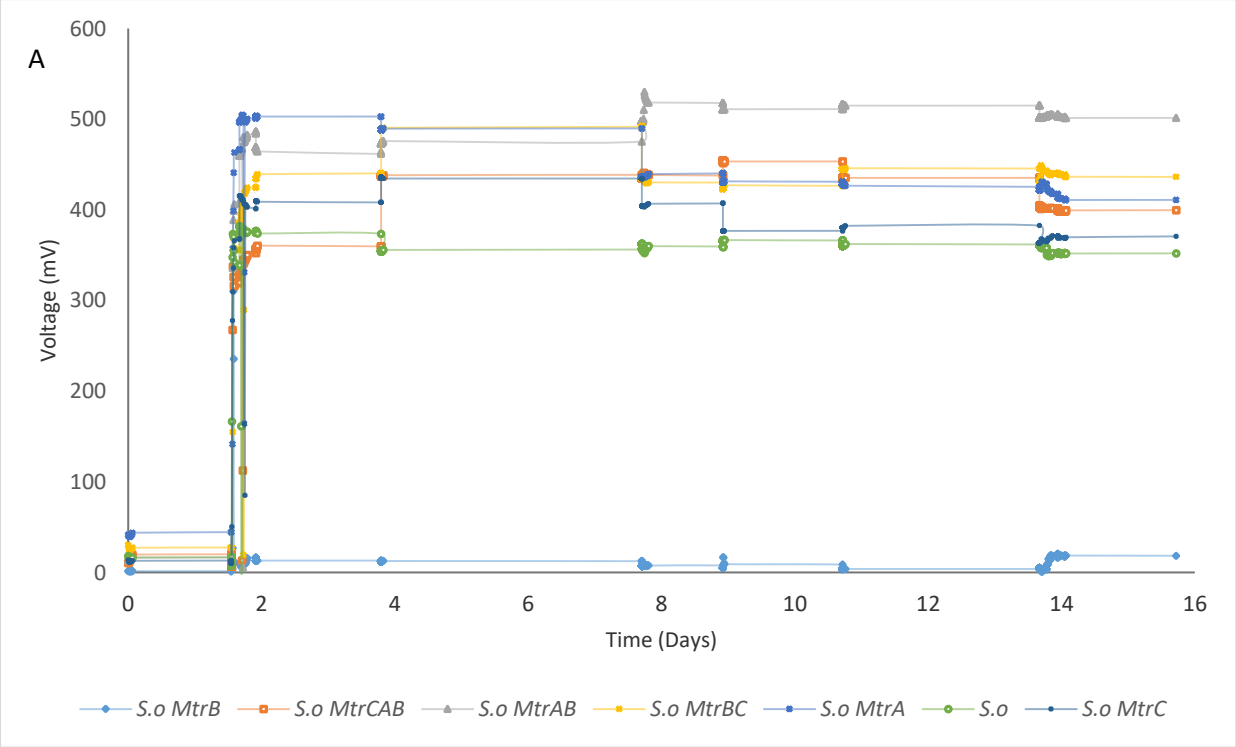

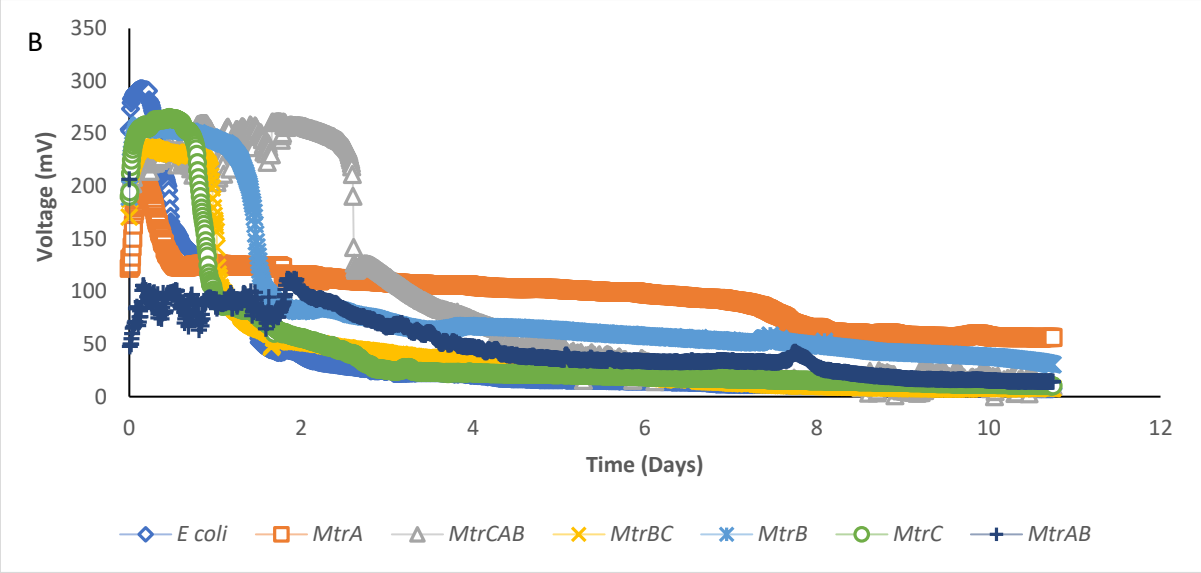

Figure 4.7. Voltage generation by S. oneidensis strains (A) and E. coli strains (B). Maximum voltage production by recombinant strains were: S. oneidensis mtrAB strain 530±6 mV compared with 376 ± 8 mV by the wild type (A); E. coli mtrCAB strain produced 257±5 mV compared with 39 ± 2 mV by the wild type (B).

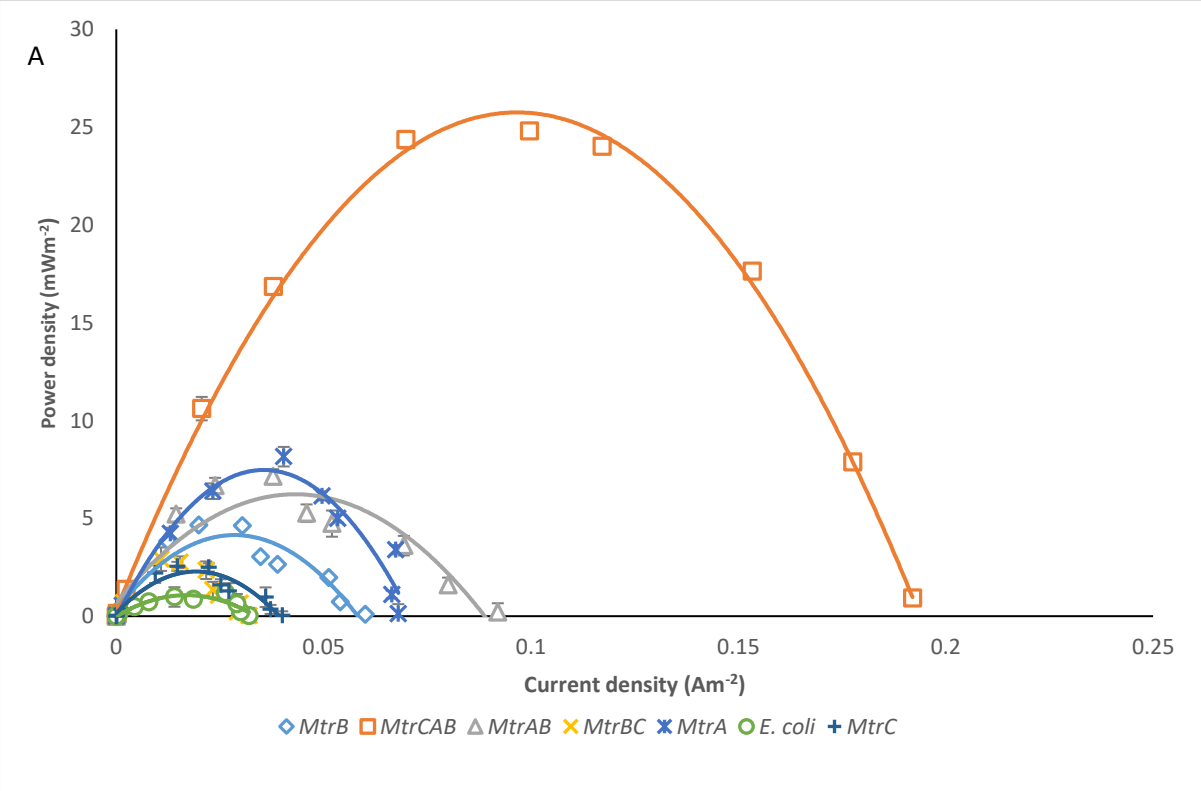

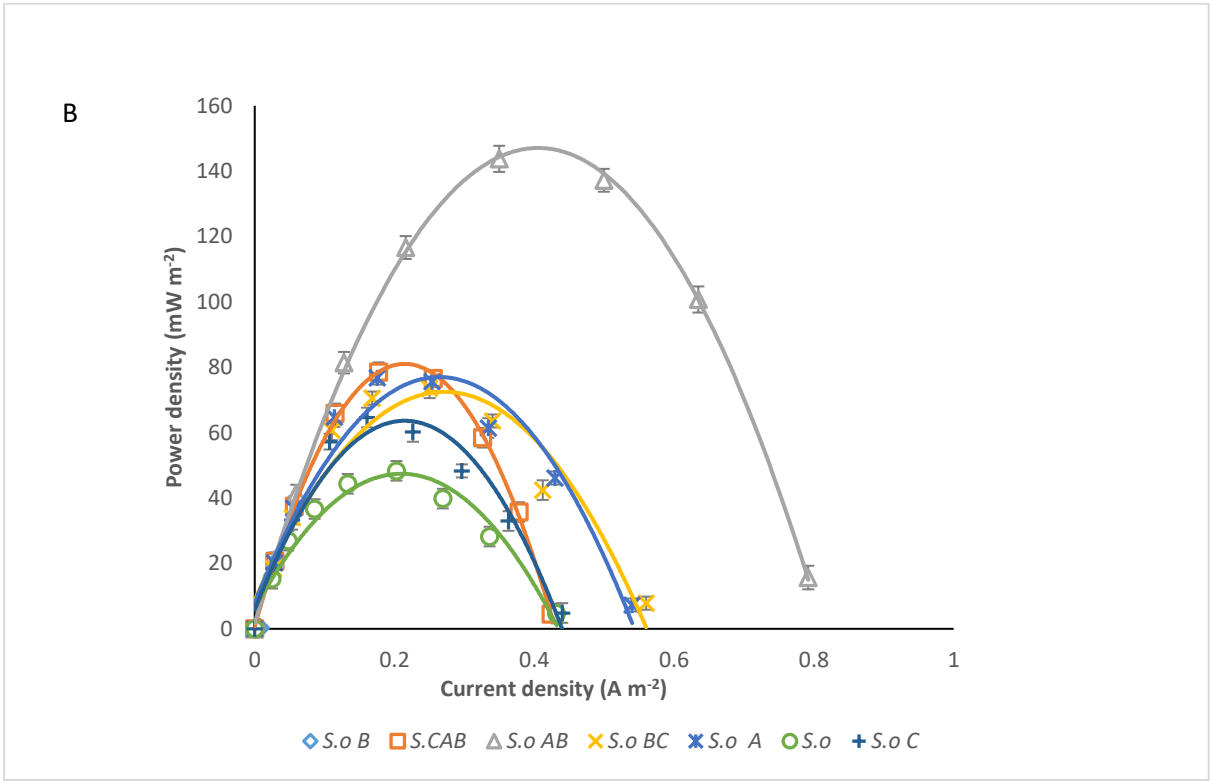
B
160
140
120
100
80
60
40
20
0
Power density (mW m-2)
0
0.2
0.4
0.6
0.8
1
Current density (A m-2)
S.o B
S.CAB
S.o AB
S.o BC
S.o A
S.o
S.o C

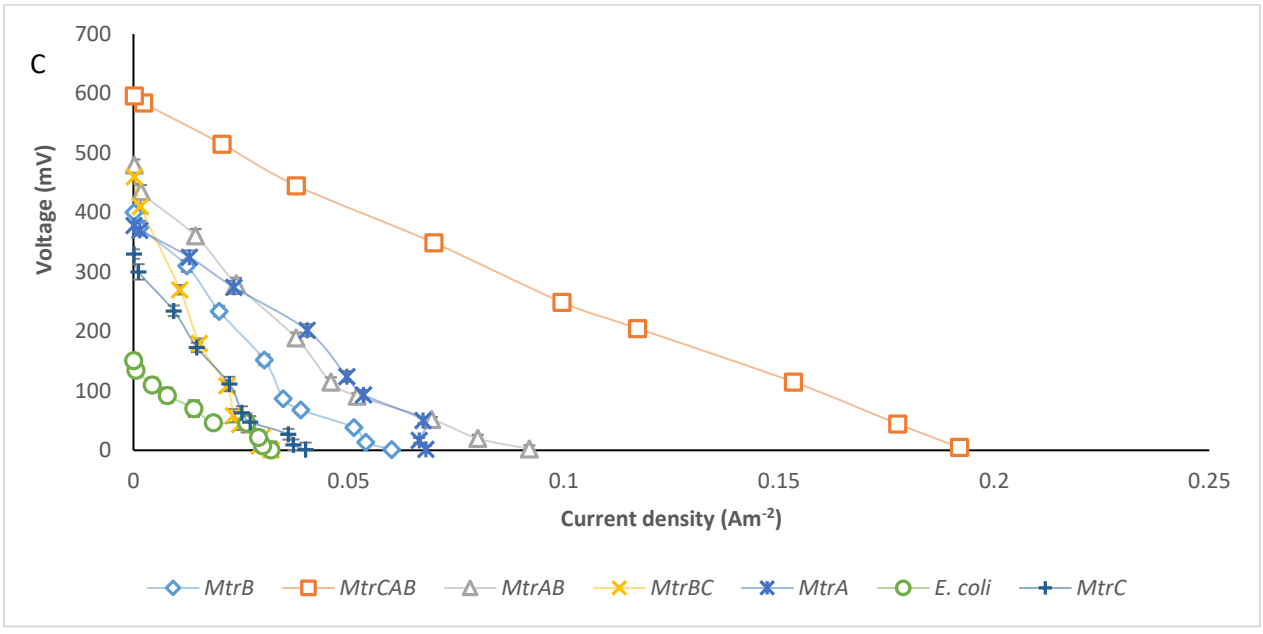
C
700
600
500
400
300
200
100
0
Voltage (mV)
0
0.05
0.1
0.15
0.2
0.25
Current density (Am-2)
MtrB
MtrCAB
MtrAB
MtrBC
MtrA
E. coli
MtrC

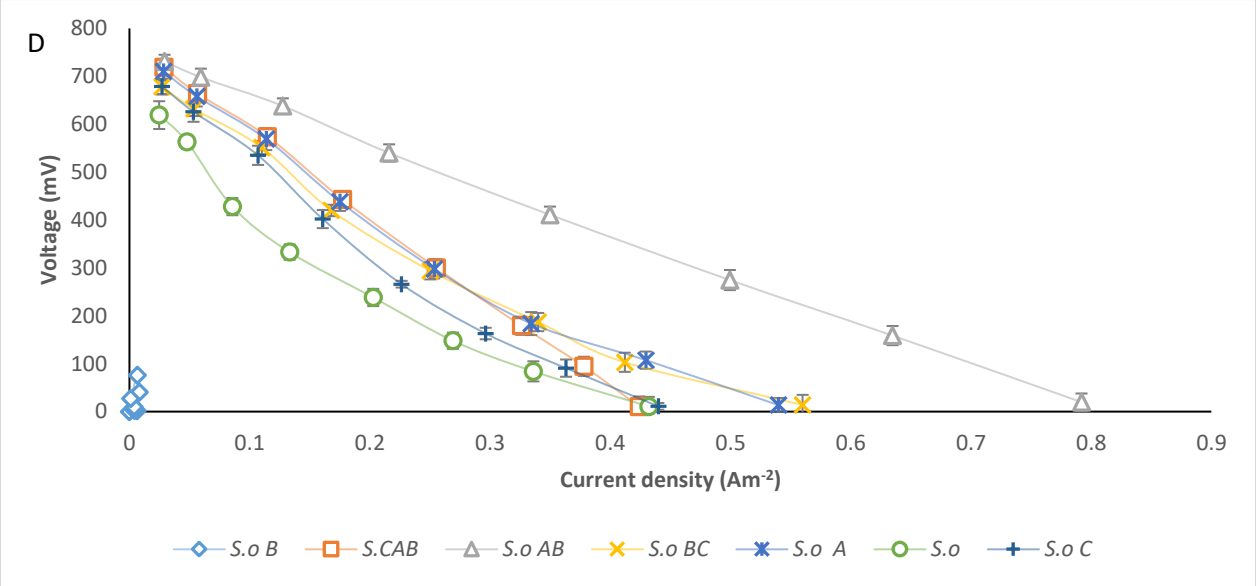

Figure 4.8: Polarization curves (C & D) and power density curves (A&B) for the experiment involving expression and overexpression of the Mtr pathway in E. coli (B&D) and in S. oneidensis (A&C) respectively. Maximum power produced by recombinant and wild types of S. oneidensis (A) and of E. coli (B) respectively are S. oneidensis mtrAB 144±4 mW m^{-2} and 48±2 mW m^{-2} for the wild type (A); E. coli 25±0.7 mW m^{-2} and 1±0.01mW m^{-2} for the wild type.

4.3.3. Analysis of COD utilization in relation to specific growth rate of wild type and recombinant *S. oneidensis* and *E. coli* constructs.

As shown in Figure 4.9, increase in specific growth rate can be correlated with COD utilization. The *mtrCAB S. oneidensis* strain and *mtrCAB E. coli* strain, both had the highest specific growth rate with corresponding COD utilization of 94% and 27% respectively. What is striking in the figure is that the MFCs utilising wild type *S. oneidensis* and wild type *E. coli* recorded COD utilization of 30% and 73% (highest recorded from *E. coli* studies) respectively.

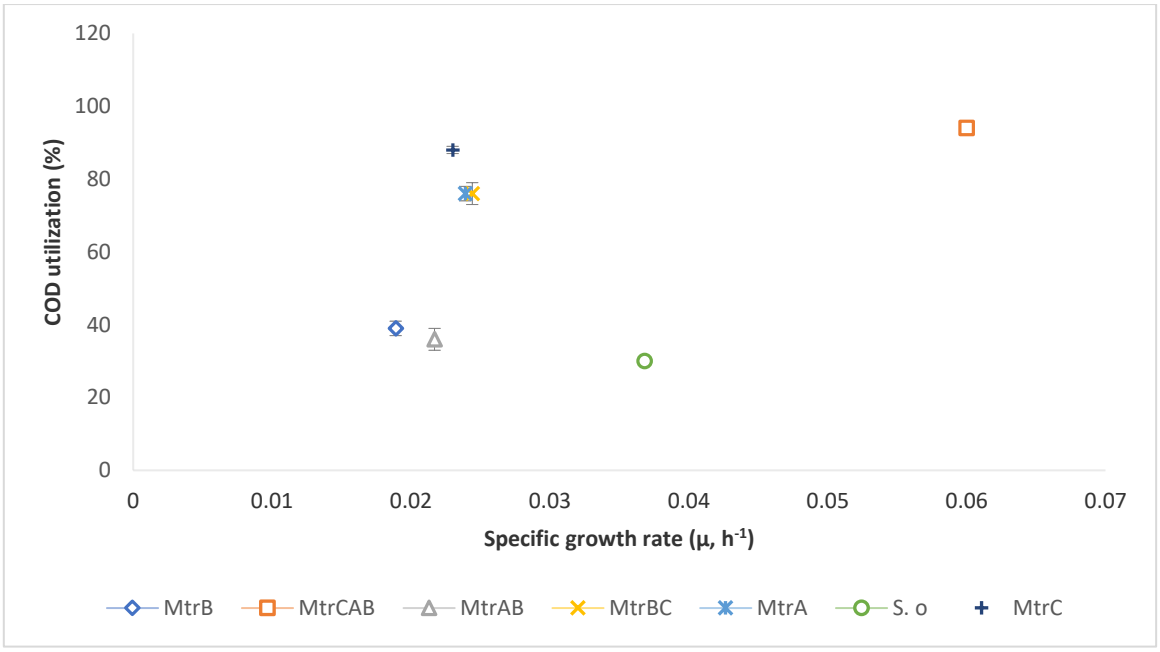

Figure 4.9. Comparison of substrate utilization (%COD) and specific growth rate (μ) for different S. oneidensis and E. coli constructs.

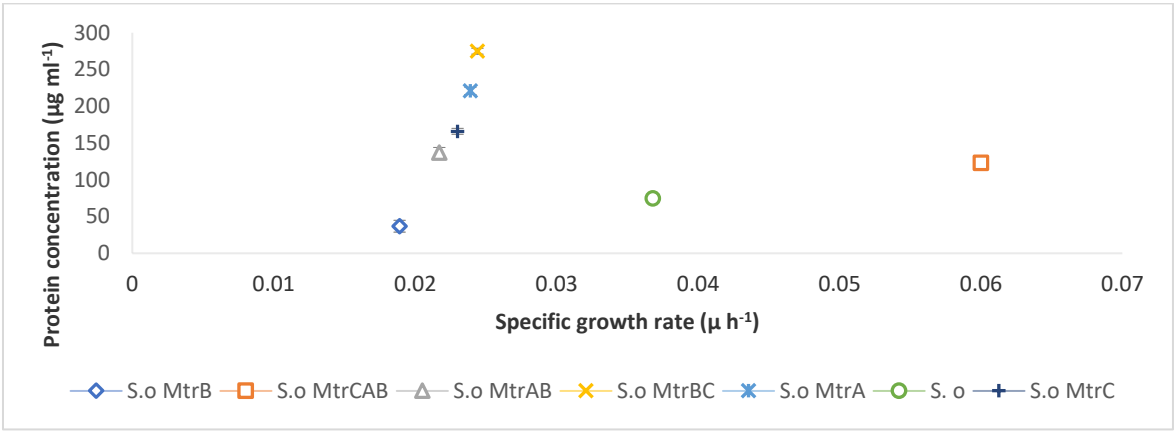

Figure 4.10. Correlation between total protein concentration in the broth sample and specific growth rate of S. oneidensis constructs at the end of investigation (day 16).

Figure 4.10 indicates a correlation between amount of protein secreted and increase in the specific growth rate of *S. oneidensis*.

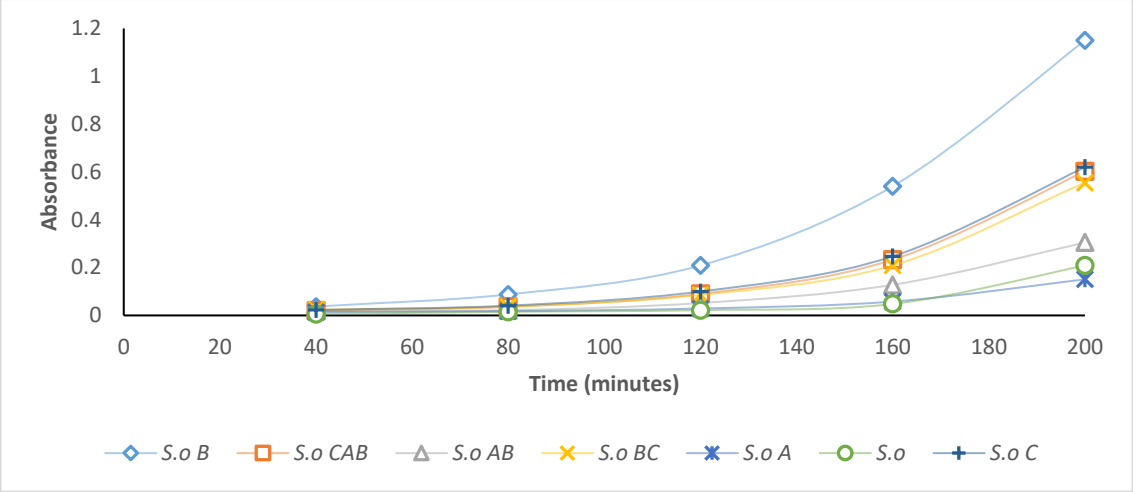

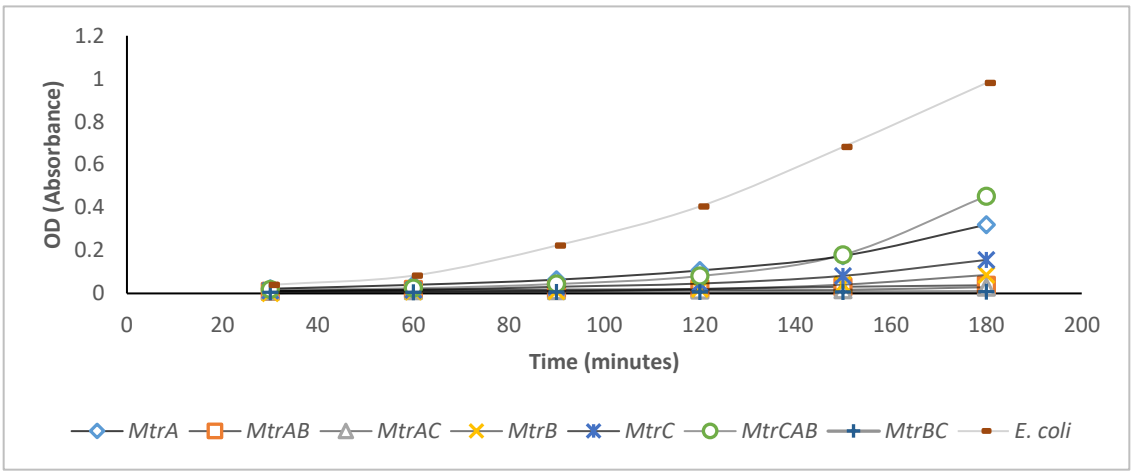

Figure 4.11. Growth curve plot measured as absorbance against time (non MFCs condition) for the recombinant and wild type strain of E. coli and S. oneidensis.

Growth analysis and specific growth studies are shown in Figure 4.11 and Table 4.3 respectively. As shown in Table 4.3 the *mtrCAB S. oneidensis* strain showed a marked increase in growth rate while other strains showed a dramatic decline in growth rate when compared with the control strain.

Table 4.3: Growth studies measured in absorbance of wild type and transformed *S. oneidensis* cells.

Time (minutes)	S.o *mtr*B (OD)	S.o *mtr*CAB (OD)	S.o *mtr*AB (OD)	S.o *mtr*BC (OD)	S.o *mtr*A (OD)	S.o (OD)	S.o *mtr*C (OD)
160	0.540	0.233	0.128	0.209	0.058	0.048	0.247
200	1.15	0.603	0.305	0.555	0.151	0.209	0.620

The *mtrCAB* strain was 1.6X faster in growth rate whereas the *mtrC construct* was 1.6X slower than the wild type. The *mtr*B strain grew slowest, 1.9X slower than the wild type (Table 4.4).

Table 4.4. Specific growth rate determination for parental and recombinant strain of *S. oneidensis* studied*:*

Specific growth rate (μ) = ($\ln x_t - \ln x_t$) / (t_0 to t_i)
E.g. for *S. oneidensis mtr*B (μ) = ln (1.15) -ln (0.54) / (200-160)
S. oneidensis mtr B (μ) = 0.0189 min^{-1} = 1.95 X slower compare to *S. oneidensis*
S. oneidensis mtr CAB (μ) = 0.06 min^{-1} = 1.63X faster compare to *S. oneidensis*
*S. oneidensis mtr*AB (μ) = 0.0217 min^{-1} = 1.7X slower compare to *S. oneidensis*
*S. oneidensis mtr*BC (μ) = 0.0244 min^{-1} = 1.51X Slower compare to *S. oneidensis*
S. oneidensis A (μ) = 0.0239 min^{-1} = 1.54X slower compare to *S. oneidensis*
S. oneidensis (μ) = 0.0368 min^{-1}
S. oneidensis C (μ) = 0.023 min^{-1} = 1.6X slower compare to *S. oneidensis*

4.3.4. Analysis of expression profiles

Results on differentially expressed genes by quantitation of total protein content in the experimental tests are shown in Table 4.5. The *mtrBC* strain had the highest protein expression which was 3.6X more than that by the wild type *S. oneidensis,* while *mtrB* strain alone recorded the lowest protein expression, 2X lower than the wild type.

Table 4.5. Bradford assay estimation of total protein content of the experimental samples.

Test (protein)	Total Protein Concentration (ug ml^{-1})	Fold increase/decrease in comparison to *S. oneidensis Test*
S. oneidensis	75	1
S. oneidensis MtrAB	137	1.8x increase
S. oneidensis MtrB	37	2x decrease
S. oneidensis MtrA	221	3X increase
S. oneidensis MtrC	166	2.2x increase
S. oneidensis MtrBC	275	3.6x increase
S. oneidensis MtrCAB	123	1.6X increase

Other experimental systems: *mtrA, mtrC, mtrAB* and *mtrCAB* strains had more protein content that the wild type.

4.3.5. Analysis of COD reduction and coulombic efficiency.

As shown in Table 4.6 comparison of %COD removal with %coulombic efficiency indicated that *mtrAB S. oneidensis* strain was very effective in COD conversion to electricity generation (28% was converted) whereas in *E. coli* the COD conversion showed a poor result. *mtrA E. coli* strain was most effective in COD conversion, converting 0.7% of the COD utilized to electricity production.

Table 4.6: Comparison of COD removal & Coulombic efficiency of work involving over-expression and expression of Mtr-pathway in S. oneidensis (test A) and E. coli (test B) respectively in MFCs.

Test A	COD removal	Coulombic efficiency (%)
S. oneidensis mtrCAB	94%	9
S. oneidensis mtrBC	76%	12
S. oneidensis mtrC	88%	9
S. oneidensis mtrB	39%	0.4
S. oneidensis mtrA	76%	12
S. oneidensis mtrAB	36%	28
S. oneidensis	30%	24

Test B	COD removal	Coulombic efficiency (%)
E. coli mtrCAB	27%	0.07
E. coli mtrBC	39%	0.03
E. coli mtrC	24%	0.04
E. coli mtrB	45%	0.04
E. coli mtrA	3%	0.70
E. coli mtrAB	21%	0.05
E. coli	73%	0.01

4.4. Discussion

S. oneidensis has gained considerable attention due to versatilities in its respiratory pathways and has been widely exploited in biotechnology and bioremediation applications. The development of efficient MFCs requires the ability to exploit interfacial electron transfer reactions to external electron acceptors (Xiong *et al*., 2011). *S. oneidensis* is a model organism capable of coupling oxidation of carbon sources to reduction of numerous terminal electron acceptors using the Mtr-pathway (Coursolle and Gralnick, 2010). Central to the utility of this pathway is the understanding of the cellular mechanisms that maintain efficient optimal function, localization, renewal and resynthesis of the MtrC (Xiong *et al*., 2011). Expression of *mtrC* in conjuction with *mtrB* and *mtrA* in *E. coli* mediated extracellular electron transfer in *E. coli* (Xiong *et al*., 2011). Previously, poor electricity production and iron (III) oxide reduction was reported when *mtrA, mtrC* and *mtrB* genes were mutated in *S. oneidensis* (Bretschger *et al*., 2007), consistent with observations that MtrC represents a terminal electron acceptor and directly bind and transfer electrons to mineral oxides (Xiong *et al*., 2011). Another study, reported limited chromium reduction by deletion of *mtrC* in *S. oneidensis* (Belchik *et al*., 2011). However, this study focused on over expression of genes observed to be involved in extracellular electron transfer pathway in *S. oneidensis*.

The experiment aimed to overexpress the protein involved in EET pathway in *S. oneidensis* individually or as operons and investigate their application and influence on MFCs performance including power production, substrate degradation rate and to study impact on growth rate and its correlation with MFCs performance, similar to previous work when the pathway were heterologous expressed *E. coli* (Jensen *et al*., 2016).

The results in Figure 4.7 and 4.8 suggested that when the *mtrB* gene were co-transformed with either *mtrA* and *mtrC* as operons in MR-1, both voltage and power production respectively were significantly improved as against expressing each gene *mtrB, mtrC* and *mtrA* alone. This might be as a result of proper localisation and insertion of these expressed cytochromes (*MtrB*) (Myers and Myers, 2002). However, this is in contrast with the result observed for *E. coli*.

The best MR-1 performance regarding power production 144±4 mW m^{-2} was when MR-1 was transformed with operon of *mtrA* and *MtrB* genes and the construct produced more power than the operon containing the three genes studied i.e. *mtrA, mtrB* and *mtrC*. This is in contrast with the result observed for *E. coli*. This suggests that both *mtrB* and *mtrA* are the possible limiting genes in the bioprocessing processing route in MR-1 and affecting power production. The power production was 3X more than that was produced by the wild type strain. Comparing the power production by *mtrCAB S. oneidensis*strain and *mtrCAB E. coli* strain, the *mtrCAB S. oneidensis* strain produced 3X more power than *mtrCAB E. coli* strain. Regarding the power production by the recombinant *E. coli* to its wild strain, the *mtrCAB* strain produced 25X more power than its wild type strain. Report of (Jensen *et al*., 2010) demonstrates 6 X and 4 X reduction of soluble and insoluble Fe (III) respectively faster by *mtrCAB E. coli* strain than parental strain of *E. coli.* However, comparing results of individual genes (*mtrA* and *mtrB*) suggests that *mtrA* gene may be the significant gene limiting power production in *S. oneidensis*.

The result on growth rate as shown in Table 4.4 suggested that overexpression of *mtrB* or *mtrA* or *mtrAB* in MR-1 negatively affects growth rate possibly due to toxicity of the protein expressed and has been observed that overexpression of membrane proteins decreased cell viability and damaged cell membranes (Goldbeck *et al*., 2013).

The result on coulombic efficiency in Table 4.6, indicated that *mtrAB* operon transformed MR-1 and *mtrA E. coli* gave the best coulombic efficiency possibly because of efficiency of substrate utilization despite reduced growth rate.

The result on improved substrate reduction indicated that complete overexpression of *MtrCAB* in *S. oneidensis* significantly improve the substrate reduction as against in *E. coli* possibly due to high degree of post translation modification of *MtrCAB* protein in *S. oneidensis* (Goldbeck *et al.,* 2013).

4.5. Concluding Remarks

The finding of the work suggests that creation of novel biologics for environmental control and electricity generation is possible by using synthetic biology and it is a promising tool that might offer solution to MFCs. By heterologous expression of

mtrCAB in a *E. coli* Top10 (a non-electroactive bacterium) power production was enhanced from 1 mW m^{-2} to 25 mW m^{-2}. By overexpressing *mtrCAB* operon in *S. oneidensis* in this present work, significantly enhanced the bioremediation of the wastewater, while overexpressing *mtrAB* operon suggests is promising steps towards enhancement of MFCs on power (144 mW m^{-2} was produced). The performance of *MtrA* as individual or in operon in *S. oneidensis* suggests the regulation of its expression should be explored for MFCs improvement.

Chapter 5

Supplementation of MFCs with quorum sensing molecule N(-3-oxodecanoyl)-L-homoserine lactone improves power production.

5.1. Quorum Sensing and its application in microbial fuel cells.

Over the past several decades, there has been an increasing appreciation among microbiologist that bacteria can perceive and respond to other bacteria (Li and Tian, 2012). The first evidence of quorum sensing was reported in *Vibrio fischeri*, a marine luminescent bacterium. *V. fischeri* can exist as free-living or in symbiotic association with fish or squids (*Euprymna scolopes*). As free-living bacteria, *V. fischeri* do not express the luciferase light-encoding genes which regulate light emission (Soto *et al*., 2012). Diverse groups of bacteria have different mechanisms for monitoring abundance in the local environment. These abilities to communicate and behave as a group for social interactions like a multi-cellular organism have presented significant benefits to bacteria in host colonisation, defence against competitors, adaptations to environment, and formation of biofilms (Li and Tian, 2012). The mechanism of communications among bacteria cells is known as quorum sensing.

Quorum sensing is a type of regulatory process that ensures that there is sufficient cell density, before some specific gene products are made (e.g. an extracellular enzyme or virulence protein). The language of communication is based on self-generated signal molecules called autoinducers or quorum sensing molecules. Quorum sensing molecules exist in two main forms: Acylated Homoserine Lactones (AHL) and Oligopepetides (Dunny and Leonard, 1997; Miller and Bassler, 2001). AHL is employed by over 25 Gram-negative bacteria species such as *V. fischeri* and *Pseudomonas aeruginosa*. AHL has been proposed to mediate intraspecies communication solely between members of the same species of Gram-negative bacterium (Coughlan *et al*., 2016). Although different forms of AHLs are produced by different species (Churchill and Chen, 2010), they all have a common homoserine lactone ring moiety with varying lengths, degree of saturation, and specific substitutions within the attached acyl side-chain (Churchill and Chen, 2010). The

concentrations of AHLs in soil range from nano-molar to milli-molar and with possible diffusion zone of 4-80 mm allowing nearby members of the same population to sense the signal and modulate gene expression accordingly (Mukherji and Prabhune, 2015). Bacteria ability to sense quorum sensing molecules has been demonstrated with a biosensor mutant *Chromobacterium violaceum* incapable of synthesizing AHL but responds to exogenously supplied of AHL by synthesising purple colour pigment violacein (Mukherji and Prabhune, 2015). When the acyl homoserine reaches a threshold concentration it binds to and activate a regulatory protein which then binds to a specific site on the DNA. The auto inducer responsible for bioluminescence in *V. fischeri* was shown to be 3-Oxo-C_6-homoserine lactone, a member of the family of N-acyl-homoserine lactones (Callahan and Dunlap, 2000). In wild type *Pseudomonas*, N-(3-oxododecanoyl)-L-homoserine lactone (Figure 5.1) is responsible for biofilm formation (Han *et al*., 2010). The lasI and lasR gene in *P. aeruginosa* direct the synthesis of the signal N-(3-oxododecanoyl) homoserine lactone (De Kievit *et al*., 2001) .This has been reported to induce *lasI* mutant of *P. aeruginosa* (producing 20% of the wild type biofilm) to form structured biofilm (Thormann *et al*., 2004). In addition, microbial biofilm is known to be an adaptation mechanism in response to environmental stresses, such as high shear forces, low nutrient availability, unfavourably pH value, and toxic chemical (Zhang *et al*., 2011). Quorum sensing molecules in Gram negative organisms are of the N-acyl homoserine lactone type and so it may be expected that a molecule such as N-(3-oxododecanoyl)-L-homoserine lactone naturally produced by *Pseudomonas aeruginosa* may induce activities such as biofilm formation in the Gram-negative *S. oneidensis.*

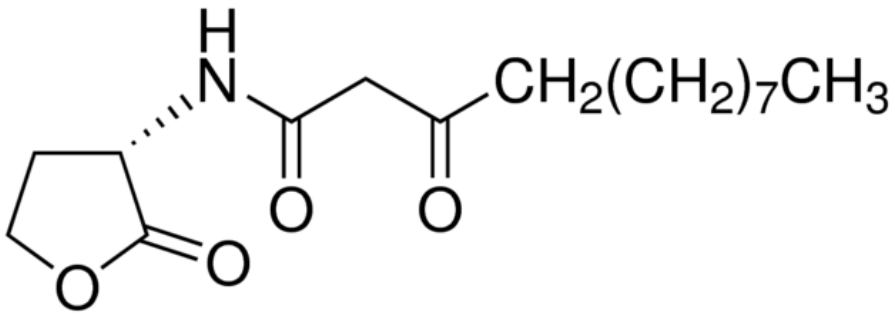

Figure 5.1. Chemical structure of N-(3-oxododecanoyl)-L-homoserine lactone (Tateda et al., 2003).

5.2. Overview of Biofilms.

Biofilms are described as highly structured entities of bacteria cells embedded in a self-produced extracellular polymeric matrix matter. Biofilm acts as a 'biological glue' accounting for about 50-90% of the biofilm composition (Karimi *et al*., 2015). Biofim attach to submerged surfaces via appendages such as flagella and fimbriae (Wood *et al*., 2011). Because of the composition of biofilms, it has also been described as microcolonies of bacterial cells enclosed in extracellular polymeric substances separated from each other by interstitial voids (Oliveira and Cunha, 2008). Microcolonies of biofilm are formed by the production of microbial products including proteins, lipid, DNA, and polysaccharides (Wood *et al*., 2011). The chemical composition of the extracellular polymeric structure (EPS) varies depending on the type of bacteria present in the biofilm, but primarily made up of polysaccharides. These polysaccharides e.g. in the case of Gram-negative bacteria are neutral or polyanionic and confers anionic properties to the EPS (Donlan, 2002). Some of the anionic polysaccharides include D-glucuronic and D-galacturonic. Several types of polysaccharide with other components such as proteins and extracellular DNA together provide structural support for the biofilm (Flemming and Wingender, 2010). The thickness of biofilms vary between species and are dependent on other environmental conditions such as pH, temperature, availability of nutrient, and oxygen concentration. The short supply of nutrients often limits bacteria growth in the natural habitat. Factors that determine initial attachments of biofilms to surfaces (Figure 5.2) include type of surface, aqueous properties of the medium and its hydrodynamics shear force exerted, and properties of the cell surface e.g. its hydrophobicity (Gyamfi-Brobbey, 2016). Cell-to-cell signalling (between bacteria cells or bacteria and host cells) plays a possible role in early attachments and detachments of bacteria to surfaces during biofilm formation.

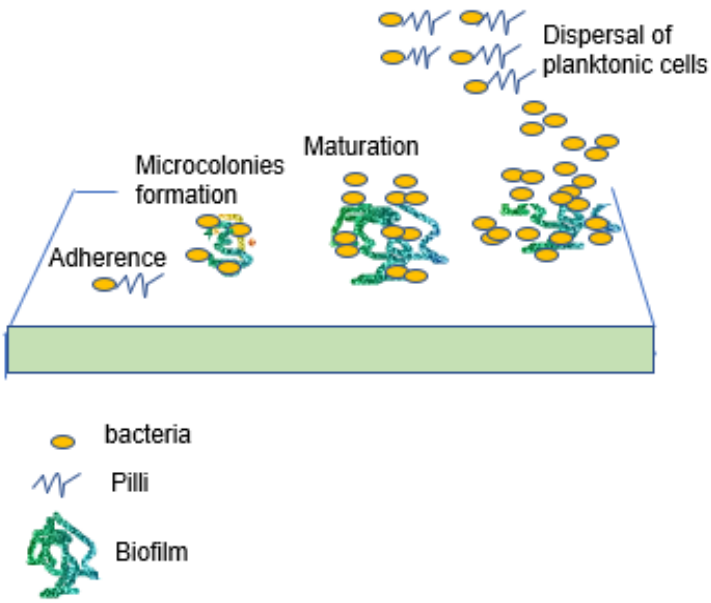

Figure 5.2. A schematic diagram illustrating the four characteristics of biofilm life cycle: the irreversible adherence of planktonic cells to surface involving action of pili and flagella (stage 1); cell division and formation of EPS leading to cell to cell adhesion thus microcolonies (stage 2); microcolonies proliferation and separation (stage 3); mature biofilm formed and dispersion of planktonic cells to initiate another life cycle (stage 4).

The suitable environment for attachment and subsequent growth of bacteria is a solid-liquid interface (Gyamfi-Brobbey, 2016). Physio-chemical properties of material surfaces such as hydrophobicity in the 96-well plates increased the rate of bacteria attachment (Cerca *et al*., 2005). Other physical forces associated with bacterial adhesion include Van da Waals forces, steric interactions, and electrostatic interaction. Hydrophobicity between bacteria cells and surfaces has been shown to enable bacteria to withstand irreversible repulsive forces that are present. However, during the stage of reversible attachments, the repulsive forces are greater than the attractive forces (Franks *et al*., 2010; Li and Tian, 2012; Garrett *et al*., 2008).

Fundamental to improving MFCs performance is to improve on its productivity and reduce its operating costs (Karmakar *et al.* 2010). One area that might fundamentally improve MFCs performance and long-time operation will be to enhance the formation of highly specialized bacterial biofilms on the electrode surface (Leech, 2015). However, as the thickness of biofilm progresses it results in the accumulation of

dead cells (Webb *et al*., 2003) and long-time operation caused biofouling of the proton exchange membrane which limit conductivity, capacity of ion transfer, and diffusion coefficient (Rahimnejad *et al*., 2015). Bacteria such as *G. sulfurreducens* and *S. oneidensis* formed electrical conductive pili capable of transferring electron transfer across considerable distance greater than 50 µm and have been shown to be involved in biofilm formation and attachment to surfaces. The thickness of biofilm growth has been observed to have a direct correlation with the current production (Choi and Chae, 2013, gya *et al*., 2010, Karra *et al*., 2013, Khan *et al*., 2016). Power output in MFCs was directly dependent on biofilm growth and composition (Okamoto *et al.*, 2012). Biofilm attachment to the electrode surface were mainly responsible for electricity production as opposed to the planktonic cells (Liu *et al*., 2007). Using Quartz crystal microbalance that monitors changes in mass on electrode to observe development of biofilm, indicated correlation of increased power production with increase in the viscoelasticity properties of the biofilm (Leech, 2015). Therefore, since AHL has been reported to mediate intraspecies communications (Coughlan *et al*., 2016) and they have a common homoserine lactone ring moiety (Churchill and Chen, 2010), it was hypothesized that exogenous supplementation of the N-(3-Oxododecanoyl)-L-Homoserine lactone would enhance biofilm formation by *S. oneidensis* leading to improved electricity production in MFCs. Therefore, this study investigated for the first time the influence of -(3-Oxododecanoyl)-L-Homoserine lactone on biofilm formation by *S. oneidensis* and influence on electricity production in MFCs.

5.3. Materials and Methods

5.3.1. Chemicals

N-(3-oxodecanoyl)-L-homoserine lactone quorum sensing molecule and some of the chemicals described in section 2.2.1 were purchased from Sigma Aldrich (UK). All chemicals used were of analytical grade and were not purified further before used.

5.3.2. Bacterial strains, maintenance, and culture

S. oneidensis strain 700550 was purchased from ATCC and was maintained, cultured and subcultured as described in section 2.2.1.

5.3.3. Experimental design

The experimental design for the use of quorum sensing molecule to enhance biofilm formation by *S. oneidensis* for electricity generation from synthetic wastewater (MSM) containing 500 mg L^{-1} glucose was investigated for 13.4 days due to time limitation under strictly anaerobic-anodic conditions in a two-chambered MFC (Figure 5.3). The inoculum was made up of 10% (v v^{-1}) of the anode working volume. The concentrations of exogenous addition of N(-3-oxodecanoyl)-L-homoserine lactone tested were 5; 10, and 20 µM. The control was MFCs with *S. oneidensis* in the anode with no quorum sensing molecule added to the anolyte medium. The experiments were done in triplicate. Performance measured include power generation, COD removal, biofilm growth, and total biofilm protein.

For all set ups the volume of inoculum used was 10% v v^{-1} of the total anolyte volume. The anode chambers with the contained mixtures were stripped of dissolved oxygen by sparging nitrogen gas for 5 minutes before setup.

All experiments were replicated three times and studied at 30^0C using a temperature controlled Stuart 160 incubator (Fisher Scientific, U.K.). Results were expressed as mean of replicates ± standard deviation.

For all set ups, the volume of inoculum used was 10% v v^{-1} of the total anolyte volume. The anode chambers with the contained mixtures were stripped of dissolved oxygen by sparging nitrogen gas for 5 minutes before setup.

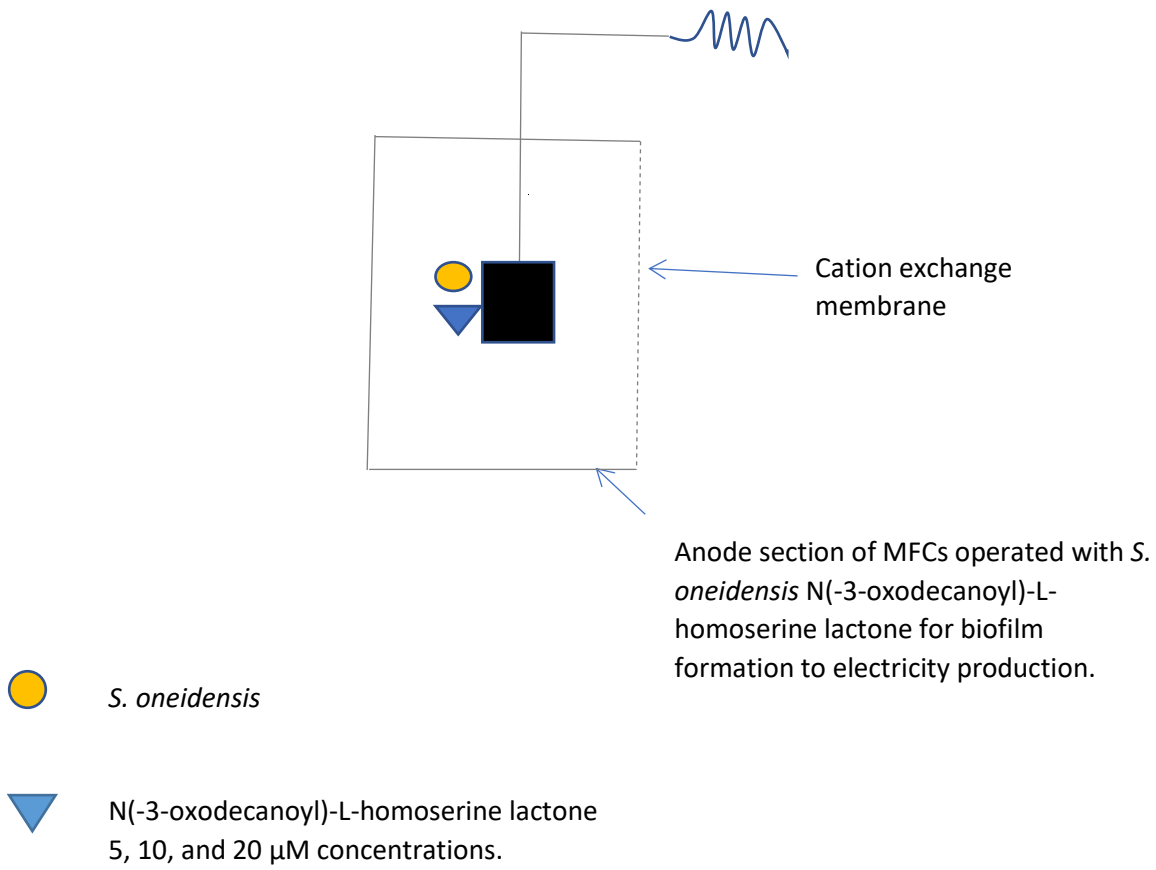

Figure 5.3. Scheme for experimental design investigating the use of N-(-3-oxodecanoyl)-L-homoserine lactone for enhancing biofilm formation and influence on electricity production in MFCs.

5.3.3.1. Modification of anolyte minimal salts medium used for the investigation of exogenous addition of quorum sensing molecule for enhancing biofilm production to power production.

The anolyte MSM for the investigation of exogenous addition of quorum sensing molecule for enhancing biofilm production and hence power production was supplemented with 500 mg L^{-1} glucose and 500 mg L^{-1} casein hydrolysate, trace element stock solution (x1) and vitamin stock solution (x1).

The catholyte used was 50 mM (pH 7) phosphate buffer containing 0.1M potassium ferricyanide, without aeration.

For all set ups, the volume of inoculum used was 10% v/v of the total anolyte volume. The anode chambers with the contained mixtures were stripped of dissolved oxygen by sparging nitrogen gas for 5 minutes before setup.

The MFC components used and all media solutions for all the experiments were sterilised by autoclaving at 121℃ for 15 minutes. The experiments were conducted in batch mode with a working volume of 200 mL in each MFC compartment. The anolyte was purged with nitrogen gas for 10 minutes through a 0.22 µm pore size diameter filter prior to inoculation.

All experiments were replicated three times and studied at 30℃ using a temperature controlled Stuart 160 incubator (Fisher Scientific, U.K.). Results were expressed as mean of replicates ± standard deviation.

The studies on *S. oneidensis biofilm* development were further investigated under non-MFCs anaerobic conditions. Firstly, using 96 sterile sterlin plates (Figure 5.4). Each well of the 96-microtiter plate has 200 µL composed of representative medium used for the investigation under MFCs condition for investigation of quorum sensing concentrations (5, 10, and 20 µM) composed of *S. oneidensis,* glucose, Minimal salt medium, vitamin mix and trace elements as described for the modification of anolyte medium. The setup is as described below and covered with the lid. The setup was further wrapped with plastic paraffin film and incubated at 30^0C.

The unattached *S. oneidensis* cells grown on microtiter plates for two days as described under experimental design for investigation of quorum sensing molecules were submerged in a small tube of water and shaked out to remove the unattached cells from the attached cells bound to the well of the microtiter plate. Solution of 0.1% Crystal Violet (125 µL) were added to each well of the microtiter plate and incubated at room temperature for 15 minutes.

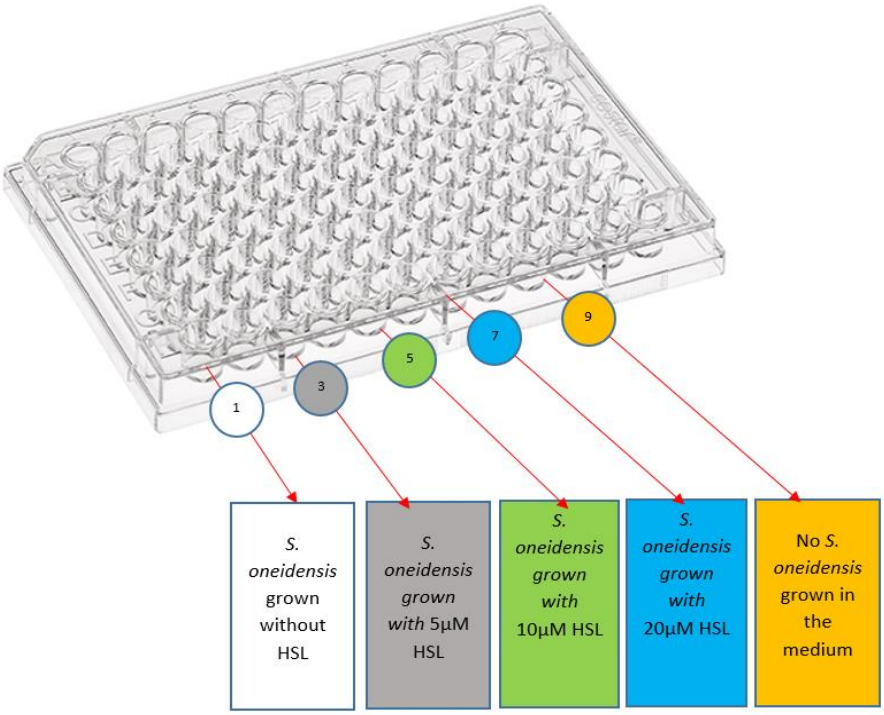

Figure 5.4. Schematic demonstration of experimental setup of biofilm studies under non-MFCs condition using 96 well Sterlin plates.

5.3.3.2. Quantification of *S. oneidensis* biofilm using crystal violet method.

The plate was rinsed 3 times after incubation by submerging in a tub of water and blotting out vigorously to remove all excess cells and dye. The plates were left to dry for 1 hour. Acetic acid 125 µL 30% (v/v) was added to each well plate to solubilize the crystal violet before quantifying using at 550 nM. Empty well with no culture were used as the blank having 125 µL 30% (v v^{-1}) acetic acid.

5.3.3.3. Quantification of *S. oneidensis* biofilm using confocal microscope.

Analysis of biofilms by using fluorescent staining and subsequent imaging is described to be challenging, because of heterogenous thickness associated with biofilm surfaces, composing of undefined regions (e.g. extracellular polymeric matrix). Hence, we used SYPRO Ruby stain for the confocal microscope examination of *C. beijerinckii,* and *S. oneidensis* biofilm formation, because it labels most classes of proteins including glycoproteins, phosphoproteins, lipoproteins, calcium binding protein and fibrillar protein and other proteins that are difficult to stain. This stain has been tested to stain matrix of *Pseudomonas aeruginosa* and some strain of *E. coli.* In-order to examine and quantify biofilm formation by *S.*

oneidensis and *C. beijerinckii* and investigation of influence of quorum sensing molecules on *S. oneidensis* to enhance biofilm formation. The cells were cultured separately on cover slips in “Corning Costa 6 Well Plates” for 2 days. The cover slips were carefully rinsed in 100mM phosphate buffer and thereafter were placed in a fresh Corning Costa 6 well plates. SYPRO Ruby stain 200 µL was added to each of the biofilm samples on the slips without offsetting the biofilm. The samples were incubated for 30 minutes protected from light. After incubation, filter sterilized water was used to remove excess stain and the stained samples were placed into a fresh Corning Costa 6 well plates (Figure 2.7, purchased from Thermofisher) covered with 3 ml of filter sterilized water and observed under a confocal microscope at 450 nm.

5.3.3.5. Extraction of Biofilm and Determination of total biofilm protein content.

Examination of biofilm formations on the anode fuel cells were done by dissembling the MFCs compartments and carbon cloth were carefully removed without touching the surface. Anode electrodes with the build-up of biofilm from the various tested systems were dipped in sterile deionised water to remove any loose cells or debris that were not part of the attached biofilm. Thereafter they were placed in the “Stomacher Bags” and equal volume of sterile distilled water were added before the biofilms were discharged using Stomacher Paddle homogeniser. The broth containing the total biofilm were further disrupted using the sonication method for total protein extraction. The total protein estimations were conducted using Thermos Scientific Pierce Bicinchoninic Acid Reagent (BCA) Protein Assay for the colorimetric detection and quantitation of the total protein. This method combines well- known reduction of Cu^{+2} from the BCA reagent to Cu^{+1} (cuprous cation) by protein in an alkaline medium (the biuret reaction) and colorimetrically detected. The water-soluble complex exhibits a strong absorbance at 562 nm. A series of dilutions of known concentrations of Bovine Serum Albumin (2 mg mL^{-1}, BSA) were prepared to prepare a set of protein standards. The concentrations of standards were ug mL^{-1} (250; 125; 50; 25; 5; 0) and assayed alongside with the unknown samples extracted by physical disruption using sonication method. Thereafter 0.1 mL of each standard and unknown samples triplicate were added to 2 ml of BCA (20 – 2,000 ug mL^{-1}). The mixtures were allowed to incubate at 37℃ for 30 minutes. The absorbance of all the samples were measured using a spectrophotometer at 562 nm after 10 minutes.

5.4. Results

5.4.1. Summary

Quorum sensing molecule N(-3-oxodecanoyl)-L-homoserine lactone was exogenously added to the anodic medium at varying concentrations: 5, 10, and 20 µM to assess effects on the regulation of the population density and hence biofilm formation by *S. oneidensis* with a view to enhance electricity production in MFCs. As summarised in Table 5.1. Power was enhanced to 184 ± 2 mW m^{-2} by the 10 µM concentration of N(-3-oxodecanoyl)-L-homoserine lactone and COD removal of 62% compared to 56 ± 3 mW m^{-2} power production with 92% COD removal by the control.

Table 5.1. Summarization of result of the influence of -(3-Oxododecanoyl)-L-homoserine lactone on biofilm formation by S. oneidensis *and influence on electricity production in MFCs*

	S. oneidensis	5 µM	10 µM	20 µM
Power Production (mWm^{-2})	56 ± 3	160 ± 5	184 ± 2	140 ± 4
% COD Reduction	92 ± 3	72 ± 1	62 ± 3	42 ± 2

5.4.2. Voltage-time profiles and polarization curves.

The influence of of N(-3-oxodecanoyl)-L-homoserine lactone on voltage-time profile is shown in Figure 5.5. What can be seen clearly is that the voltage pattern were closely similar. The peak voltage produced was by 10 uM (538 mV), followed by 20uM (526 mV) and lastly by 5 uM (484 mV). The control had lowest voltage of 261 mV.

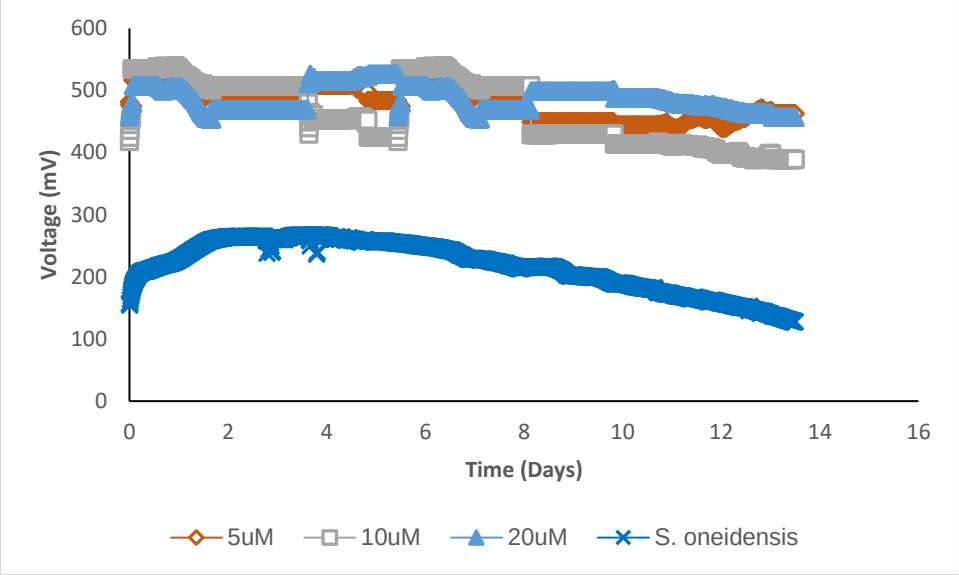

Figure 5.5. Voltage production using N(-3-oxodecanoyl)-L-homoserine lactone.

The influence on polarisation and power density curves are shown in Figure 5.6A and 5.6B respectively. What stands out is that the power produced across the HSL stimulated tested studies are statistically significant ($p < 0.05$) higher than the control. The order of power produced are 10 uM (184 mWm^{-2}) > 5 uM (160 mWm^{-2}) > 20 uM (140 mWm^{-2}) > control (56 mWm^{-2}).

A

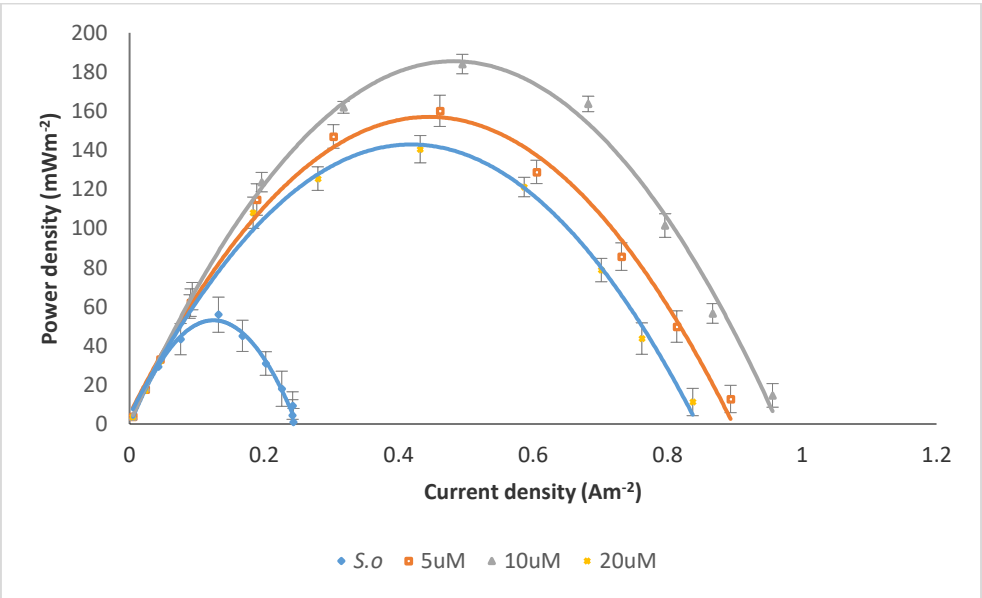

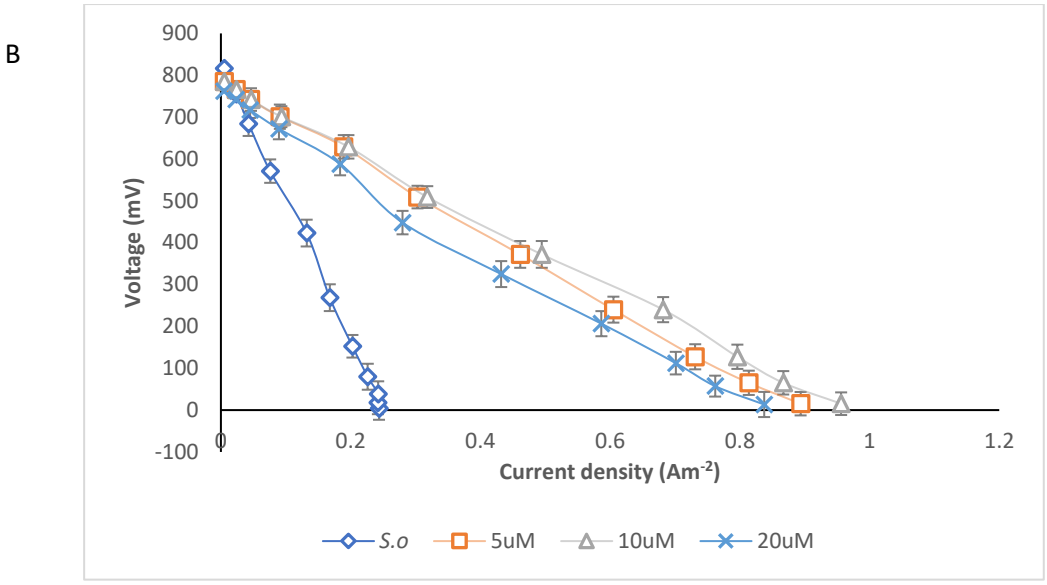

Figure 5.6. Power production of S. oneidensis influenced using N(-3-oxodecanoyl)-L-homoserine lactone: (10 µM, 184.02 mW m^{-2}) (5 µM, 160.1 mW m^{-2})(20 µM, 140.5 mW m^{-2}) (control, 56 mW m^{-2}) using N(-3-oxodecanoyl)-L-homoserine lactone.

5.4.3. Quantitative and Qualitative analysis of biofilm formation by *S. oneidensis* influenced by N(-3-oxodecanoyl)-L-homoserine lactone.

The influence of varying concentrations of N(-3-oxodecanoyl)-L-homoserine lactone studied on biofilm growth under anaerobic non-MFCs condition is shown in Figure 5.7. What is interesting is that 20 uM produced the highest growth of 1.09 OD compared to the control which recorded the lowest (0.7 OD).

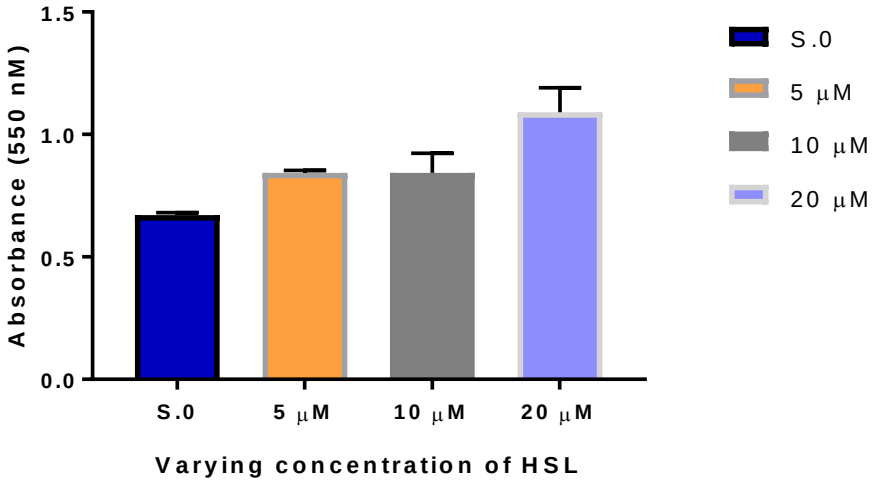

Figure 5.7. Quantification of biofilm formation influenced by HSL under non-MFCs condition. Error bars mean standard deviation from the mean (n = 3)

What is also interesting is that 5 uM produced growth of 0.83 OD similar to the growth of 0.84 OD produced by 10 uM concentrations. Images from confocal microscope (Figure 5.8) showed marked increase of biofilm developed by the 10 µM concentration which was densest compared to all the tested conditions.

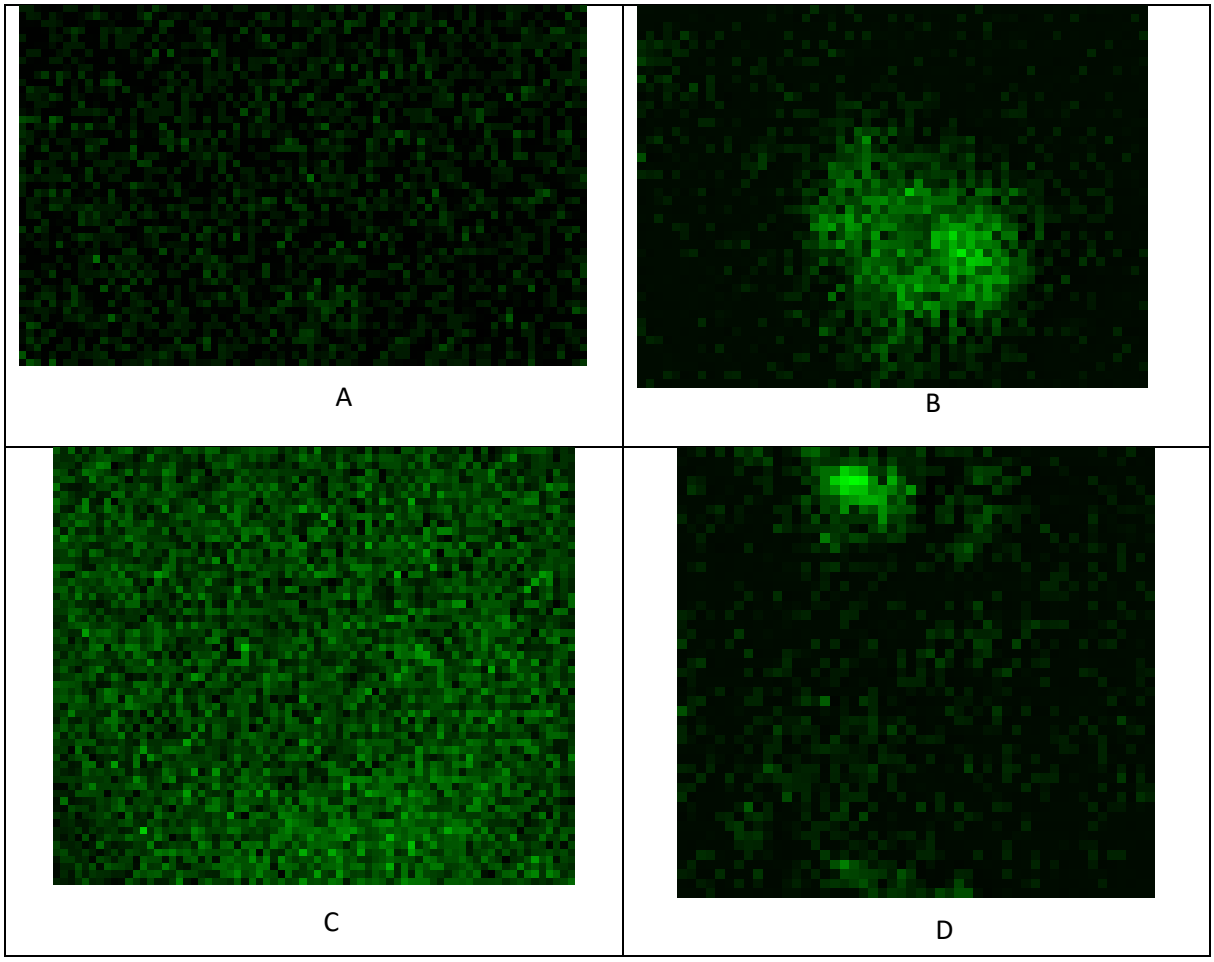

Figure 5.8. Images from confocal microscope analysis of (A). S. oneidensis biofilm (B) with 5 uM N(-3-oxodecanoyl)-L-homoserine lactone (C) with 10 uM N(-3-oxodecanoyl)-L-homoserine lactone (D) with 20 uM N(-3-oxodecanoyl)-L-homoserine lactone grown under non-MFCs condition on microscope slide in six well plates grown at 30℃ for 2 days under complete anaerobic condition.

5.4.4. Analysis of Biofilm formation discharged from the tested anode conditions.

The total concentration of protein extracted from the biofilm discharged from the various anode tested conditions are shown in Table 5.2. What can be clearly seen is

that as the concentration of HSL increases, the protein concentration increases except in the case of 20 µM.

The highest protein of 2.94 mg mL^{-1} was produced by 10 µM while the control produced the least of 0.2 mg mL^{-1}. The 20 µM concentration produced 1.71 mg mL^{-1}.

Test	Protein concentration (mg mL^{-1})
S. oneidensis	0.222
5µM	1.60 ± 0.01
10µM	2.94 ± 0.01
20µM	1.71 ± 0.01

Table 5.2. Protein quantitation from biofilm discharged from electrode in MFCs condition influenced by varying concentration of N(-3-oxodecanoyl)-L-homoserine lactone.

The result of percentage of COD reduction and amount of percentage of coulombic efficiency recovered are shown in Table 5.3. What can be clearly seen is that as COD decreases, the concentration of HSL increases. The control achieved the best COD reduction of 92%.

Table 5.3: Comparison of COD with the CE from MFCs investigated by stimulation of S. oneidensis with varying concentrations of N(-3-oxodecanoyl)-L-homoserine lactone.

Test	COD (%)	CE (%)
S. oneidensis	92 ± 3	4.7± 1
5 µM	72 ± 1	13 ± 1
10 µM	62 ± 3	15 ± 2
20 µM	42 ± 2	23 ± 2

The result of coloumbic efficiency demonstrated that the higher the substrate consumed the lower the amount of CE recovered. The 20 µM had the best coulombic efficiency of 23% transfer. The coulombic efficiency increases as the concentration of HSL increases.

5.5.6. Analysis of DNA composition of the biofilm discharged from the investigation of exogenous addition of N(-3-oxodecanoyl)-L-homoserine lactone.

The analysis of DNA contents of the biofilm is shown in Figure 5.9. The result demonstrated that as the concentration of HSL increases the DNA synthesized increases. HSL of 20 µM produced 47 ng μL^{-1}, 10 µM produced 36 ng μL^{-1}, 5 µM produced 16 ng μL^{-1} and control produced 3 ng μL^{-1}.

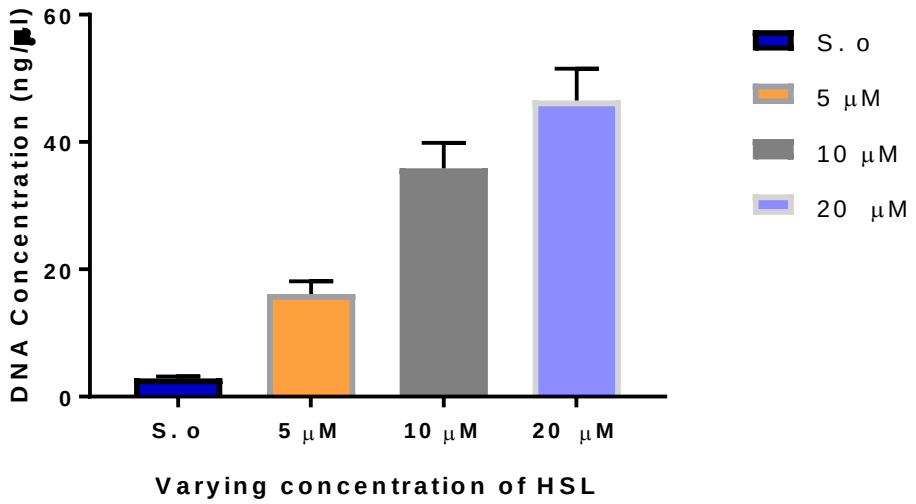

Figure 5.9. Quantitation of DNA extracted from anodic biofilm discharged, growth influenced by varying concentration of N(-3-oxodecanoyl)-L-homoserine lactone.

5.6. Discussion.

The aim of this study was to enhance electricity production in MFCs by using quorum sensing molecules (N(-3-oxodecanoyl)-L-homoserine lactone) to enhance biofilm formation by *S. oneidensis*. Although, different operating parameters such as pH, substrate concentration, temperature, external resistance, anaerobic and aerobic processes have been shown to directly affect biofilm formation, however, optimal biofilm formation and minimal oxygen invasion in the anode chamber has been shown to improve power generation (Saratale *et al*., 2017). *S. oneidensis* form biofilms by secreting extracellular polysaccharide and plays a significant role in

extracellular electron transfer (Uno *et al*., 2017) which could form a large tower biofilm 40 µM in height (Read *et al*., 2010). Increase in biofilm has been shown to be accompanied with increase in cell number (Murphy *et al*., 2016).This investigation focussed on using N(-3-oxodecanoyl)-L-homoserine lactone a quorum sensing molecule to enhance biofilm formation by *S. oneidensis* in-order to enhance biofilm formation for electricity recovery in microbial fuel cells as previous studies have reported direct correlation between levels of biofilm formation and power production (Song *et al*., 2016), coulombic efficiency (Zhang *et al*., 2017) azo dye degradation (Cao *et al*., 2017) and nitrogen removal. The production of current in microbial fuel cell has been shown to be related to the development of electronic conductive biofilm by electrode interaction (Malvankar *et al*., 2012). Bacteria develop biofilms on the electrode which allow opportunity for extracellular electron transfer (Read *et al*., 2010).

MFCs performance are conventionally evaluated through coulombic efficiency and power output. Hence, parameters considered for improving MFCs performance includes: power generation, percentage of COD removal and coulombic efficiency.

Understanding ways bacteria drive metabolic flux through processes such as biofilm formation, cytochrome transport protein, or through improve cell density could potentially be exploited to drive COD degradation route to electricity production (Rabaey and Verstraete, 2005). A combination of high power density, high COD reduction of substrate and high coulombic efficiency are important for MFCs towards real world practical application (Rahimnejad *et al*. 2015)

Figure 5.5 and Figure 5.6 demonstrated that quorum sensing molecules can be utilized to improve voltage and power production in MFCs respectively. Although, the voltage patterns of the tests with varied N(-3-oxodecanoyl)-L-homoserine lactone concentrations studied were closely similar, but were significantly higher than the control by more than 37%. Previous report have demonstrated that mutant strain of *P. aeruginosa* deficient in synthesising pyocyanin and phenazine-1-carboxyamide achieved 5% of power produced by the wild type and was restored to 50% by addition of pyocyanin (Rabaey *et al*., 2005). The power result in this study suggested that N(-3-oxodecanoyl)-L-homoserine lactone between 5 µM and 10 µM

concentration can be used to enhance power production in MFCs. The power produced increased more than X3 when 10 µM of (-3-oxodecanoyl)-L-homoserine lactone was used. It has also been shown that the amount of AHL determine the biofilm formation (Taghadosi *et al*., 2015) and over 1µM concentration of (-3-oxodecanoyl)-L-homoserine lactone was observed to increase biofilm in *Pseudomonas aeruginosa* (Xia *et al*., 2012).

Figure 5.7 and Figure 5.8 indicated that the *S. oneidensis* under MFCs and non-MFCs altered with N(-3-oxodecanoyl)-L-homoserine lactone produced biofilm formation in correlation with the concentration of quorum sensing molecule. The result indicated that the rate of biofilm formation increases proportionally to the concentration of the ASL. The increase is associated with power production (Figure 6.2).

Table 5.2 of this study indicated that 10 µM concentration N(-3-oxodecanoyl)-L-homoserine lactone produced the highest biofilm protein. There are direct correlations between the concentration of N(-3-oxodecanoyl)-L-homoserine lactone, the biofilm proteins produced, the power production produced, and voltage produced. Suggesting that approach might be the goal to enhancing electricity production in MFCs.

Table 5.3 suggested that N(-3-oxodecanoyl)-L-homoserine lactone inhibit COD reduction by the *S. oneidensis*, although the result of coulombic efficiency indicated coulombs recovered was increased as the concentration increases. Therefore, this suggests that COD was utilized effectively for electricity generation. In the case of 10 µM concentration, 24% of coulombs was transferred, while 55% was transferred in the case of 20 µM concentration for power production (Figure 5.6A).

The result of total DNA of the biofilm composition (Figure 5.9) which could represent the population density of the biofilm corroborates the result of biofilm formation under non-MFCs condition, suggesting that the mode of respiration of *S. oneidensis* has little role to play on its biofilm formation. The increase in the concentration of N(-3-oxodecanoyl)-L-homoserine lactone associated with the concentration of DNA result was also consistent with the levels of coulombic efficiency result (Table 5.3). This is supported by the claim that efficiency of MFCs can be correlated with the biomass of

biofilm formed on the electrode and coulombic efficiency was increased from 89% to 99% (Eaktasang *et al*., 2013) and biofilms attached anode enabled increase of CE from supernatanat consortium of 29.6% to 50% (Liu *et al*., 2008).

5.7. Concluding remarks.

The present work demonstrated that MFCs could be successfully improved regarding power production by using quorum sensing molecules. This work demonstrates that HSL can be used for interspecies communication. It further demonstrates that modification of industrial wastewater with (-3-oxodecanoyl)-L-homoserine lactone to a concentration of 10 µM concentration can potentially make MFCs a sustainably wastewater treatment process. This work also suggests that concentration of (-3-oxodecanoyl)-L-homoserine lactone from 5 µM to 19 µM concentrations need to be further studied in order to judge the best concentration for MFCs application.

Chapter 6

Conclusions

The first study (Chapter 2) investigating the use of co-cultures to enhance electricity production in MFCs demonstrated that cleverly defined co-cultures can be used to improve substrate degradation leading to improved electricity production. By using co-cultures of *S. oneidensis* and *C. beijerinckii* , electricity production from synthetic wastewater containing glucose as model carbon source was improved from either 60±3 mWm^{-2} (*C. beijerinckii*) or 48±2 mW m^{-2} (*S. oneidensis*) to 87±4 mW m^{-2} for the co-culture at day 15. Substrate (glucose) consumption was improved from 20% (*S. oneidensis*) to 67% by the co-culture. This could be due to the advantages of the fermentative organism employed that enhanced the degradation of glucose to 67% alone. In the second co-culture studies, electricity production was improved from either 1 mWm^{-2} (*S. cerevisiae*) or 74 mW m^{-2} (*C. beijerinckii*) to 80 mw m^{-2} by the co-culture of *G. sulfurreducens*, *S. cerevisiae* and *C. beijerinckii*. In the second study at 11 day of the studies, glucose utilization was improved from 40% (*C*. *beijerinckii*) or 35% (*G. sulfurreducens*) to 55% by the co-culture of *C. beijerinckii* and *G. sulfurreducens*.

The relative abundance of the electrochemically active bacteria in the co-cultures changed during the course of the experiments with *S. oneidensis* showing more abundancy in the first study of co-culture work and *G. sulfurreducens* in the second study of the co-culture work relative to *C. beijerinckii* in both studies. This work further suggests that the electroactive organisms (*S.oneidensis* and *Geobacter sulphurreducens*) irrespective of their specific growth rate were the abundant organism when co-cultured with other non-electrogenic bacteria in MFCs. The pure culture of *S. oneidensis* can potentially generate 4.6 mWm^{-2} which is higher than 4.25 mW m^{-2} when co-cultured with *C. beijerinckii* for electricity production from 500 mg L^{-1} phenol contaminated wastewater. Pure cultures of *C. beijerinckii* could be used to achieve 99% remediation of phenol at levels of 500 mg L^{-1} within 35 days in a contaminated wastewater system if applied. The efficiency of *S. oneidensis* for energy generation and remediation at a level of 500 mg L^{-1} phenol contaminated wastewater was improved by exogenous supplementation of Riboflavin

(concentration level of 40 µM) with power generation increasing from 4.6 mW m^{-2} to 54 mW m^{-2}. Also at a concentration level of 30 µM Riboflavin, phenol concentration was reduced from 500 mg L^{-1} to 52 mg L^{-1} (ca. 90% removal) within 8 days of operation.

In the second study (Chapter 3), the understanding of the relative contribution of direct electron transfer and mediated electron transfer utilized by *S. oneidensis* and which could generally be used by most other electrogenic bacteria was investigated in MFCs. The outcome of the investigation revealed that direct electron transfer made a 74% contribution to overall electron transfer when a dialysis membrane was used to localise *S. oneidensis* cells on the electrode and generated 114±6 mW m^{-2} power which was more than the contribution made by the mediated electron transfer process by *S. oneidensis* (32± 8 mW m^{-2}). The results were corroborated by another study where *S. oneidensis* cells were entrapped in alginate beads for studying mediated electron transfer process utilized by *S. oneidensis* (in which case power generation was 36± 6 mWm^{-2}).

In the third study (Chapter 4), the possibility of using Synbiota Rapid DNA prototyping assembly method to engineer *E. coli* and *S. oneidensis* for the understanding of the expression of the proteins involved in the transfer of electrons from the periplasmic membrane of *S. oneidensis* to the outer membrane was investigated. The genes were studied individually and also by combination of the genes as operons. The outcome of the investigation suggested that the complete operon *MtrCAB* coding for the Mtr pathway is required for a non-electrogenic bacterium to generate electricity. By the heterologous expression of the proteins in *E. coli*, power was increased from 1±0.01 mW m^{-2} to 25±0.7 mW m^{-2} by the *MtrCAB* mutant strain. Overexpression of the *mtrAB* in *S. oneidensis* enhanced extracellular electron for power generation from 48±2 mW m^{-2} to 144±4 mW m^{-2}. The overexpression of *MtrB* in *S. oneidensis* inhibited the growth rate and power production. Overexpression of *mtrCAB* operon in *S. oneidensis* enhanced glucose utilization from 30% to 94%. The expression of *mtrC* or *mtrA* individually in *S. oneidensis* can be used to improve glucose utilization from 30% to 88% or 76% respectively. These results suggest the importance of these two genes in

mtrCAB operon with respect to substrate conversion by *S. oneidensis* in MFCs applied for bioremediation processes.

The fourth study (Chapter 5), investigated the possibility of using quorum sensing molecules for stimulation of *S. oneidensis* for the enhancement of biofilm formation with the possibility for increasing power generation in MFCs. The quorum sensing molecule used for this study was (-3-oxodecanoyl)-L-homoserine lactone which is naturally used by *Pseudomonas aeruginosa* for biofilm formation. The work demonstrated that supplementation of industrial wastewater with (-3-oxodecanoyl)-L-homoserine lactone to a concentration of 10 µM concentration can potentially make MFCs a sustainably process of wastewater treatment. The study generated the best power output of all the approaches presented in this thesis i.e. 184 ± 2 mW m^{-2} equivalent to 2.3 W m^{-3} of anode chamber assuming for an electrode area of 25 cm^2 and an anode chamber volume of 200 mL. Confocal electron microscope analysis of the microorganisms studied under non MFCs conditions revealed the stimulation of *S. oneidensis* by (-3-oxodecanoyl)-L-homoserine lactone for dense biofilm formation compared with the sparsely- formed biofilm without (-3-oxodecanoyl)-L-homoserine lactone. This demonstrates the possibility that the enhanced power generation in Chapter 4, 5 and 6 might be as a result of development of biofilm on the electrode.

This work has significantly contributed to previous knowledge in that by using cleverly defined co-cultures, substrate conversion to electricity production can be improved. It has also contributed to knowledge on the understanding of the relative contributions of extracellular electron transfer processes utilized by *S. oneidensis* to electrodes. This work also expanded the knowledge of application of synthetic biology for introducing different combinations of extracellular electron transfer pathways in a non-electrochemically active bacterium (*E. coli*) and also by overexpressing different combinations of the pathway in *S. oneidensis*. This work further contributed to previous knowledge that *S. oneidensis* can recognise and communicate with 3-oxodecanoyl)-L-homoserine lactone for increasing biofilm formation and power generation in MFCs.

Chapter 7

7.0 Future work

The results from this study underscore several areas of future work so as to enhance electricity production from industrial wastewater using microbial fuel cell technology.

7.1. Further design of synthetic microbial consortia

The work presented in this thesis utilised cocultures of fermentative organisms (e.g. *C. beijerinckii*) with exo-electrons with a view of increasing substrate conversion and ultimately electricity production. Facultative organisms e.g. *S. cerevisiae* were all used to consume oxygen from the anode. Further work should explore cocultures with other ecological relationships e.g. mutualism, amensalism etc. (Figure 7.1). Algae-bacterial interactions for example have been less studied yet algae could remove organic compounds and nutrients e.g. nitrogen from wastewater.

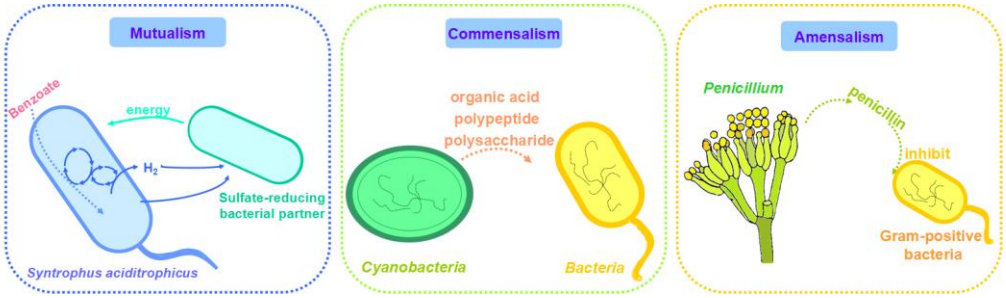

Figure 7.1. Microbial relationships that could further be explored in designing defined co-cultures for improving electricity production from MFCs.

Fungal bacterial interactions should also be explored. A very large number of organic molecules in wastewater are susceptible to the actions of various strains of white rot fungi, and even recalcitrant compounds e.g. polycyclic aromatic compounds can be degraded. Studies by Fernandez de Bios et al., 2013 used a defined culture of the fungus *Trametes versicolor* and the electroactive bacteria *S. oneidensis* in the anode chamber of an H-type microbial fuel cell so that the bacterium would use the networks of the fungus to transport the electrons to the anode. Their system, which was linked to azo dye degradation in the cathode chamber, generated stable electricity (stable voltage of approximately 1000 mV across 1000 Ohms resistance) that was enhanced when electro-Fenton reactions occurred in the cathode chamber.

Strains could be genetically engineered and cultivated in co-culture with electrogenic microorganisms to confer certain characteristics e.g. utilise a wide range of substrates e.g. C6 and C5 sugars, produce vitamins, amino acids needed for growth, produce redox mediators e.g. riboflavin etc. (Figure 7.2)

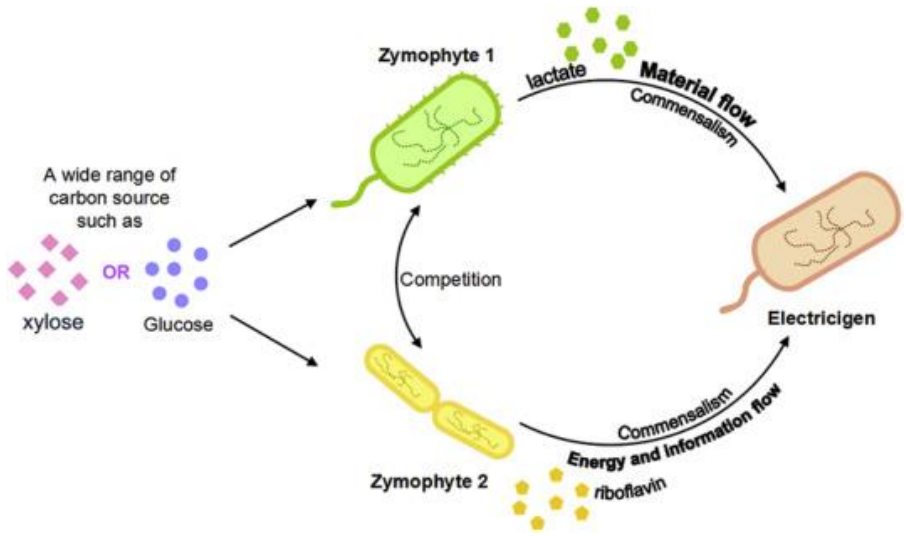

Figure 7.2. Defined consortium of two microorganisms which compete for carbons sources while interacting with electrogens. The three microorganism combination could in theory produce more electricity than individual microbes. Adapted from Ding et al., (2016).

7.2. Strategies to improve electron transfer

In this present work, direct electron transfer mechanism contributed significantly to power production. Hence, it is recommended for future investigation to investigate ways of coupling bacteria to electrodes e.g. by encapsulating *S. oneidensis* cells in conductive polymer and coating the cells with nanoparticles for generating artificial nanowires (Alfonta, 2010).

This work indicated that mediated electron transfer also contributes to electricity production although not to the same extent as direct electron transfer. Future work should target improving the permeability of *S. oneidensis* cell membrane to redox mediators. This could be achieved by heterologously expressing the porin protein OprF e.g. from *Pseudomonas aeruginosa* PAO1 into *S. oneidensis*. Some studies have suggested that in addition to increased membrane permeability of redox

mediators between bacteria and anodes, such expression can increase substrate uptake and metabolite excretion (Yong *et al*., 2013).

7.3. Modulating expression of genes involved in extracellular electron transfer

The investigation for better understanding of the Mtr-pathway for bioelectricity production suggested that the *mtrA* gene strongly influenced power production in *S. oneidensis* although the recombinant cells grew slower compared to the wild type strain. Hence, it is recommended for future work to investigate the regulation of the expression of the *mtrA* gene using strong, weak and inducible promoters. Another area of synthetic biology application suggested for possibility of MFCs improvement is by engineering *S. oneidensis* with the curli operon genes (*Csg BAC*) for curli overproduction. Curli are highly aggravative amyloid fibers (2-5 mm diameter) that protrude on the surface of *E. coli* and salmonella which are devoted to increasing adherence abilities of bacteria and formation of biofilm on abiotic surfaces. It is known to bind to metal ions and have affinity for metals such as Cu^{2+} and Fe^{3+} (Drogue *et al*., 2012).

7.4. Improving biofilm formation.

This work demonstrated that supplementation of microbial fuel cells with 10 µM concentrations of (N-3-oxodecanoyl)-L-homoserine lactone significantly enhanced power production and this was correlated with increased biofilm formation. Hence, it is recommended for future investigation to investigate concentrations beyond 20 uM not considered in this study. It would also be useful if quorum sensing molecules (if any) produced by *S. oneidensis* could be extracted and identified. The supplementation of MFCs with compounds that enhance production of quorum sensing molecules e.g. phenolic plant compounds such as Vanillin, 4-hydroxybenzoic and Gallic acids at concentration within 40 to 400 µg mL^{-1} should also be investigated (Plyuta *et al*., 2013). Although biofilm formation was correlated to increased power production, no information on the viability of the cells in the biofilm was generated. Further studies should probe the viability of cells in MFC biofilms using a Baclight™ live/dead stain.

7.5. Development of photosynthetic biocathodes

To make MFC technology competitive, the cost of materials for operational needs to be low. Another area that should be considered for future investigation is the use of photosynthetic biocathodes e.g. algae as a possible replacement for expensive platinum catalyst used in MFC cathodes. Algae provides a useful way generating oxygen, used as a terminal electron acceptor, in situ in MFC cathodes, utilisation of CO_2 produced in the anode and ultimately conversion of solar energy to electricity (Lee *et al*., 2015; Liu *et al*., 2015). Algae can utilize the carbon dioxide produced by the end product of metabolism (Velasquez-Orta *et al*., 2009; Gajda *et al*., 2015). Hence, elementary CO_2 produced in the anode can be diverted to the cathode for algae utilization.

References

Abboud, R., Popa, R., Souza-Egipsy, V., Giometti, C. S., Tollaksen, S., Mosher, J. J., Findlay, R. H. & Nealson, K. H. 2005. Low-temperature growth of *Shewanella oneidensis* MR-1. *Applied and Environmental Microbiology,* **71:** 811-816.

Alfonta, L. 2010. Genetically engineered microbial fuel cells. *Electroanalysis,* **22:** 822-831.

AL-Shehri, A. 2015. Employment of microbial fuel cell technology to biodegrade naphthalene and benzidine for bioelectricity generation. *International Journal of Current Microbiology and Applied Sciences,* **4:** 134-149.

Bader, J., Mast-Gerlach, E., Popovic, M.K., Bajpai, R., Stahl, U. 2010. Relevance of microbial co-culture fermentations in biotechnology. Journal of *Applied Microbiology* **109:** 371-387.

Baranitharan, E., Khan, M.R., Prasad, D., Teo, W.F. A., Tan, G.Y.A. & Jose, R. 2015. Effect of biofilm formation on the performance of microbial fuel cell for the treatment of palm oil mill effluent. *Bioprocess and Biosystems Engineering,* **38:** 15-24.

Barabasi, A.-L. & Oltvai, Z. N. 2004. Network biology: understanding the cell's functional organization. *Nature Reviews Genetics,* **5:** 101.

Belchik, S. M., Kennedy, D. W., Dohnalkova, A. C., Wang, Y., Sevinc, P. C., Wu, H., Lin, Y., Lu, H. P., Fredrickson, J. K. & SH, L. 2011. Extracellular reduction of hexavalent chromium by cytochromes MtrC and OmcA of *Shewanella oneidensis* MR-1. *Applied and Environmental Microbiology,* **77:** 4035-4041.

Biffinger, J. C., Byrd, J. N., Dudley, B. L. & Ringeisen, B. R. 2008. Oxygen exposure promotes fuel diversity for< i> *Shewanella oneidensis*</i> microbial fuel cells. *Biosensors and Bioelectronics,* **23:** 820-826.

Biffinger, J. C., Ray, R., Little, B. J., Fitzgerald, L. A., Ribbens, M., Finkel, S. E. & Ringeisen, B. R. 2009. Simultaneous analysis of physiological and electrical

output changes in an operating microbial fuel cell with *Shewanella oneidensis*. *Biotechnology and Bioengineering,* **103:** 524-531.

Bretschger, O., Onraztsova, A., Sturm, C. A., Chang, I. S., Gorby, Y. A., Reed, S. B., Culley, D. E., Reardon, C. L., Barua, S. & Romine, M. F. 2007. Current production and metal oxide reduction by *Shewanella oneidensis* MR-1 wild type and mutants. *Applied and Environmental Microbiology,* **73:** 7003-7012.

Bourdakos N, Marsili E, Mahadevan R. 2013. A defined co-culture of *Geobacter sulphrreducens and Escherichia coli* in a membrane less microbial fuel cell. *Biotechnology and Bioengineering*, **111(4)**:709-718.

Bourdakos, N., Marsili, E. & Mahadevan, R. 2014. A defined co-culture of *Geobacter sulfurreducens* and *Escherichia coli* in a membrane-less microbial fuel cell. *Biotechnology and Bioengineering,* **111:** 709-718.

Burnett, L. C., Lunn, G. & Coico, R. 2009. Biosafety: guidelines for working with pathogenic and infectious microorganisms. *Current Protocols in Microbiology***,** 1A. 1.1-1A. 1.14.

Caccavo, F., Lonergan, D. J., Lovley, D. R., Davis, M., Stolz, J. F. & Mcinerney, M. J. 1994. *Geobacter sulfurreducens* sp. nov., a hydrogen-and acetate-oxidizing dissimilatory metal-reducing microorganism. *Applied and Environmental Microbiology,* **60:** 3752-3759.

Cao, X., Wang, H., Li, X.-Q., Fang, Z. & Li, X.-N. 2017. Enhanced degradation of azo dye by a stacked microbial fuel cell-biofilm electrode reactor coupled system. *Bioresource Technology,* **227:** 273-278.

Carpentier, W., De Smet, L., Van Beeumen, J. & Brigé, A. 2005. Respiration and growth of *Shewanella oneidensis* MR-1 using vanadate as the sole electron acceptor. *Journal of Bacteriology,* **187:** 3293-3301.

Casali, N. & Preston, A. 2003. *E. coli plasmid vectors: methods and applications*, Springer Science & Business Media. 27-28.

Chen, S., Liu, G., Zhang, R., Qin, B. & Luo, Y. 2012. Development of the microbial electrolysis desalination and chemical-production cell for desalination as well as acid and alkali productions. *Environmental Science & Technology,* **46:** 2467-2472.

Choi, S. & Chae, J. 2013. Optimal biofilm formation and power generation in a micro-sized microbial fuel cell (MFC). *Sensors and Actuators A: Physical,* **195:** 206-212.

Choi, O. & Sang, B.I. 2016. Extracellular electron transfer from cathode to microbes: application for biofuel production. *Biotechnology for Biofuels,* **9:** 11-25.

Chouler, J. & Di Lorenzo, M. 2015. Water quality monitoring in developing countries; can microbial fuel cells be the answer? *Biosensors,* **5:** 450-470.

Chouler, J., Padgett, G. A., Cameron, P. J., Preuss, K., Titirici, M.-M., Ieropoulos, I. & Di lorenzo, M. 2016. Towards effective small scale microbial fuel cells for energy generation from urine. *Electrochimica Acta,* **192:** 89-98.

Chouler, J., Bentley, I., Vaz, F., O'Fee, A., Cameron, P. J. & Di Lorenzo, M. 2017. Exploring the use of cost-effective membrane materials for Microbial Fuel Cell based sensors. *Electrochimica Acta,* **231:** 319-326.

Chu, M. I., Hartig, A., Freese, E. B. & Freese, E. 1981. Adaptation of glucose-grown *Saccharomyces cerevisiae* to gluconeogenic growth and sporulation. *Microbiology,* **125:** 421-430.

Coates, J. D., Phillips, E., Lonergan, D. J., Jenter, H. & Lovley, D. R. 1996. Isolation of *Geobacter* species from diverse sedimentary environments. *Applied and Environmental Microbiology,* **62:** 1531-1536.

Conrad, R. 1999. Contribution of hydrogen to methane production and control of hydrogen concentrations in methanogenic soils and sediments. *FEMS Microbiology Ecology,* **28:** 193-202.

Coppi, M. V. 2005. The hydrogenases of *Geobacter sulfurreducens*: a comparative genomic perspective. *Microbiology,* **151:** 1239-1254.

Coughlan, L. M., Cotter, P. D., Hill, C. & Alvarez-Ordóñez, A. 2016. New weapons to fight old enemies: novel strategies for the (bio) control of bacterial biofilms in the food industry. *Frontiers in Microbiology,* **7:** 1641.

Coursolle, D. & Gralnick, J. A. 2010. Modularity of the Mtr respiratory pathway of *Shewanella oneidensis* strain MR-1. *Molecular Microbiology,* **77:** 995-1008.

Dannys, E., Green, T., Wettlaufer, A., Madhurnathakam, C. & Elkamel, A. 2016. Wastewater treatment with microbial fuel cells: a design and feasibility study for scale-up in microbreweries. *J Bioprocess Biotech,* **6:** 2-8.

Daw, J., Hallett, K., Dewolfe, J. & Venner, I. 2012. Energy efficiency strategies for municipal wastewater treatment facilities. *Contract,* **303:** 275-3000.

Dunny, G. M. & Leonard, B. A. 1997. Cell-cell communication in gram-positive bacteria. *Annual Reviews in Microbiology,* **51:** 527-564.

De Kievit, T. R., Gillis, R., Marx, S., Brown, C. & Iglewski, B. H. 2001. Quorum-sensing genes in *Pseudomonas aeruginosa* biofilms: their role and expression patterns. *Applied and Environmental Microbiology,* **67:** 1865-1873.

Demirel, B., Yenigun, O. & Onay, T. T. 2005. Anaerobic treatment of dairy wastewaters: a review. *Process Biochemistry,* **40:** 2583-2595.

Donlan, R. M. 2002. Biofilms: microbial life on surfaces. *Emerging Infectious Diseases,* **8:** 881-890.

Drogue, B., Thomas, P., Balvay, L., Prigent-Combaret, C. & Dorel, C. 2012. Engineering adherent bacteria by creating a single synthetic curli operon. *Journal of Visualized Experiments: JoVE*, **69:** 4176.

Duina, A. A., Miller, M. E. & Keeney, J. B. 2014. Budding yeast for budding geneticists: a primer on the *Saccharomyces cerevisiae* model system. *Genetics,* **197:** 33-48.

Eaktasang, N., Kang, C. S., Ryu, S. J., Suma, Y. & Kim, H. S. 2013. Enhanced current production by electroactive biofilm of sulfate-reducing bacteria in the microbial fuel cell. *Environmental Engineering Research,* **18:** 277-281.

Escapa, A., San-Martín, M. I. & Morán, A. 2014. Potential use of microbial electrolysis cells in domestic wastewater treatment plants for energy recovery. *Frontiers in Energy Research,* **2:** 19.

Fernández de Dios M.A, González del Campo A, Fernández F. J, Rodrigo M, Pazos M, Sanromán M.A. 2013. Bacterial–fungal interactions enhance power generation in microbial fuel cells and drive dye decolourisation by an ex situ and in situ electro-Fenton process. *Bioresource Technology*, **148:** 39-46

Fernando, E., Keshavarz, T., Kyazze, G., 2012. Enhanced bio-decolourisation of acid orange 7 by *Shewanella oneidensis* through co-metabolism in a microbial fuel cell. *International Biodeterioration and Biodegradation*, **72:** 1-9.

Fernando, E., Keshavarz, T., Kyazze, G., 2013. Simultaneous co-metabolic decolourisation of azo dye mixtures and bio-electricity generation under thermophillic (50 °C) and saline conditions by an adapted anaerobic mixed culture in microbial fuel cells. *Bioresource Technology***, 127:** 1-8.

Fierer N., Jackson J.A, Vilgalys R, Jackson R.B. 2005. Assessment of soil microbial community structure by use of taxon-specific quantitative PCR assays. *Applied and Environmental Microbiology*, **71**(7): 4117-4120.

Finch, A. S., Mackie, T. D., Sund, C. J. & Sumner, J. J. 2011. Metabolite analysis of *Clostridium acetobutylicum*: Fermentation in a microbial fuel cell. *Bioresource Technology,* **102:** 312-315.

Flemming, H.-C. & Wingender, J. 2010. The biofilm matrix. *Nature Reviews Microbiology,* 8**:** 623.

Franks, A. E., Malvankar, N. & Nevin, K. P. 2010. Bacterial biofilms: the powerhouse of a microbial fuel cell. *Biofuels,* **1:** 589-604.

Friman, H., Schechter, A., Ioffe, Y., Nitzan, Y. & Cahan, R. 2013. Current production in a microbial fuel cell using a pure culture of *Cupriavidus basilensis* growing in acetate or phenol as a carbon source. *Microbial Biotechnology,* **6:** 425-434.

Gajda, I., Greenman, J., Melhuish, C. & Ieropoulos, I. 2015. Self-sustainable electricity production from algae grown in a microbial fuel cell system. *Biomass and Bioenergy,* **82:** 87-93.

Garrett, T. R., Bhakoo, M. & Zhang, Z. 2008. Bacterial adhesion and biofilms on surfaces. *Progress in Natural Science,* **18:** 1049-1056.

Gavala, H., Kopsinis, H., Skiadas, I., Stamatelatou, K. & Lyberatos, G. 1999. Treatment of dairy wastewater using an upflow anaerobic sludge blanket reactor. *Journal of Agricultural Engineering Research,* **73:** 59-63.

Gyamfi-Brobbey, G. 2016. *The microbiology of diabetic foot infections: a Ghanaian perspective.* PhD thesis, University of Westminster.

Goel, R. K., Flora, J. R. & Chen, J. P. 2005. Flow equalization and neutralization. *Physicochemical Treatment Processes.* Humana Press, New Jersey.

Goldbeck C.P., Jensen H.M., Teravest M.A., Beedle N, Appling Y, Hepler M, Cambray G, Mutalik V, Angenent L.T., Ajo-Franklin C.M. **2013**. Tuning promoter strengths for improved synthesis and function of electron conduits in *Escherichia coli.* ACS Synthetic Biology **2**: 150-159.

Gomez-Flores, M., Nakhla, G. & Hafez, H. 2017. Hydrogen production and microbial kinetics of *Clostridium termitidis* in mono-culture and co-culture with *Clostridium beijerinckii* on cellulose. *AMB Express,* **7:** 84.

Guerrero-Lemus, R. & Shephard, L. E. 2017. Waste-to-Energy. *Low-Carbon Energy in Africa and Latin America.* Springer.

Hanahan, D., 1985. Techniques for transformation of E. coli. *DNA cloning*, **1:** 09 - 135.

Harnisch, F., Aulenta, F.,Schröder, U. **2011.** Microbial Fuel Cells and Bioelectrochemical Systems: Industrial and Environmental Biotechnologies Based on Extracellular Electron Transfer. In: MooYoung, M. *Comprehensive Biotechnology*. 2nd ed. Amsterdam: Elsevier. 643-659.

Harwani, D. 2013. Bacteria eating pollution and generating electricity. *International Journal of Pharma and Biosciences,* **4:** 996-1002.

Heidelberg, J. F., Paulsen, I. T., Nelson, K. E., Gaidos, E. J., Nelson, W. C., Read, T. D., Eisen, J. A., Seshadri, R., Ward, N. & Methe, B. 2002. Genome sequence of the dissimilatory metal ion–reducing bacterium *Shewanella oneidensis*. *Nature Biotechnology,* **20:** 1118-1123.

Horan, N., Smyth, M. & May, A. 2011. Optimisation of digester performance and gas yield through analysis of VFA speciation. 16th European Bio-solids and Organic Resources Conference, 20th to 21st, Lead.

Howard, E. C., Hamdan, L. J., Lizewski, S. E. & Ringelsen, B. R. 2012. High frequency of glucose-utilizing mutants in *Shewanella oneidensis* MR-1. *FEMS Microbiology Letters,* **327:** 9-14.

Hughes, T. R., Marton, M. J., Jones, A. R., Roberts, C. J., Stoughton, R., Armour, C. D., Bennett, H. A., Coffey, E., Dai, H. & He, Y. D. 2000. Functional discovery via a compendium of expression profiles. *Cell,* **102:** 109-126.

Hunt, K. A., Flynn, J. M., Naranjo, B., Shikhare, I. D. & Gralnick, J. A. 2010. Substrate-level phosphorylation is the primary source of energy conservation during anaerobic respiration of *Shewanella oneidensis* strain MR-1. *Journal of Bacteriology,* **192:** 3345-3351.

Ieropoulos, I., Melhuish, C., Greenman, J. & Horsfield, I. 2005. EcoBot-II: An artificial agent with a natural metabolism. *International Journal of Advanced Robotic Systems,* **2:** 295-300.

Jensen, H. M., Albers, A. E. 2010. Engineering of a synthetic electron conduit in living cells. *Proceedings of the National Academy of Sciences*. **107**(45): 19213-19218.

Jensen, H. M., Albers, A. E., Malley, K. R., Londer, Y. Y., Cohen, B. E., Helms, B. A., Weigele, P., Groves, J. T. & Ajo-Franklin, C. M. 2010. Engineering of a synthetic electron conduit in living cells. *Proceedings of the National Academy of Sciences,* **107:** 19213-19218.

Jensen, H. M., Teravest, M. A., Kokish, M. G. & Ajo-Franklin, C. M. 2016. CymA and Exogenous Riboflavins Improve Extracellular Electron Transfer and Couple It to Cell Growth in Mtr-Expressing *Escherichia coli*. *America Chemical Society Synthetic Biology*, **5:** 679-688.

Jeremiasse, A. W., Hamelers, H. V. & Buisman, C. J. 2010. Microbial electrolysis cell with a microbial biocathode. *Bioelectrochemistry,* **78:** 39-43.

Jiang, X., Hu, J., Fitzgerald, L. A., Biffinger, J. C., Xie, P., Ringeisen, B. R. & Lieber, C. M. 2010. Probing electron transfer mechanisms in Shewanella oneidensis MR-1 using a nanoelectrode platform and single-cell imaging. *Proceedings of the National Academy of Sciences,* **107:** 16806-16810.

Jiang, S. T., Guan, Y. J. & Bai, S. L. 2012. Power generation from phenol degradation using a microbial fuel cell. Advanced Materials Research, Trans Tech Publ, **512:** 1432-1437.

Karmakar, S., Kundu, K. & Kundu, S. 2010. Design and development of microbial fuel cells. *Current research technology and development topics in applied microbiology and microbial biotechnology. Microbiology Book Series. Spain: Formatex,* **2:** 1029-1034.

Karman, S. B., Diah, S. Z. M. & Gebeshuber, I. C. 2015. Raw materials synthesis from heavy metal industry effluents with bioremediation and phytomining: a biomimetic resource management approach. *Advances in Materials Science and Engineering,* 2015.

Karra, U., Manickam, S. S., Mccutcheon, J. R., Patel, N. & Li, B. 2013. Power generation and organics removal from wastewater using activated carbon nanofiber (ACNF) microbial fuel cells (MFCs). *International Journal of Hydrogen Energy,* **38:** 1588-1597.

Khan, M. R., Baranitharan, E., Prasad, D. & Cheng, C. K. 2016. Fast Biofilm Formation and Its Role on Power Generation in Palm Oil Mill Effluent Fed Microbial Fuel Cell. MATEC Web of Conferences, EDP Sciences.

Kouzuma, A., Kasai, T., Hirose, A. & Watanabe, K. 2015a. Catabolic and regulatory systems in *Shewanella oneidensis* MR-1 involved in electricity generation in microbial fuel cells. *Frontiers in microbiology,* **6:** 609- 620.

Kouzuma, A., Kato, S. & Watanabe, K. 2015b. Microbial interspecies interactions: recent findings in syntrophic consortia. *Frontiers in microbiology,* **6:** 477- 485.

Kracke, F., Vassilev, I. & Krömer, J. O. 2015. Microbial electron transport and energy conservation–the foundation for optimizing bioelectrochemical systems. *Frontiers in Microbiology,* **6:** 575- 593.

Kraytsberg, A. & Ein-Eli, Y. 2014. Review of advanced materials for proton exchange membrane fuel cells. *Energy & Fuels,* **28:** 7303-7330.

Kyazze G, Popov A, Dinsdale R, Esteves S, Hawkes F, Premier G, Guwy A. 2010. Influence of catholyte pH and temperature on hydrogen production from acetate using a two chamber concentric tubular microbial electrolysis cell. *International Journal of Hydrogen Energy*, **35**(15): 7716-7722.

Lagunas, R. 1993. Sugar transport in Saccharomyces cerevisiae. *FEMS Microbiology Reviews,* **10:** 229-242.

Lai, X., Cao, L., Tan, H., Fang, S., Huang, Y. & Zhou, S. 2007. Fungal communities from methane hydrate-bearing deep-sea marine sediments in South China Sea. *The ISME Journal,* **1:** 756.

Leech, D. 2015. *Properties of electrode-attached biofilms for application to microbial fuel cells (Doctoral Dissertation). National University of Ireland Galway.*

Li, Y.-H. & Tian, X. 2012. Quorum sensing and bacterial social interactions in biofilms. *Sensors,* **12:** 2519-2538.

Liu, Z., Du, Z., Lian, J., Zhu, X., Li, S. & Li, H. 2007. Improving energy accumulation of microbial fuel cells by metabolism regulation using Rhodoferax ferrireducens as biocatalyst. *Letters in Applied Microbiology,* **44:** 393-398.

Liu, Z., Li, H., Liu, J. & Su, Z. 2008. Effects of inoculation strategy and cultivation approach on the performance of microbial fuel cell using marine sediment as bio-matrix. *Journal of Applied Microbiology,* **104:** 1163-1170.

Liu, T., Rao, L., Yuan, Y. & Zhuang, L. 2015. Bioelectricity generation in a microbial fuel cell with a self-sustainable photocathode. *The Scientific World Journal,* 2015: 1-8.

Liu X-W, Sun X-F, Huang Y-X, Li D-B, Zeng R-J, Lu X, Sheng G-P, Li W-W, Cheng Y-Y, Wang S-G, Yu H-Q. **2013.** Photoaautotrophic cathodic oxygen reduction catalysed by a green algae, *Chlamydomonas reinhardtii. Biotechnology and Bioengineering*, **110**(1): 173-179.

Liu, W.-F. & Cheng, S.-A. 2014. Microbial fuel cells for energy production from wastewaters: the way toward practical application. *Journal of Zhejiang University Science a,* **15:** 841-861.

Logan, B.E., 2008. *Microbial fuel cells.* Hoboken, N.J.: Hoboken, N.J. Wiley-Interscience.

Logan, B. E. & Rabaey, K. 2012. Conversion of wastes into bioelectricity and chemicals by using microbial electrochemical technologies. *Science,* **337:** 686-690.

Logan, B. E., Wallack, M. J., Kim, K.-Y., He, W., Feng, Y. & Saikaly, P. E. 2015. Assessment of microbial fuel cell configurations and power densities. *Environmental Science & Technology Letters,* **2:** 206-214.

Longo, S., D'Antoni, B. M., Bongards, M., Chaparro, A., Cronrath, A., Fatone, F., Lema, J. M., Mauricio-Iglesias, M., Soares, A. & Hospido, A. 2016. Monitoring and diagnosis of energy consumption in wastewater treatment plants. A state of the art and proposals for improvement. *Applied Energy,* **179:** 1251-1268.

Luo H, Liu G, Zhang R, Jin S. 2009**.** Phenol degradation in microbial fuel cells. Chemical Engineering Journal, **147**: 259-264.

Luo, X., Zhang, F., Liu, J., Zhang, X., Huang, X. & Logan, B. E. 2014. Methane production in microbial reverse-electrodialysis methanogenesis cells (MRMCs) using thermolytic solutions. *Environmental science & technology,* **48:** 8911-8918.

Malvankar, N. S. & Lovley, D. R. 2012. Microbial nanowires: a new paradigm for biological electron transfer and bioelectronics. *ChemSusChem,* **5:** 1039-1046.

Mansoorian, H.J., Mahvi, A.H., Jafari, A.J. & Khanjani, N. 2014. Evaluation of dairy industry wastewater treatment and simultaneous bioelectricity generation in a catalyst-less and mediator-less membrane microbial fuel cell. *Journal of Saudi Chemical Society.* 1-13.

Mehanna, M., Kiely, P. D., Call, D. F. & Logan, B. E. 2010. Microbial electrodialysis cell for simultaneous water desalination and hydrogen gas production. *Environmental science & technology,* **44:** 9578-9583.

Miller, M. B. & Bassler, B. L. 2001. Quorum sensing in bacteria. *Annual Reviews in Microbiology,* **55:** 165-199.

Moestedt, J., Müller, B., Westerholm, M. & Schnürer, A. 2016. Ammonia threshold for inhibition of anaerobic digestion of thin stillage and the importance of organic loading rate. *Microbial Biotechnology,* **9:** 180-194.

Mohan, S. V., Raghavulu, S. V. & Sarma, P. 2008. Influence of anodic biofilm growth on bioelectricity production in single chambered mediatorless microbial fuel cell using mixed anaerobic consortia. *Biosensors and Bioelectronics,* **24:** 41-47.

Moscoviz, R., De Fouchécour, F., Santa-Catalina, G., Bernet, N. & Trably, E. 2017. Cooperative growth of Geobacter sulfurreducens and Clostridium pasteurianum with subsequent metabolic shift in glycerol fermentation. *Scientific reports,* 7: 44334 -443343

Mrozik, A. & Piotrowska-Seget, Z. 2010. Bioaugmentation as a strategy for cleaning up of soils contaminated with aromatic compounds. *Microbiological Research,* **165:** 363-375.

Mukherji, R. & Prabhune, A. 2015. Enzyme purification and kinetic characterization of AHL lactonase from *Bacillus* sp. RM1 a novel and potent quorum quencher isolated from Fenugreek root nodule rhizosphere. *International Journal of Current Microbiology and Applied Science,* **4:** 909-924.

Murphy, M. F., Edwards, T., Hobbs, G., Shepherd, J. & Bezombes, F. 2016. Acoustic vibration can enhance bacterial biofilm formation. *Journal of Bioscience and Bioengineering,* **122:** 765-770.

Myers, C. R. & Myers, J. M. 2002. MtrB is required for proper incorporation of the cytochromes OmcA and OmcB into the outer membrane of *Shewanella putrefaciens* MR-1. *Applied and Environmental Microbiology,* **68:** 5585-5594.

Napoli, F., Olivieri, G., Russo, M. E., Marzocchella, A. & Salatino, P. 2010. Butanol production by *Clostridium acetobutylicum* in a continuous packed bed reactor. *Journal of industrial microbiology & biotechnology,* **37:** 603-608.

Ng, W. J. & Tjan, K. W. 2006. *Industrial wastewater treatment*, World Scientific. Imperial Collge Press, London.

Niessen, J., Schroder, U. & Scholz, F. 2004. Exploiting complex carbohydrates for microbial electricity generation–a bacterial fuel cell operating on starch. *Electrochemistry Communications,* **6:** 955-958.

Nimje, V. R., Chen, C.-C., Chen, H.-R., Chen, C.-Y., Tseng, M.-J., Cheng, K.-C., Shih, R.-C. & Chang, Y.-F. 2012. A single-chamber microbial fuel cell without an air cathode. *International journal of Molecular Sciences,* **13:** 3933-3948.

Noar, J., Makwana, S. & Bruno-Bárcena, J. M. 2014. Complete genome sequence of solvent-tolerant *Clostridium beijerinckii* strain SA-1. *Genome announcements,* **2:** e01310-14.

Oh, S.-E. & Logan, B. E. 2007. Voltage reversal during microbial fuel cell stack operation. *Journal of Power Sources,* **167:** 11-17.

Okamoto, A., Hashimoto, K. & Nakamura, R. 2012. Long-range electron conduction of *Shewanella* biofilms mediated by outer membrane c-type cytochromes. *Bioelectrochemistry,* **85:** 61-65.

Oliveira, A. & Cunha, M. 2008. Bacterial biofilms with emphasis on coagulase-negative staphylococci. *Journal of Venomous Animals and Toxins including Tropical Diseases,* **14:** 572-596.

Oliveira V.B., Simoes M, Melo L.F. Pinto A.M.F.R. 2013. Overview on the developments of microbial fuel cells*. Biochemical Engineering Journal*, **73**: 53-64.

Oram, J. & Jeuken, L. J. 2016. A Re-evaluation of Electron-Transfer Mechanisms in Microbial Electrochemistry: Shewanella Releases Iron that Mediates Extracellular Electron Transfer. *ChemElectroChem,* **3:** 829-835.

Ostergaard, S., Olsson, L. & Nielsen, J. 2000. Metabolic engineering of *Saccharomyces cerevisiae*. *Microbiology and Molecular Biology Reviews,* **64:** 34-50.

Pandhal, J. & Noirel, J. 2014. Synthetic microbial ecosystems for biotechnology. *Biotechnology letters,* **36:** 1141-1151.

Pandit, S., Khilari, S., Roy, S., Pradhan, D. & Das, D. 2014. Improvement of power generation using *Shewanella putrefaciens* mediated bioanode in a single chambered microbial fuel cell: Effect of different anodic operating conditions. *Bioresource technology,* **166:** 451-457.

Pant, D., Van Bogaert, G., Diels, L. & Vanbroekhoven, K. 2010. A review of the substrates used in microbial fuel cells (MFCs) for sustainable energy production. *Bioresource Technology,* **101:** 1533-1543.

Permana, D., Rosdianti, D., Ishmayana, S., Rachman, S. D., Putra, H. E., Rahayuningwulan, D. & Hariyadi, H. R. 2015. Preliminary Investigation of Electricity Production Using Dual Chamber Microbial Fuel Cell (DCMFC) with *Saccharomyces cerevisiae* as Biocatalyst and Methylene Blue as an Electron Mediator. *Procedia Chemistry,* **17:** 36-43.

Potter, M. C. 1911. Electrical effects accompanying the decomposition of organic compounds. *Proceeding Royal Society London B,* **84:** 260-276.

Pham, T., Rabaey, K., Aelterman, P., Clauwaert, P., De Schamphelaire, L., Boon, N. & Verstraete, W. 2006. Microbial fuel cells in relation to conventional anaerobic digestion technology. *Engineering in Life Sciences,* **6:** 285-292.

Plyuta, V., Zaitseva, J., Lobakova, E., Zagoskina, N., Kuznetsov, A. & Khmel, I. 2013. Effect of plant phenolic compounds on biofilm formation *by Pseudomonas aeruginosa*. *Apmis,* **121:** 1073-1081.

Qu Y, Feng Y, Wang X, Logan B.E. 2012. Use of a co-culture to enable current production by *Geobacter sulphurreducens*. Applied and Environmental Microbiology. **78(9):**3484-3487.

Qureshi, N., Annous, B.A., Ezeji, T.C., Karcher, P., & Maddox, I.S. 2005. Biofilm reactors for industrial bioconversion processes: employing potential of enhanced reaction rates. *Microbial Cell Factories*, **4**(1): 24 45

Rabaey K, Boon N, Hofte M, Verstraete W. 2005. Microbial phenazine production enhances electron transfer in biofuel cells. Environmental Science and Technology, **39**(9)**:** 3401 – 3408.

Rabaey, K. & Verstraete, W. 2005. Microbial fuel cells: novel biotechnology for energy generation. *TRENDS in Biotechnology,* **23:** 291-298.

Rahimnejad, M., Adhami, A., Darvari, S., Zirepour, A. & Oh, S.-E. 2015. Microbial fuel cell as new technology for bioelectricity generation: A review. *Alexandria Engineering Journal,* **54:** 745-756.

Read, S. T., Dutta, P., Bond, P. L., Keller, J. & Rabaey, K. 2010. Initial development and structure of biofilms on microbial fuel cell anodes. *BMC microbiology,* **10:** 98 -108

Ren Z, Wang T.E, Regan J.M. 2007. Electricity production from cellulose in a microbial fuel cell using a defined binary culture. *Environmental Science and Technology.* **41**: 4781-4786.

Ren, H., Lee, H.-S. & Chae, J. 2012. Miniaturizing microbial fuel cells for potential portable power sources: promises and challenges. *Microfluidics and Nanofluidics,* **13:** 353-381.

Rosenbaum, M.A., Bar, H.Y., Beg, Q.K Segre, D., Booth, J., Cotta, M.A. & Angenent, L. T. 2011. *Shewanella oneidensis* in a lactate-fed pure-culture and a glucose-fed co-culture with Lactococcus lactis with an electrode as electron acceptor. *Bioresource Technology,* **102:** 2623-2628.

Roth, T. L., Milenkovic, L. & Scott, M. P. 2014. A rapid and simple method for DNA engineering using cycled ligation assembly. *PloS one,* 9**,** e107329.

Saeed, H. M., Husseini, G. A., Yousef, S., Saif, J., Al-Asheh, S., Fara, A. A., Azzam, S., Khawaga, R. & Aidan, A. 2015. Microbial desalination cell technology: a review and a case study. *Desalination,* **359:** 1-13.

Sandoval-Espinola, W. J., Chinn, M. & Bruno-Barcena, J. M. 2015. Inoculum optimization of *Clostridium beijerinckii* for reproducible growth. *FEMS Microbiology Letters,* **362:** 164.

Santoro, C., Serov, A., Villarrubia, C. W. N., Stariha, S., Babanova, S., Artyushkova, K., Schuler, A. J. & Atanassov, P. 2015. High catalytic activity and pollutants resistivity using Fe-AAPyr cathode catalyst for microbial fuel cell application. *Scientific Reports,* **5:** 16596- 165106.

Saratale, G. D., Saratale, R. G., Shahid, M. K., Zhen, G., Kumar, G., Shin, H.-S., Choi, Y.-G. & Kim, S.-H. 2017b. A comprehensive overview on electro-active biofilms, role of exo-electrogens and their microbial niches in microbial fuel cells (MFCs). *Chemosphere,* **178:** 534-547.

Schlafer, S. & Meyer, R. L. 2017. Confocal microscopy imaging of the biofilm matrix. *Journal of microbiological methods,* 138**:** 50-59.

Scott, K., Murano, C. & Rimbu, G. 2007. A tubular microbial fuel cell. *Journal of Applied Electrochemistry,* 37**,** 1063 -1068.

Sekar, N. & Ramasamy, R. P. 2013. Electrochemical impedance spectroscopy for microbial fuel cell characterization. *J Microb Biochem Technol S,* 6.

Serres, M. H. & Riley, M. 2006. Genomic analysis of carbon source metabolism of Shewanella oneidensis MR-1: predictions versus experiments. *Journal of Bacteriology,* **188:** 4601-4609.

Simon, A. J. & Ellington, A. D. 2016. Recent advances in synthetic biosafety. *F1000Research,* 5: 1-13.

Singh, D. & Srivastava, B. 2002. Removal of phenol pollutants from aqueous solutions using various adsorbents. *Journal of Scientific and Industrial Research,* **61:** 208-218.

Song T-S, Wu X-Y, Zhou C-C. 2014. Effect of different acclimation methods on the performance of microbial fuel cells using phenol as substrate. *Bioprocess and Biosystems Engineering,* **37**:133-138.

Song, Y.-H., Hidayat, S., Kim, H.-K. & Park, J.-Y. 2016. Hydrogen production in microbial reverse-electrodialysis electrolysis cells using a substrate without buffer solution. *Bioresource Technology,* **210:** 56-60.

Stanbury, P. F., Whitaker, A. & Hall, S. J. 2013. *Principles of Fermentation Technology*, Elsevier, London.

Sun, J., LI, W., Li, Y., Hu, Y. & Zhang, Y. 2013. Redox mediator enhanced simultaneous decolorization of azo dye and bioelectricity generation in air-cathode microbial fuel cell. *Bioresource Technology,* **142:** 407-414.

Sutaryo, S., Ward, A. & Moller, H. 2014. Ammonia inhibition in thermophilic anaerobic digestion of dairy cattle manure. *Journal of the Indonesian Tropical Animal Agriculture,* **39:** 83-90.

Taghadosi, R., Shakibaie, M. R. & Masoumi, S. 2015. Biochemical detection of N-Acyl homoserine lactone from biofilm-forming uropathogenic *Escherichia coli* isolated from urinary tract infection samples. *Reports of biochemistry & Molecular Biology,* **3(2):** 56-61.

Tang, Y. J., Meadows, A. L., Kirby, J. & Keasling, J. D. 2007. Anaerobic central metabolic pathways in *Shewanella oneidensis* MR-1 reinterpreted in the light of isotopic metabolite labeling. *Journal of Bacteriology,* **189:** 894-901.

Tateda, K., Ishii, Y., Horikawa, M., Matsumoto, T., Miyairi, S., Pechere, J. C., Standiford, T. J., Ishiguro, M. & Yamaguchi, K. 2003. The *Pseudomonas*

aeruginosa autoinducer N-3-oxododecanoyl homoserine lactone accelerates apoptosis in macrophages and neutrophils. *Infection and Immunity,* **71:** 5785-5793.

Thormann, K. M., Saville, R. M., Shukla, S., Pelletier, D. A. & Spormann, A. M. 2004. Initial phases of biofilm formation in *Shewanella oneidensis* MR-1. *Journal of Bacteriology,* **186:** 8096-8104.

Tian, M., Du, D., Zhou, W., Zeng, X. & Cheng, G. 2017. Phenol degradation and genotypic analysis of dioxygenase genes in bacteria isolated from sediments. *Brazilian Journal of Microbiology,* **48:** 305-313.

Torres, L., Krüger, A., Csibra, E., Gianni, E. & Pinheiro, V. B. 2016. Synthetic biology approaches to biological containment: pre-emptively tackling potential risks. *Essays in Biochemistry,* **60:** 393-410.

Uno, M., Phansroy, N., Aso, Y. & Ohara, H. 2017. Starch-fueled microbial fuel cells by two-step and parallel fermentation using *Shewanella oneidensis* MR-1 and Streptococcus bovis 148. *Journal of Bioscience and Bioengineering,* **124:** 189-194.

Van der Gast CJ, Whiteley AS, Starkey M, Knowles CJ, Thompson IP. 2003. Bioaugmentation strategies for remediating mixed chemical effluents. *Biotechnology Progress*, **19(4):** 1156-1161.

Venkateswaran, K., Moser, D. P., Dollhopf, M. E., Lies, D. P., Saffarini, D. A., Macgregor, B. J., Ringelberg, D. B., White, D. C., Nishijima, M. & Sano, H. 1999. Polyphasic taxonomy of the genus Shewanella and description of Shewanella oneidensis sp. nov. *International Journal of Systematic and Evolutionary Microbiology,* **49:** 705-724.

Velasquez-orta, S. B., Curtis, T. P. & Logan, B. E. 2009. Energy from algae using microbial fuel cells. *Biotechnology and bioengineering,* **103:** 1068-1076.

Verduyn, C., Postma, E., Scheffers, W. A. & Van Dijken, J. P. 1990. Physiology of *Saccharomyces cerevisiae* in Anaerobic Glucose-Limited Chemostat Culturesx. *Microbiology,* **136:** 395-403.

Visioli, L. J., Alves, E. A., Trindade, A., Kuhn, R. C., Schwaab, M. & Mazutti, M. A. 2015. Evaluation of biobutanol production by *Clostridium beijerinckii* NRRL B-592 using sweet sorghum as carbon source. *Ciência Rural,* **45:** 1707-1712.

Wang, L., Trawick, J. D., Yamamoto, R. & Zamudio, C. 2004. Genome-wide operon prediction in *Staphylococcus aureus*. *Nucleic acids research,* **32:** 3689-3702.

Watanabe, K. 2008. Recent developments in microbial fuel cell technologies for sustainable bioenergy. *Journal of Bioscience and Bioengineering,* **106:** 528-536.

Webb, J. S., Thompson, L. S., James, S., Charlton, T., Tolker-Nielsen, T., Koch, B., Givskov, M. & Kjelleberg, S. 2003. Cell death in *Pseudomonas aeruginosa* biofilm development. *Journal of Bacteriology,* **185:** 4585-4592.

Wood, T. K., Hong, S. H. & Ma, Q. 2011. Engineering biofilm formation and dispersal. *Trends in Biotechnology,* **29:** 87-94

Wright, M. H., Farooqui, S. M., White, A. R. & Greene, A. C. 2016. Production of manganese oxide nanoparticles by Shewanella species. *Applied and environmental microbiology,* **82:** 5402-5409.

Wright, O., Stan, G.-B. & Ellis, T. 2013. Building-in biosafety for synthetic biology. *Microbiology,* **159:** 1221-1235.

Wrighton, K., Thrash, J., Melnyk, R., Bigi, J., Byrne-Bailey, K., Remis, J., Schichnes, D., Auer, M., Chang, C. & Coates, J. 2011. Evidence for direct electron transfer by a Gram-positive bacterium isolated from a microbial fuel cell. *Applied and Environmental Microbiology,* **77:** 7633-7639.

Wong, T. S., Roccatano, D. & Schwaneberg, U. 2007. Steering directed protein evolution: strategies to manage combinatorial complexity of mutant libraries. *Environmental Microbiology,* **9:** 2645-2659.

Wu, P. & Tan, M. 2012. Challenges for sustainable urbanization: a case study of water shortage and water environment changes in Shandong, China. *Procedia Environmental Sciences,* **13:** 919-927.

Xia, S., Zhou, L., Zhang, Z. & Li, J. 2012. Influence and mechanism of N-(3-oxooxtanoyl)-L-homoserine lactone (C8-oxo-HSL) on biofilm behaviors at early stage. *Journal of Environmental Sciences,* **24:** 2035-2040.

Xinmin, L., Jianjun, W. & Benyue, G. 2016. Series and parallel connection of anaerobic fluidized bed microbial fuel cells (MFCs). *International Journal of Applied Microbiology and Biotechnology Research,* **4:** 7-14.

Xiong, Y., Chen, B., Shi, L., Fredrickson, J. K., Bigelow, D. J. & Squier, T. C. 2011. Targeted protein degradation of outer membrane decaheme cytochrome MtrC metal reductase in *Shewanella oneidensis* MR-1 measured using biarsenical probe crash-edt2. *Biochemistry,* **50:** 9738-9751.

Yong, Y. C., Yu, Y. Y., Yang, Y., Liu, J., Wang, J. Y. & Song, H. 2013. Enhancement of extracellular electron transfer and bioelectricity output by synthetic porin. *Biotechnology and Bioengineering,* **110:** 408-416.

Zacharoff, L., Chan, C. H. & Bond, D. R. 2016. Reduction of low potential electron acceptors requires the CbcL inner membrane cytochrome of *Geobacter sulfurreducens. Bioelectrochemistry,* **107:** 7-13.

Zhang, Y., Baranov, P. V., Atkins, J. F. & Gladyshev, V. N. 2005. Pyrrolysine and selenocysteine use dissimilar decoding strategies. *Journal of Biological Chemistry*.

Zhang, L., Zhu, X., Li, J., Liao, Q. & Ye, D. 2011. Biofilm formation and electricity generation of a microbial fuel cell started up under different external resistances. *Journal of Power Sources,* **196:** 6029-6035.

Zhang, X., Ye, X., Finneran, K.T., Zilles, J.L. & Morgenroth, E. 2013. Interactions between *Clostridium beijerinckii* and *Geobacter metallireducens* in co-culture fermentation with anthrahydroquinone-2,6-disulfonate (AH2QDS) for enhanced biohydrogen production from xylose. *Biotechnology and Bioengineering,* **110**(1): 164-172.

Zhao, F., Slade, R.C. 2009. "Techniques for the study and development of microbial fuel cells: an electrochemical perspective." *Chemical Society Reviews* **. 38**(7): 1926-1939.

Zhao, X., Condruz, S., Chen, J. & Jolicoeur, M. 2016. A quantitative metabolomics study of high sodium response in *Clostridium acetobutylicum* ATCC 824 acetone-butanol-ethanol (ABE) fermentation. *Scientific Reports,* **6:** 28307.

Zhao, Y.-G., Zhang, Y., She, Z., Shi, Y., Wang, M., Gao, M. & Guo, L. 2017. Effect of Substrate Conversion on Performance of Microbial Fuel Cells and Anodic Microbial Communities. *Environmental Engineering Science,* **34:** 666-674.

Zhou M, He H, Tin T, Wang H. 2012. Power generation enhancement in novel microbial carbon capture cells with immobilised *Chrorella vulgaris*. *Journal of Power Sources*, **214**: 216-219.

Zhuang, L., Chen, Q., Zhou, S., Yuan, Y. & Yuan, H. 2012. Methanogenesis control using 2-Bromoethanesulfonate for enhanced power recovery from sewage sludge in air-cathode microbial fuel cells. *International Journal of Electrochemical Science* ***7*****:** *6512-6523.*

Web references

iGEM York 2013. MFC Engineered *Escherichia coli.* [online] available at: http://2013.igem.org/Team:York_UK

RDP 2015. Compliance manual. [onloine] available at: http://synbiota-tinker-studio.wikidot.com/compliance-manual.

Synbiota 2015. RDP™ Assembly. [onloine] available at:http://synbiota-tinker-studio.wikidot.com/dna-assembly.

Appendix

Appendix 1: Ethanol, Butyric and Acetic Standards analysed using Gas Chromatography (FID).

Ethanol 50mg/L

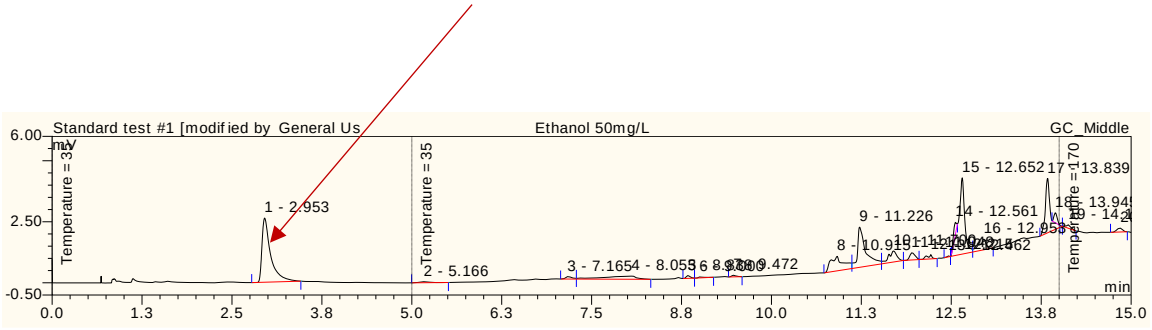

No.	Peakname	Ret.Time	Area
		min	mV*min
1	Ethanol	2.953	0.3690

Ethanol concentration at 100mg/L

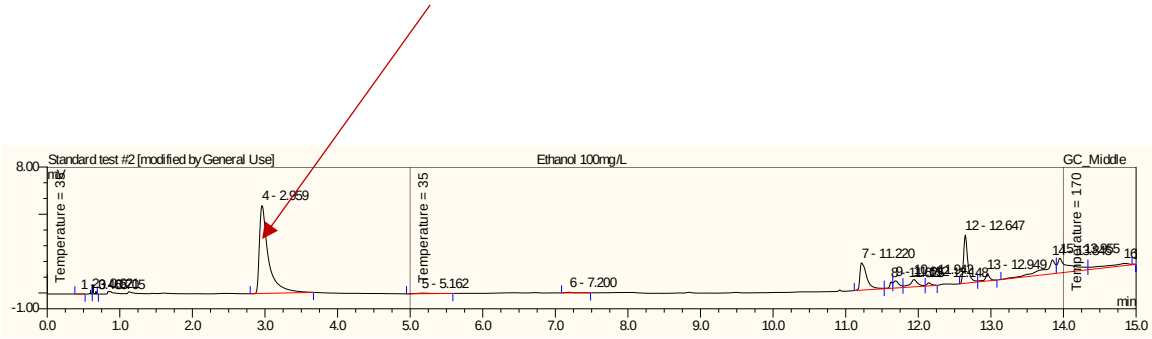

No.	Peakname	Ret.Time	Area
		min	mV*min
1	Ethanol	2.959	0.8060

Ethanol 200mg/L

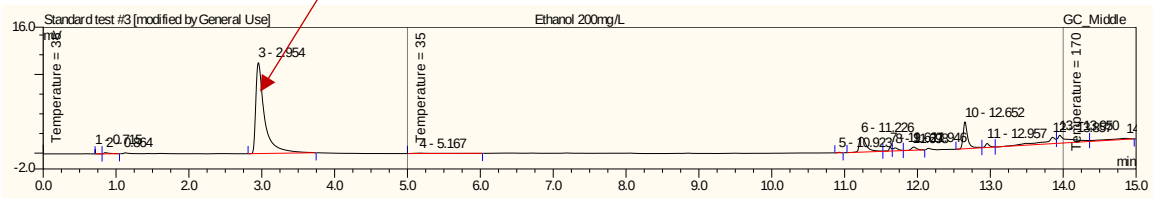

No.	Peakname	Ret.Time	Area
		min	mV*min
1	Ethanol	2.954	1.6158

Ethanol 500mg/L

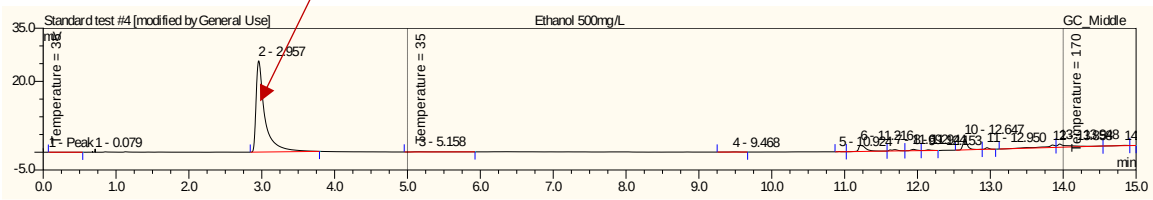

No.	Peakname	Ret.Time	Area
		min	mV*min
2	Ethanol	2.957	3.6014

Butyric acid peak at 200mg/L

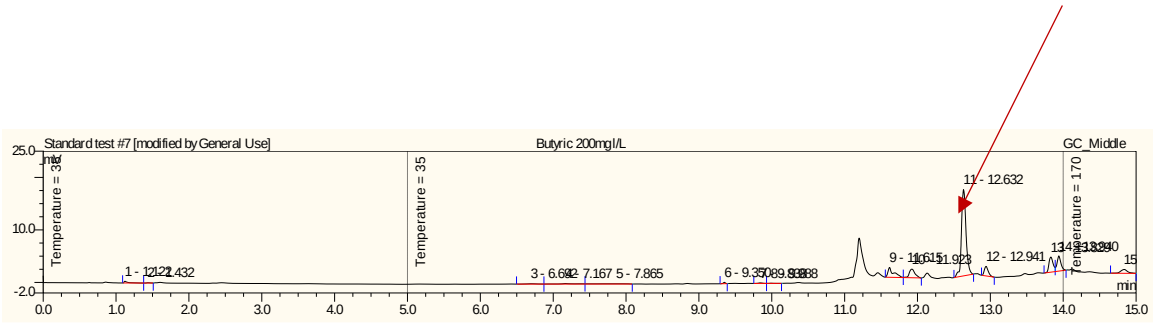

No.	Peakname	Ret.Time	Area
		min	mV*min
9	n.a.	12.643	0.8805

Butyric acid peak at 400mg/L

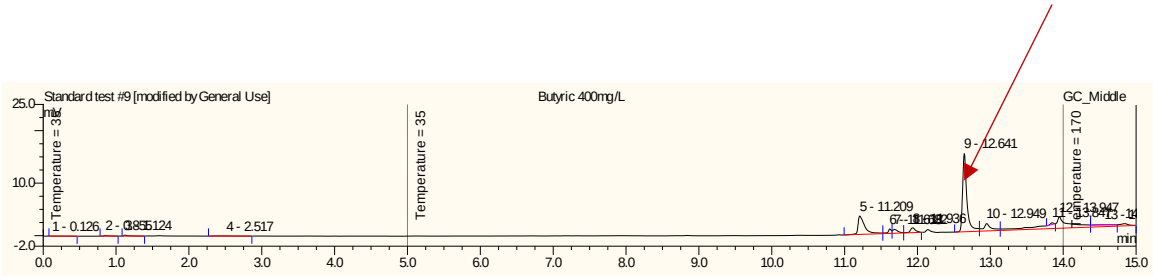

No.	Peakname	Ret.Time	Area
		min	mV*min
1	n.a.	12.641	1.0206

Butyric acid peak at 800mg/L

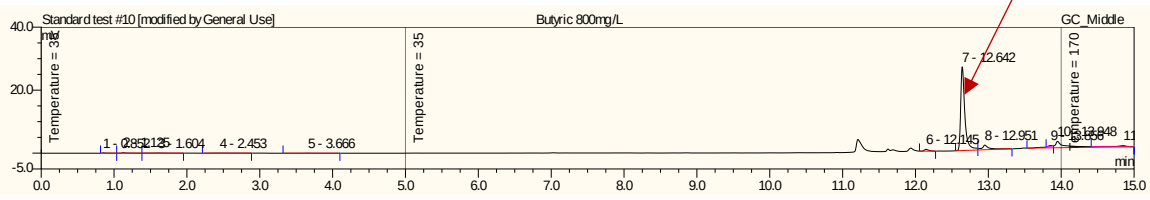

No.	Peakname	Ret.Time	Area
		min	mV*min
1	n.a.	12.642	1.7451

Acetic acid peak at 200mg/L

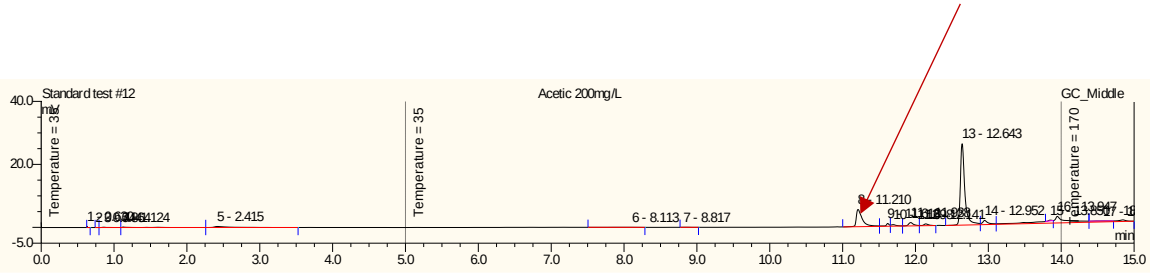

No.	Peakname	Ret.Time	Area
		min	mV*min
8	n.a.	11.210	0.5264

Acetic acid peak at 400mg/L

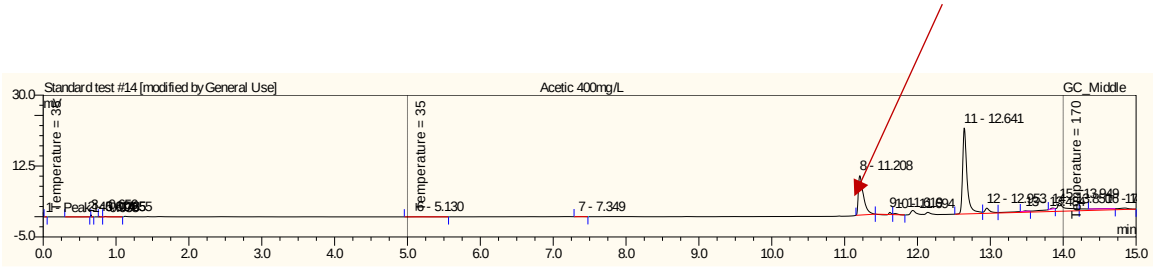

No.	Peakname	Ret.Time	Area
		min	mV*min
1	n.a.	11.208	0.7931

Acetic acid peak at 800mg/L

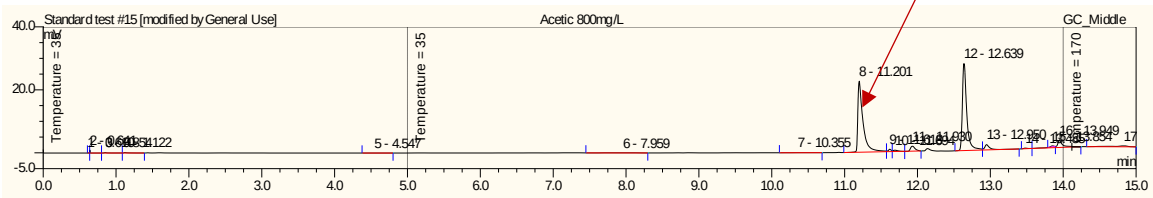

No.	Peakname	Ret.Time	Area
		min	mV*min
1	Acetic acid	11.201	1.8348

Appendix 2: Standard Curve of Protein (Albumin) using Bradford Assay.

A

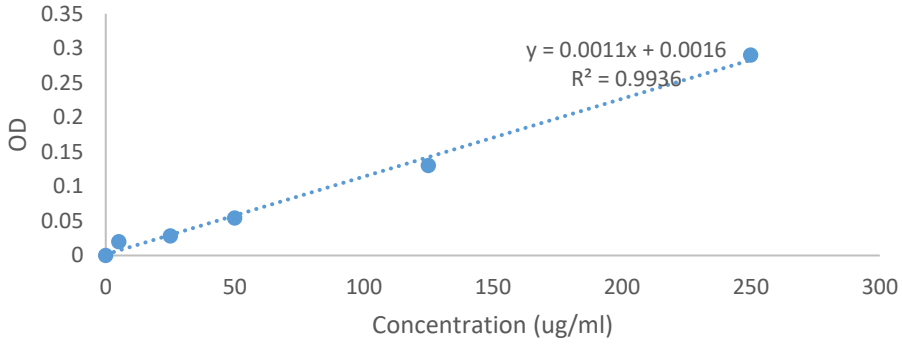

B

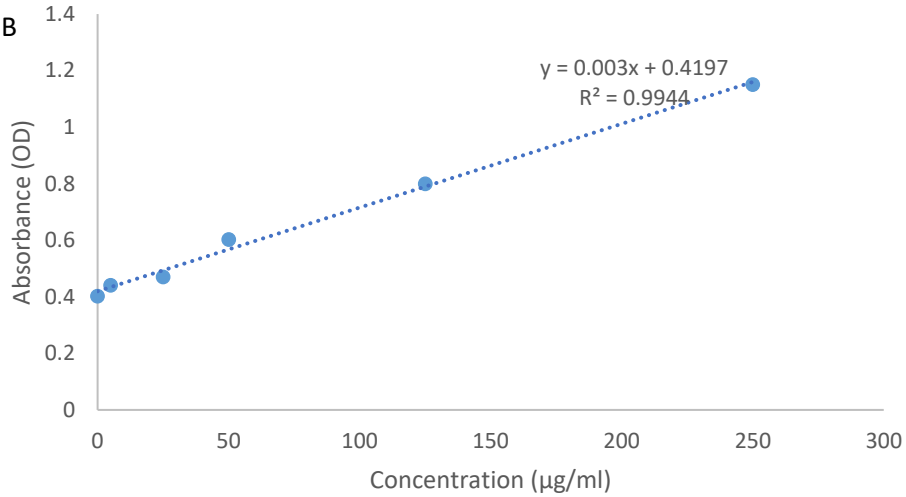

Appendix 3: Gas chromatography analysis of metabolic products of glucose utilization by *S. oneidensis.*

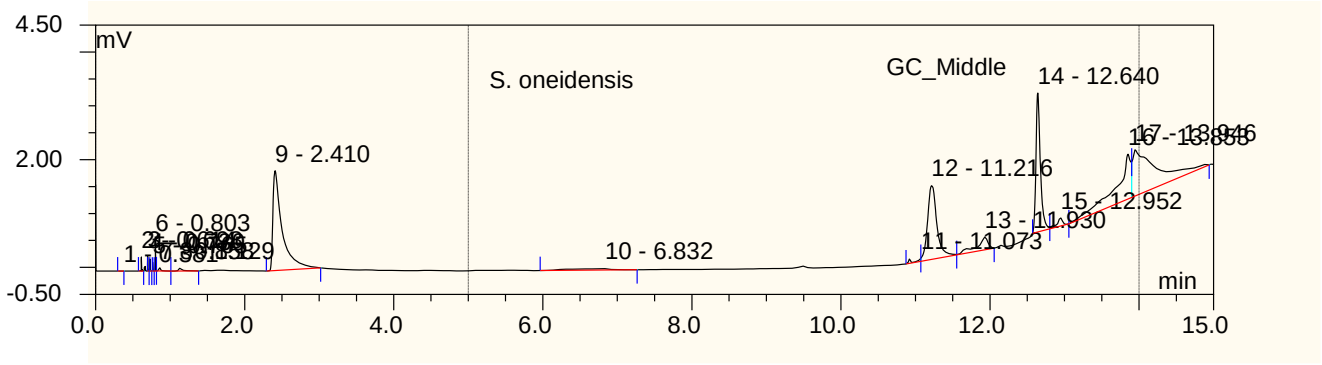

Appendix 4: Journal Publications & Conference proceedings.

Journal Publications

Fapetu, S., Keshavarz, T., Clements, M. & Kyazze, G. 2016. Contribution of direct electron transfer mechanisms to overall electron transfer in microbial fuel cells utilising *Shewanella oneidensis* as biocatalyst. *Biotechnology letters.38(9): 1465-1473.*

Gomaa, O. M., Fapetu, S., Kyazze, G. & Keshavarz, T. 2017. The role of riboflavin in decolourisation of Congo red and bioelectricity production using *Shewanella oneidensis* MR1 under MFC and non-MFC conditions. *World Journal of Microbiology and Biotechnology. 33(3): 56 – 62.*

Conference proceedings

- **Fapetu, S.A**., Keshavarz, T., Clements, M.O. and Kyazze, G. 2017. Overexpression of the Mtr pathway in *Shewanella oneidensis* for bioelectricity production. (Society for Applied Microbiology) 6th ECS Research Symposium. University of Westminster 19 Apr 2017 Society for Applied Microbiology.
- Gomaa, O., **Fapetu, S**., Kyazze, G. and Keshavarz, T. 2016. Applying synthetic biology as a tool to understand simultaneous bioenergy production and biodegradation process. Aulenta, F. and Majone, M. (ed.) EU-ISMET 2016: The 3rd European Meeting of the International Society for Microbial Electrochemistry and Technology. Department of Chemistry (NEC) Sapienza, University of Rome, Rome, Italy 26 to end of 28 Sep 2016 ISMET.
- **Fapetu, S.,** Keshavarz, T., Clements, M.O. and Kyazze, G. 2016. Enhancing electricity production from wastewater using microbial fuel cells. Aulenta, F. and Majone, M. (ed.) EU-ISMET 2016: The 3rd European Meeting of the International Society for Microbial Electrochemistry and Technology. Department of Chemistry (NEC) Sapienza, University of Rome, Rome, Italy 26 to end of 28 Sep 2016 ISMET.

Appendix 5. *Shewanella oneidensis* MR-1 chromosome, complete genome

NCBI Reference Sequence: NC_004347.2

GenBank Graphics

>NC_004347.2:c1859279-1858278 Shewanella oneidensis MR-1 *mtrA* (1002 bp) *gene sequence*,

ATGAAGAACTGCCTAAAAATGAAAAACCTACTGCCGGCACTTACCATCACAATGGCAATGTC
TGCAGTTA
TGGCATTAGTCGTCACACCAAACGCTTATGCGTCGAAGTGGGATGAGAAAATGACGCCAGA
GCAAGTCGA
AGCCACCTTAGATAAGAAGTTTGCCGAAGGCAACTACTCCCCTAAAGGCGCCGATTCTTGCT
TGATGTGC
CATAAGAAATCCGAAAAAGTCATGGACCTTTTCAAAGGTGTCCACGGTGCGATTGACTCCTC
TAAGAGTC
CAATGGCTGGCCTGCAATGTGAGGCATGCCACGGCCCACTGGGTCAGCACAACAAAGGCG
GCAACGAGCC
GATGATCACTTTTGGTAAGCAATCAACCTTAAGTGCCGACAAGCAAAACAGCGTATGTATGA
GCTGTCAC
CAAGACGATAAGCGTATGTCTTGGAATGGCGGTCACCATGACAATGCCGATGTTGCTTGTGC
TTCTTGTC
ACCAAGTACACGTCGCAAAAGATCCTGTGTTATCTAAAAACACGGAAATGGAAGTCTGTACT
AGCTGCCA
TACAAAGCAAAAAGCGGATATGAATAAACGCTCAAGTCACCCACTCAAATGGGCACAAATG
ACCTGTAGC
GACTGTCACAATCCCCATGGGAGCATGACAGATTCCGATCTTAACAAGCCTAGCGTGAATG
ATACCTGTT
ATTCCTGTCACGCCGAAAAACGCGGCCCAAAACTTTGGGAGCATGCACCCGTCACTGAGAA
TTGTGTCAC
TTGCCACAATCCTCACGGTAGTGTGAATGACGGTATGCTGAAAACCCGTGCGCCACAGCTA
TGTCAGCAA
TGTCACGCCAGCGATGGCCACGCCAGCAACGCCTACTTAGGTAACACTGGATTAGGTTCAA
ATGTCGGTG
ACAATGCCTTTACTGGTGGAAGAAGCTGCTTAAATTGCCATAGTCAGGTTCATGGTTCTAAC
CATCCATC
TGGCAAGCTATTACAGCGCTAA

Appendix 6. *Shewanella oneidensis* MR-1 chromosome, complete genome

NCBI Reference Sequence: NC_004347.2

GenBank Graphics

>NC_004347.2:c1861363-1859348 Shewanella oneidensis MR-1 *mtrC* (2016bp) chromosome, complete genome.

ATGATGAACGCACAAAAATCAAAAATCGCACTGCTGCTCGCAGCAAGTGCCGTCACAATGG
CCTTAACCG
GCTGTGGTGGAAGCGATGGTAATAACGGCAATGATGGTAGTGATGGTGGTGAGCCAGCAG
GTAGCATCCA
GACGTTAAACCTAGATATCACTAAAGTAAGCTATGAAAATGGTGCACCTATGGTCACTGTTT
TCGCCACT
AACGAAGCCGACATGCCAGTGATTGGTCTCGCAAATTTAGAAATCAAAAAAGCACTGCAATT
AATACCGG
AAGGGGCGACAGGCCCAGGTAATAGCGCTAACTGGCAAGGCTTAGGCTCATCAAAGAGCT
ATGTCGATAA
TAAAAACGGTAGCTATACCTTTAAATTCGACGCCTTCGATAGTAATAAGGTCTTTAATGCTCA
ATTAACG
CAACGCTTTAACGTTGTTTCTGCTGCGGGTAAATTAGCAGACGGAACGACCGTTCCCGTTGC
CGAAATGG
TTGAAGATTTCGACGGCCAAGGTAATGCGCCGCAATATACAAAAAATATCGTTAGCCACGA
AGTATGTGC
TTCTTGCCACGTAGAAGGTGAAAAGATTTATCACCAAGCTACTGAAGTCGAAACTTGTATTT
CTTGCCAC
ACTCAAGAGTTTGCGGATGGTCGCGGCAAACCCCATGTCGCCTTTAGTCACTTAATTCACAA
TGTGCATA
ATGCCAACAAAGCTTGGGGCAAAGACAATAAAATCCCTACAGTTGCACAAAATATTGTCCAA
GATAATTG
CCAAGTTTGTCACGTTGAATCCGACATGCTCACCGAGGCAAAAAACTGGTCACGTATTCCAA
CAATGGAA
GTCTGTTCTAGCTGTCACGTAGACATCGATTTTGCTGCGGGTAAAGGCCACTCTCAACAACT
CGATAACT
CCAACTGTATCGCCTGCCATAACAGCGACTGGACTGCTGAGTTACACACAGCCAAAACCAC
CGCAACTAA
GAACTTGATTAATCAATACGGTATCGAGACTACCTCGACAATTAATACCGAAACTAAAGCAG
CCACAATT

AGTGTTCAAGTTGTAGATGCGAACGGTACTGCTGTTGATCTCAAGACCATCCTGCCTAAAGT GCAACGCT

TAGAGATCATCACCAACGTTGGTCCTAATAATGCAACCTTAGGTTATAGTGGCAAAGATTCA ATATTTGC

AATCAAAAATGGAGCTCTTGATCCAAAAGCTACTATCAATGATGCTGGCAAACTGGTTTATA CCACTACT

AAAGACCTCAAACTTGGCCAAAACGGCGCAGACAGCGACACAGCATTTAGCTTTGTAGGTT GGTCAATGT

GTTCTAGCGAAGGTAAGTTTGTAGACTGTGCAGACCCTGCATTTGATGGTGTTGATGTAACT AAGTATAC

CGGCATGAAAGCGGATTTAGCCTTTGCTACTTTGTCAGGTAAAGCACCAAGTACTCGCCACG TTGATTCT

GTTAACATGACAGCCTGTGCCAATTGCCACACTGCTGAGTTCGAAATTCACAAAGGCAAACA ACATGCAG

GCTTTGTGATGACAGAGCAACTATCACACACCCAAGATGCTAACGGTAAAGCGATTGTAGG CCTTGACGC

ATGTGTGACTTGTCATACTCCTGATGGCACCTATAGCTTTGCCAACCGTGGTGCGCTAGAGC TAAAACTA

CACAAAAAACACGTTGAAGATGCCTACGGCCTCATTGGTGGCAATTGTGCCTCTTGTCACTC AGACTTCA

ACCTTGAGTCTTTCAAGAAGAAAGGCGCATTGAATACTGCCGCTGCAGCAGATAAAACAGG TCTATATTC

TACGCCGATCACTGCAACTTGTACTACCTGTCACACAGTTGGCAGCCAGTACATGGTCCATA CGAAAGAA

ACCCTGGAGTCTTTCGGTGCAGTTGTTGATGGCACAAAAGATGATGCTACCAGTGCGGCAC AGTCAGAAA

CCTGTTTCTACTGCCATACCCCAACAGTTGCAGATCACACTAAAGTGAAAATGTAA.

Appendix 7: *Shewanella oneidensis* MR-1 chromosome, complete genome

NCBI Reference Sequence: NC_004347.2

GenBank Graphics

>NC_004347.2:c1858265-1856172 Shewanella oneidensis MR-1 *mtrB* (2094bp) chromosome, complete genome

ATGAAATTTAAACTCAATTTGATCACTCTAGCGTTATTAGCCAACACAGGCTTGGCCGTCGCT
GCTGATG
GTTATGGTCTAGCGAATGCCAATACTGAAAAAGTGAAATTATCCGCATGGAGCTGTAAAGGC
TGCGTCGT
TGAAACGGGCACATCAGGCACTGTGGGTGTCGGTGTCGGTTATAACAGCGAAGAGGATATT
CGCTCTGCC
AATGCCTTTGGTACATCCAATGAAGTGGCGGGTAAATTTGATGCCGATTTAAACTTTAAAGG
TGAAAAGG
GTTATCGTGCCAGTGTTGATGCTTATCAACTCGGTATGGATGGCGGTCGCTTAGATGTCAAT
GCGGGCAA
ACAAGGCCAGTACAACGTCAATGTGAACTATCGCCAAATTGCTACCTACGACAGCAATAGC
GCCCTATCG
CCCTACGCGGGTATTGGTGGCAATAACCTCACGTTACCGGATAACTGGATAACAGCAGGTT
CAAGCAACC
AAATGCCACTCTTGATGGACAGCCTCAATGCCCTCGAACTCTCACTTAAACGTGAGCGCACG
GGGTTGGG
ATTTGAATATCAAGGTGAATCCCTGTGGAGCACCTATGTTAACTACATGCGTGAAGAGAAAA
CCGGCTTA
AAACAAGCCTCTGGTAGCTTCTTCAACCAATCGATGATGTTAGCAGAGCCGGTGGATTACAC
CACTGACA
CCATTGAAGCGGGTGTCAAACTCAAGGGTGATCGTTGGTTTACCGCACTCAGTTACAATGGG
TCAATATT
CAAAAACGAATACAACCAATTGGACTTTGAAAATGCTTTTAACCCCACCTTTGGTGCTCAAA
CCCAAGGT
ACGATGGCACTCGATCCGGATAACCAGTCACACACCGTGTCGCTGATGGGACAGTACAACG
ATGGCAGCA
ACGCACTGTCGGGTCGTATTCTGACCGGACAAATGAGCCAAGATCAGGCGTTAGTGACGGA
TAACTACCG

TTATGCTAATCAGCTCAATACCGATGCCGTCGATGCCAAAGTCGATCTACTGGGTATGAACC
TGAAAGTC
GTTAGCAAAGTGAGCAATGATCTTCGCTTAACAGGTAGTTACGATTATTACGACCGTGACAA
TAATACCC
AAGTAGAAGAATGGACTCAGATCAGCATCAACAATGTCAACGGTAAGGTGGCTTATAACAC
CCCTTACGA
TAATCGTACGCAACGCTTTAAAGTTGCCGCAGATTATCGCATTACCCGCGATATCAAACTCG
ATGGTGGT
TATGACTTCAAACGTGACCAACGTGATTATCAAGACCGTGAAACCACGGATGAAAATACCGT
TTGGGCCC
GTTTACGTGTAAACAGCTTCGATACTTGGGACATGTGGGTAAAAGGCAGTTACGGTAACCGT
GACGGCTC
ACAATACCAAGCGTCTGAATGGACCTCTTCTGAAACCAACAGCCTGTTACGTAAGTACAATC
TGGCTGAC
CGTGACAGAACTCAAGTCGAAGCACGGATCACCCATTCGCCATTAGAAAGCCTGACTATCG
ATGTTGGTG
CCCGTTACGCGTTAGATGATTATACCGATACTGTGATTGGATTAACTGAGTCAAAAGACACC
AGTTATGA
TGCCAACATCAGTTATATGATCACCGCTGACTTACTGGCAACCGCCTTCTACAATTACCAAA
CCATTGAG
TCTGAACAGGCGGGTAGCAGCAATTACAGCACCCCAACGTGGACAGGCTTTATAGAAGATC
AGGTAGATG
TGGTCGGTGCAGGTATCAGCTACAACAATCTGCTGGAGAACAAGTTACGCCTAGGACTGGA
CTACACCTA
TTCCAACTCCGACAGTAACACTCAAGTCAGACAAGGTATCACTGGCGACTATGGTGATTATT
TTGCCAAA
GTGCATAACATTAACTTATACGCTCAATATCAAGCCACCGAGAAACTCGCGCTGCGCTTCGA
TTACAAAA
TTGAGAACTATAAGGACAATGACGCCGCAAATGATATCGCCGTTGATGGCATTTGGAACGTC
GTAGGTTT
TGGTAGTAACAGCCATGACTACACCGCACAAATGCTGATGCTGAGCATGAGTTACAAACTCT
AA